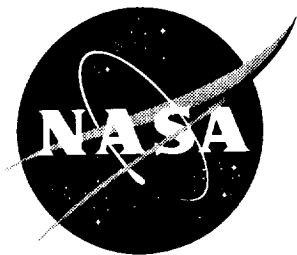


NASA/TM-2000-210293



X-38 Landing Gear Skid Test Report

George K. Gafka
NASA Johnson Space Center, Houston, Texas

Robert H. Daugherty
NASA Langley Research Center, Hampton, Virginia

June 2000

The NASA STI Program Office ... in Profile

Since its founding, NASA has been dedicated to the advancement of aeronautics and space science. The NASA Scientific and Technical Information (STI) Program Office plays a key part in helping NASA maintain this important role.

The NASA STI Program Office is operated by Langley Research Center, the lead center for NASA's scientific and technical information. The NASA STI Program Office provides access to the NASA STI Database, the largest collection of aeronautical and space science STI in the world. The Program Office is also NASA's institutional mechanism for disseminating the results of its research and development activities. These results are published by NASA in the NASA STI Report Series, which includes the following report types:

- **TECHNICAL PUBLICATION.** Reports of completed research or a major significant phase of research that present the results of NASA programs and include extensive data or theoretical analysis. Includes compilations of significant scientific and technical data and information deemed to be of continuing reference value. NASA counterpart of peer-reviewed formal professional papers, but having less stringent limitations on manuscript length and extent of graphic presentations.
- **TECHNICAL MEMORANDUM.** Scientific and technical findings that are preliminary or of specialized interest, e.g., quick release reports, working papers, and bibliographies that contain minimal annotation. Does not contain extensive analysis.
- **CONTRACTOR REPORT.** Scientific and technical findings by NASA-sponsored contractors and grantees.

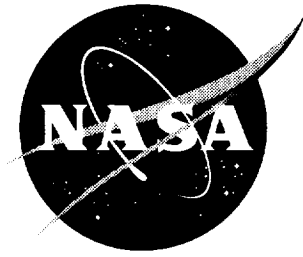
- **CONFERENCE PUBLICATION.** Collected papers from scientific and technical conferences, symposia, seminars, or other meetings sponsored or co-sponsored by NASA.
- **SPECIAL PUBLICATION.** Scientific, technical, or historical information from NASA programs, projects, and missions, often concerned with subjects having substantial public interest.
- **TECHNICAL TRANSLATION.** English-language translations of foreign scientific and technical material pertinent to NASA's mission.

Specialized services that complement the STI Program Office's diverse offerings include creating custom thesauri, building customized databases, organizing and publishing research results ... even providing videos.

For more information about the NASA STI Program Office, see the following:

- Access the NASA STI Program Home Page at <http://www.sti.nasa.gov>
- E-mail your question via the Internet to help@sti.nasa.gov
- Fax your question to the NASA STI Help Desk at (301) 621-0134
- Phone the NASA STI Help Desk at (301) 621-0390
- Write to:
NASA STI Help Desk
NASA Center for AeroSpace Information
7121 Standard Drive
Hanover, MD 21076-1320

NASA/TM-2000-210293



X-38 Landing Gear Skid Test Report

George K. Gafka
NASA Johnson Space Center, Houston, Texas

Robert H. Daugherty
NASA Langley Research Center, Hampton, Virginia

National Aeronautics and
Space Administration

Langley Research Center
Hampton, Virginia 23681-2199

June 2000

Available from:

NASA Center for AeroSpace Information (CASI)
7121 Standard Drive
Hanover, MD 21076-1320
(301) 621-0390

National Technical Information Service (NTIS)
5285 Port Royal Road
Springfield, VA 22161-2171
(703) 605-6000

X-38 Landing Gear Skid Test Report

Edwards Air Force Base Lakebed

George K. Gafka
NASA Johnson Space Center

Robert H. Daugherty
NASA Langley Research Center

ABSTRACT

NASA incorporates skid-equipped landing gear on its series of X-38 flight test vehicles. The X-38 test program is the proving ground for the operational Crew Return Vehicle (CRV), a vehicle designed to return the crew from the International Space Station in the event of an emergency where no other means of escape is possible. The vehicle is envisioned to land at a relatively low speed by making use of a gliding parafoil. The skid-equipped landing gear is designed to attenuate the vertical landing energy of the vehicle at touchdown using crushable materials within the struts themselves. The vehicle then slides out as the vehicle horizontal energy is dissipated through the skids. A series of tests was conducted at Edwards Airforce Base (EAFB) in an attempt to quantify the drag force produced while "dragging" various X-38 landing gear skids across lakebed regions of varying surface properties. These data were then used to calculate coefficients of friction for each condition. Coefficient of friction information is critical for landing stability analysis as well as for landing gear load and interface load analysis. The skid specimens included full- and sub-scale V201 (space test vehicle) nose and main gear designs, a V131/V132 (atmospheric flight test vehicles) main gear skid (actual flight hardware), and a newly modified, full-scale V201 nose gear skid with substantially increased edge curvature as compared to its original design. Results of the testing are discussed along with comments on the relative importance of various parameters that influence skid stability and other dynamic behavior.

Table of Contents

List of Figures.....	3
List of Tables	4
Introduction.....	5
Test Equipment	5
Test Plan	7
Test Matrix Reduction Study	7
Multi-Speed / Constant Speed Discussion	7
Resulting Test Procedure	8
Small Crab Angle Effects on Test Matrix Size	9
Data Acquisition / Data Reduction	11
Results and Discussion	11
Test Run Observations.....	11
Drag Force Mechanisms	11
Skid Behavior.....	12
Surface / Soil Effects	14
Skid Geometry Effects	16
Skid Redesign	21
Conclusions and Recommendations	23
Appendix A: V201 Skid Drawings.....	26
Appendix B: Planned and Actual Test Runs	29
Appendix C: Graphical Depiction of Test Matrix	34
Appendix D: Raw Test Data	36

List of Figures

Figure 1. NASA Langley's ITTV	6
Figure 2. Typical skid installation on ITTV	6
Figure 3. Multi-speed vs. constant-speed comparison	8
Figure 4. Graphical depiction of typical test run	9
Figure 5. "Small" crab angle comparison	10
Figure 6. Examples of the three drag force-producing mechanisms	12
Figure 7. Examples of horizontal plowing on medium and soft surfaces	13
Figure 8. General skid stability break-down	14
Figure 9. Sketch showing tendency of drag force to create pitch-down	14
Figure 10. Effect of surface strength on drag force coefficient versus speed.	15
Figure 11. Sketch showing the effect of leading edge curvature	16
Figure 12. Free body diagram of typical skid forces	17
Figure 13. Sketch of relative positions of geometric variables at zero crab.	18
Figure 14. Sketch of relative positions of geometric variables at large crab	18
Figure 15. Originally-proposed V201 nose gear skid buried after diverging	20
Figure 16. V131 main gear skid design is unstable	20
Figure 17. Modified full-scale nose gear skid (201NR)	21
Figure 18. Modified nose skid design produces lower overall drag forces	22
Figure 19. Redesigned nose gear skid provides floatation on soft surface	23

List of Tables

Table 1. Initial test matrix	7
Table 2. Reduced test matrix	10
Table 3. Calculated bearing pressure for each skid at 5000 lb. load	16

Introduction

NASA incorporates skid-equipped landing gear on its series of X-38 flight test vehicles. The X-38 test program is the proving ground for the operational Crew Return Vehicle (CRV), a vehicle designed to return the crew from the International Space Station in the event of an emergency where no other means of escape is possible. The vehicle is envisioned to land at a relatively low speed by making use of a gliding parafoil. The skid-equipped landing gear is designed to attenuate the vertical landing energy of the vehicle at touchdown using crushable materials within the struts themselves. The vehicle then slides out as the vehicle horizontal energy is dissipated through friction forces acting on the skids. The X-38 program includes atmospheric flight test vehicles designated to date as V131 and V132, as well as a space test vehicle designated as V201. It should be noted that the skids utilized on these two types of vehicles are vastly different.

A series of tests was conducted at Edwards Airforce Base (EAFB) in an attempt to quantify the drag force produced while “dragging” various X-38 landing gear skids across lakebed regions of varying surface properties. These data were then used to calculate coefficients of friction for each condition. Coefficient of friction information is critical for landing stability analysis as well as for landing gear load and interface load analysis.

Test Equipment

The skid tests were conducted using NASA Langley’s Instrumented Tire Test Vehicle (ITTV). The ITTV consists of an approximately 28,000-lb. truck to which a pneumatically driven test fixture loading system is attached. A specially designed force measurement dynamometer allows a variety of aircraft landing gear components, such as tires, to be mounted to the test fixture. In this case, the main gear skids used on both the V131 and V132 (X-38 atmospheric flight test vehicles) as well as the candidate skids for the space test vehicle V201 were mounted to the test fixture using adapter plates. The forces and moments associated with tire or skid drag testing (i.e. vertical load, drag load, side load, aligning torque, and overturning torque) were measured and recorded by an onboard electronic data acquisition system. Continuous time histories were taken by strain gages, speed sensors, and distance sensors for each test run. The test fixture loading system at the rear of the ITTV can be seen below in figure1. For this skid test program, the fixture was used to generate its maximum downward load of approximately 5000lb.

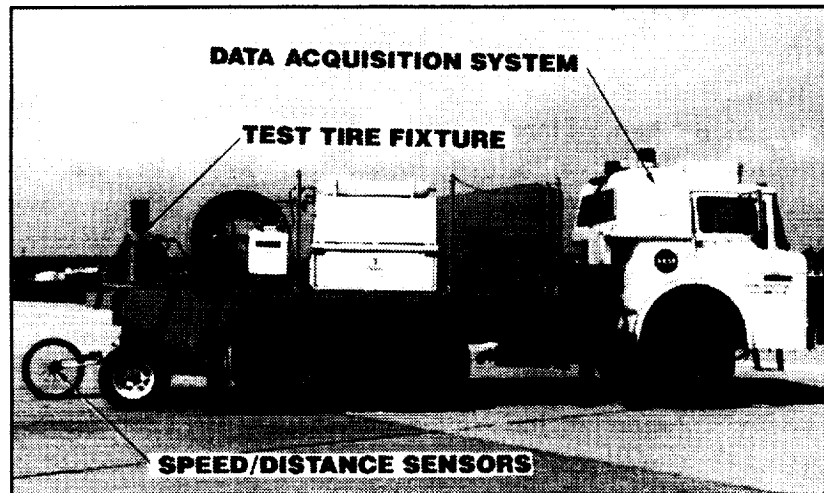


Figure 1. NASA Langley's ITTV.

The test plan called for the testing of five different skids:

- V131/V132 main gear (actual flight hardware, denoted as "131")
- the current V201 nose gear design (edge curvature radius approx. 0.75 inches, denoted as "201N")
- the current V201 main gear design (edge curvature radius approx. 1.58 inches, denoted as "201M")
- a sub-scale V201 nose gear design (50% scale, denoted as "201NS")
- a sub-scale V201 main gear design (40% scale, denoted as "201MS")

The V201 series skids were solid aluminum plate replicas of the latest skid design at the time. It should be noted that, while not originally in the test plan, yet another skid "specimen" was tested later in the test program. This "specimen" was the 201N skid described above but modified as will be discussed later, and is denoted as "201NR". Due to the limited downward force capability of the ITTV (~5000lb), the sub-scale replicas were manufactured to better simulate actual vehicle landing loads by attempting to match the skid/ground bearing pressures to those expected for flight. In other words, by reducing the size of the skid, and therefore the skid contact area, the bearing pressure is increased without increasing load. See Appendix A for detailed drawings of each V201 skid. Figure 2 shows a close-up of a typical installation of a skid specimen on the test fixture of the ITTV.

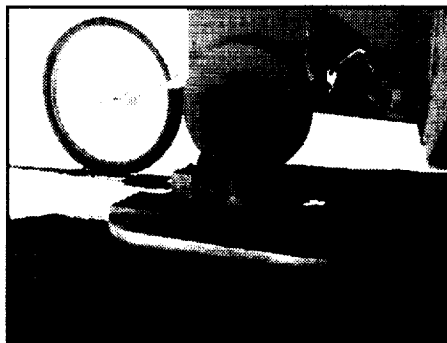


Figure 2. Typical skid installation on ITTV.

Test Plan

Test Matrix Reduction Study

Table 1 shows the initially-proposed test matrix developed during pre-test planning:

Table 1. Initial test matrix.

θ_c (deg)	V_g (ft/s)					
	15	35	50	56	65	76
0	✓	✓	✓	✓	✓	✓
2	✓	✓	✓	✓	✓	✓
5	✓	✓	✓	✓	✓	✓
10	✓	✓	✓	✓	✓	✓
30	✓	✓	✓	✓	✓	✓
45	✓	✓	✓	✓	✓	✓

This matrix shows planned test runs using six different crab or yaw angles, θ_c (NOTE: for these tests only, crab angle and yaw angle are used interchangeably) at each of six different test speeds. It was planned to conduct these tests on each of two different strength surfaces, on five different skid specimens, and with two different vertical loads. Combining all of these desired test parameters resulted in a test matrix that grew to a total of 720 runs.

Multi-Speed / Constant Speed Discussion

Due to the large number of initially-proposed test cases coupled with the limited amount of test time on the lakebed, a test matrix reduction was necessary. However, instead of removing individual test matrix cases, LaRC proposed a plan to acquire an entire “row” of test matrix data per test run by continuously taking data while decelerating the ITTV from 76 ft/sec down to 0 ft/sec (52 mph to 0 mph).

This data acquisition procedure had to be verified prior to testing. First, some preliminary tests were conducted near NASA LaRC with a “dummy” skid prior to shipping the ITTV out to EAFB. These preliminary drag tests were conducted at constant speeds as well as continuously-decelerating speeds to verify consistent friction results with respect to speed (i.e. “constant speed” results matched up with “multi-speed” results at their respective speed.). The tests revealed that this manner of data acquisition was acceptable. This test approach was again verified using the actual test hardware at EAFB.

Figure 3 clearly illustrates the acceptability of acquiring data in this manner. Note the discrete data points from the “multi-speed” run (continuous data acquisition while decelerating). These data points are used to form a linear approximation of drag force coefficient versus speed. Processing the data in this manner eliminates the noise from the

raw data. Next, note that the “constant speed” data points (data at only one speed per entire test run) match closely with their respective location on the “multi-speed” plot. The slight discrepancy in results is certainly within an acceptable range and also within the “noise-floor” of the data accuracy.

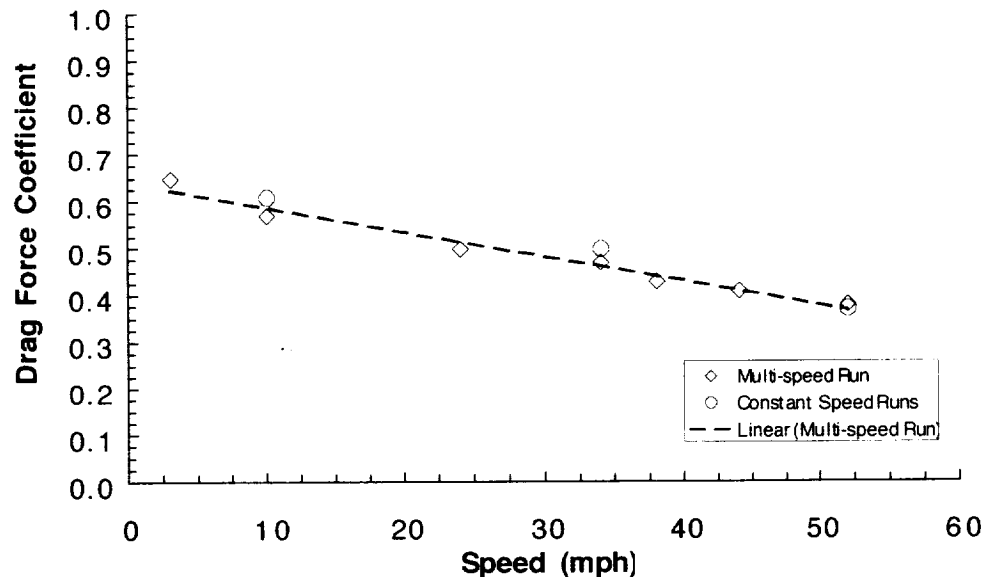


Figure 3. Multi-speed vs. constant-speed comparison: Drag force coefficient versus speed using V201 full-scale nose gear skid (201N).

Resulting Test Procedure

To ensure a consistent method of data acquisition the following test run sequence was developed (see figure 4).

- The vehicle was accelerated to maximum speed prior to the test section (the test section was typically 900 feet long).
- The data recorders were activated just prior to the test section and the ITTV operator was given a “proceed with test” command from the data operator.
- The ITTV operator would lower the test fixture at the beginning of the test section and “5 seconds of distance” (about 300 feet) was dedicated to achieving ground contact and full load buildup on the skid specimen.
- After the 5-second period, the ITTV would pass a cone at which point the operator would begin a constant deceleration and the vehicle would be brought to a stop in approximately 500 feet.
- The data recorders were deactivated after the vehicle was stopped.

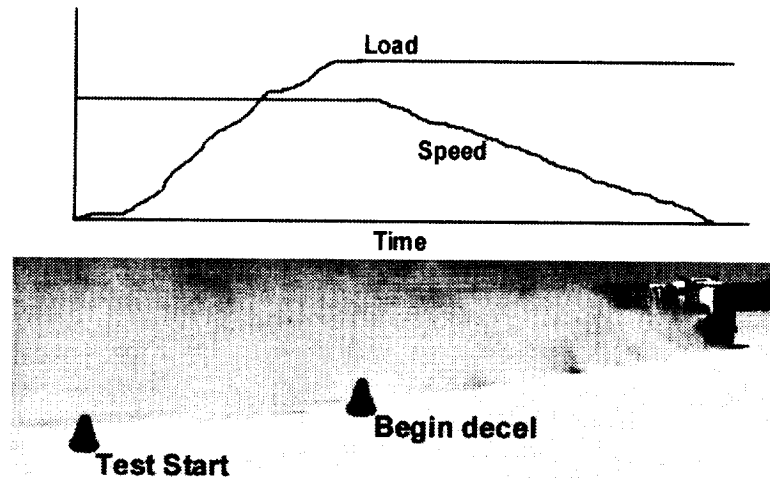


Figure 4. Graphical depiction of typical test run.

The test runs were staggered such that each pass was made over a fresh, undisturbed surface to ensure data accuracy. In other words, test data were not acquired over previously tested soil or in a tire track left from a previous run. This was particularly important for testing on the softer regions of the lakebed.

Small Crab Angle Effects on Test Matrix Size

It was believed that any friction property changes due to small crab angles (2 degrees and 5 degrees) would be negligible and well within the “noise-floor” of the data accuracy. Therefore, NASA LaRC recommended removing the “small” crab angle (referred to as yaw angle in the test data) test runs from the test matrix.

Preliminary tests were conducted to compare the drag force coefficient versus speed for the following crab angles: 0 degrees, 2 degrees, and 5 degrees. Figure 5 illustrates the results from these test runs. Note that all three plots are virtually identical and overlay each other quite closely. Therefore, it was reasonable to assume that the geometric effects (i.e. effect of small leading edge contour change, effect of small center of pressure to center of load location change, and effect of small side force component change) from small crab angles on coefficient of friction were negligible. Thus, all 2- and 5-degree crab angle test runs were eliminated from the test matrix. This resulted in an updated matrix (shown in Table 2) that, when combined with the previous multi-speed discussion, required only 80 test runs as compared to the originally-planned 720 runs.

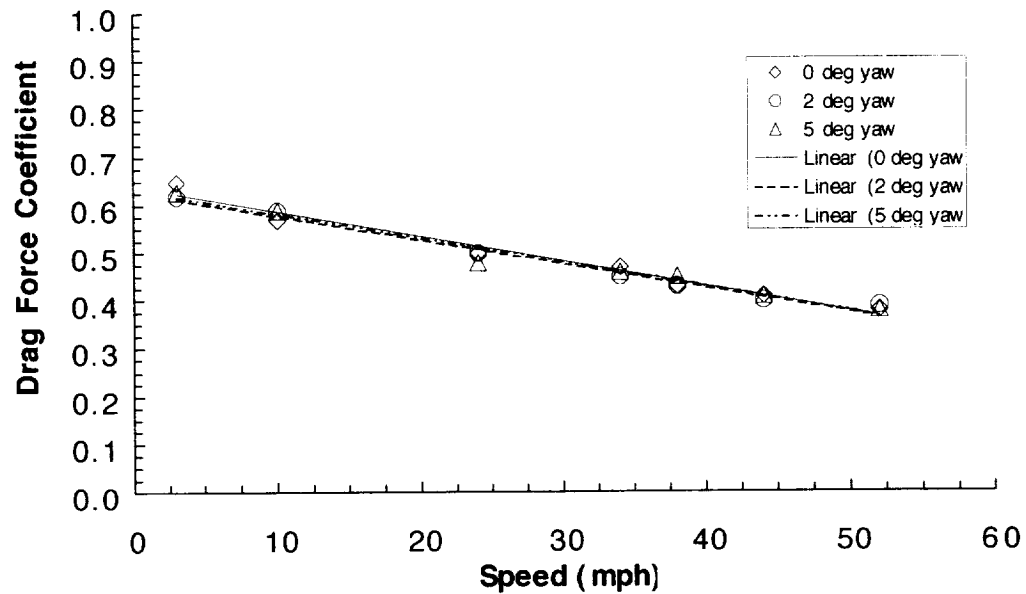


Figure 5. “Small” crab angle comparison: Drag force coefficient versus speed using V201 full-scale nose gear skid.

Table 2. Reduced test matrix.

θ_c (deg)	V_g 76 to 0 ft/sec
0	✓
10	✓
30	✓
45	✓

Appendix B contains the list of all planned test runs. Along the way, some of the planned test runs were omitted due to hardware safety concerns, some of the tests were not needed due to similarity to other tests, and some additional test runs were added to gain a more complete understanding of skid behavior. Runs with an “ITTV Run Number” appended to them were actually conducted. Appendix C graphically shows the places in the high-load portion of the test matrix that were tested and those that were not. The values shown in Appendix C represent the drag force coefficients at the conditions shown.

Data Acquisition / Data Reduction

Raw data (provided in Appendix D) acquired from each test run were in the form of load-cell component force time histories for normal, drag, and side loads. ITTV speed and distance were also measured. All data were recorded at 10 samples per second. The drag and side loads were measured in the test specimen coordinate plane, so true drag force (force parallel and opposite the velocity vector) and true side force (force perpendicular to the velocity vector) would require an angular transformation using the yaw or crab angle. Rather than apply the required transformation to the drag load itself, the drag force coefficient was calculated by dividing the drag force time histories by the normal force time histories and then the angular transformation was applied to the drag force coefficient. Thus, when these data are presented, the drag forces shown are in skid coordinates, and the drag force coefficients are in velocity vector coordinates.

For runs conducted with crab angle present, the side forces as well as the drag forces were evaluated. If no true side load was present, then the measured side and drag loads should each resolve into the same true drag load. In each case, it was confirmed that the total drag loads in the velocity vector coordinates were pure. For example, in tests conducted at a 45 degree crab angle, the measured side and drag forces were equal thus indicating no true side load as compared to the velocity vector was being produced and that all of the forces generated by the skid were parallel and opposite the velocity vector.

Results and Discussion

Test Run Observations

One of the first and most significant observations was that, as expected, “friction” in the classical sense (i.e. a block of wood sliding down a wedge) had very little to do with any results labeled “coefficient of friction”. In fact, it is far more accurate to refer to this *energy attenuation mechanism* as merely a “drag force coefficient.” Therefore, this will be the terminology used from this point forward.

Drag Force Mechanisms

The drag force (and thus, the drag force coefficient after division by the normal load) produced by the skid specimens appears to ultimately result from combinations of the drag forces produced by several mechanisms. Figure 6 shows a photograph of the results of each of the following drag-producing mechanisms:

- a. Forces due to conventional friction as described above. (figure 6a)
- b. Direct mechanical interference forces produced in the path of the plowing skid specimen (plowing appears to be influenced heavily by surface strength). (figure 6b)
- c. Forces produced by the imparting of momentum to the soil particles that are “thrown” laterally by the plowing action in a direction not parallel to the velocity

vector (e.g. the “side plume” of dirt left after certain testing on soft surfaces). (figure 6c)



Figure 6a. Forces due mainly to friction.



Figure 6b. Forces due mainly to plowing.



Figure 6c. Significant forces dedicated to “side plume”.

Figure 6. Examples of the three drag force-producing mechanisms.

The landing gear skids act more like snow skis than any classic, molecular-type representation of a friction problem, especially as the test surface gets softer. Therefore, keeping this “ski” analogy in mind aids tremendously in understanding both the test results and V201 skid design modifications discussed later in this report.

Skid Behavior

Qualitatively, the skid behavior can be separated into three distinct types of behavior:

- **skiing or terra-planing** (stable)
- **horizontal plowing** (meta-stable plowing)
- **nose-dive plowing** (unstable plowing)

A **skiing or terra-planing** behavior has occurred when the skid appears to glide over the surface. On a hard surface, a mark is barely visible after each test. On a soft surface, the loose material is brushed out to the sides keeping the nose of the skid relatively high and

clean. This type of behavior is the most favorable because it is the most stable and corresponds to the lowest drag force coefficients. This behavior also roughly corresponds to drag force-producing mechanism (a) above and is shown in figure 6a.

A horizontal plowing behavior occurs when the skid breaks through the surface and plows but stays consistently level once it has penetrated to its “steady state” depth. Typically not seen on extremely hard surfaces, this behavior was observed to occur both on surfaces of medium and low hardness with certain skid designs. In addition, this behavior typically becomes more evident towards the end of a test run when the vehicle is traveling fairly slowly. This will be discussed in greater detail later. Although not “catastrophic” in nature, this type of behavior is unfavorable and is referred to as “meta-stable”. The drag force coefficients for a horizontal plowing behavior also tend to be somewhat higher than those recorded for a terra-planing behavior. Figures 7a and 7b show two examples of horizontal plowing behavior. Figure 7a shows the behavior on the medium-strength surface with the originally-proposed full-scale V201 nose gear skid (201N), and Figure 7b shows this behavior on a very low-strength surface with the modified V201 nose gear skid (201NR, to be discussed later).

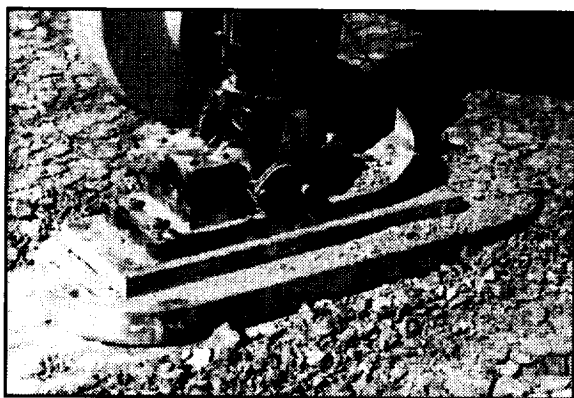


Figure 7a. Meta-stable on medium surface.



Figure 7b. Meta-stable on soft surface.

Figure 7. Examples of horizontal plowing on medium and soft surfaces.

A nose-dive plowing behavior occurs when the nose pitches down and the skid digs into the ground divergently. This is considered both a catastrophic and a totally unacceptable skid behavior. Most skid test runs that displayed this behavior resulted in fixture damage, sheared fixture bolts, and a substantial loss of steering control for the test truck driver. On the medium-strength surface, the only reason that nose-dive plowing did not completely diverge and damage the hardware was because the fixture was able to fully extend and “bottom out”, thereby eliminating the vertical load on the skid. Because this medium-strength soil density was not as great as the soil density of the hard surface, the fixture was able to tolerate the drag loads produced by nose-dive plowing on the softer surface. Obviously, the drag force coefficients for these runs were sizably higher than for runs exhibiting other behaviors and in some cases the values were off-scale and not even measurable. An example of a test in which the drag force coefficient was quite large is seen in figure 6c.

Both horizontal plowing and nose-dive plowing exhibit all three drag force-producing mechanisms from above but it is surmised that the frictional forces from mechanism (a) are substantially overshadowed by the other two mechanisms (b and c). The amount of contribution to total drag force by mechanism b or c may be related to not only the surface density but also to the relative stability produced by the geometry of the skid itself. In other words, a skid that is either designed or operated such that the center of load is not *behind* the center of pressure will exhibit nose-dive plowing and throw a lot of soil laterally. However, a skid designed with an appropriate load and pressure center, (depending on leading edge curvature and soil strength), may have a meta-stable horizontal plowing behavior and not produce as much “side plume”. Figure 8 illustrates the three skid behaviors in general stability terminology.

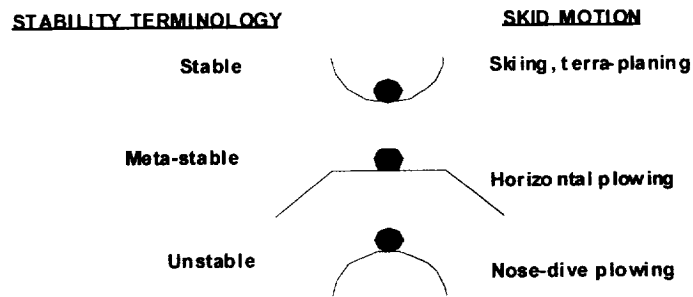


Figure 8. General skid stability break-down.

These three skid behaviors, or motions, come about as a result of the complex interaction of the skid geometry itself and the type of surface (which may be described with a soil hardness value and/or a soil density value and/or a cone index value described later).

Surface/Soil Effects

Surface Hardness: The soil or surface hardness (or density) appears to determine how deeply the skid penetrates (even if it is a “stable” skid design). This penetration provides an initial elevation (relative to the skid pitch pivot point) where the combination of drag forces is coincident. Figure 9 shows a sketch of a skid with limited penetration and one can note the pitch-down moment tendency associated with the drag force as drawn. Note that the drag force is not necessarily parallel to the velocity vector

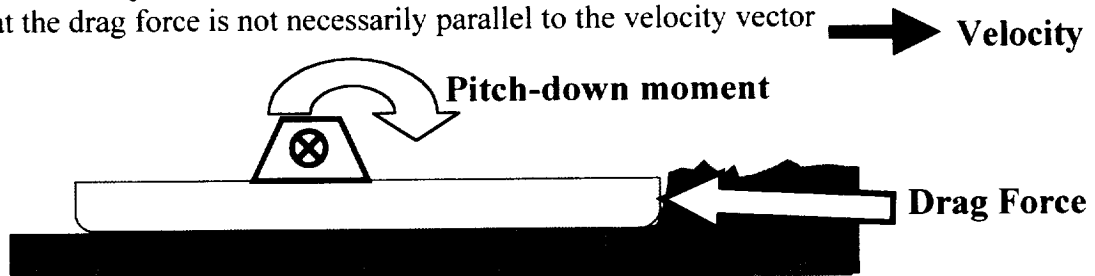


Figure 9. Sketch showing tendency of drag force to create pitch-down moments and unstable behavior.

Figure 10 presents test data showing the effect of soil strength (or hardness) on the drag behavior of a skid at a yaw angle of 45 degrees.

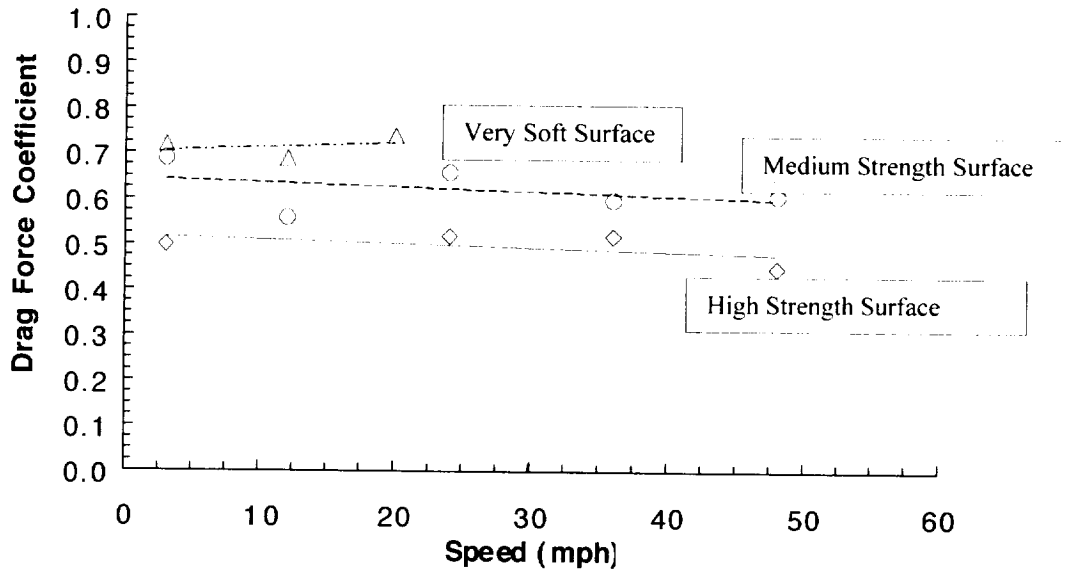


Figure 10. Effect of surface strength on drag force coefficient versus speed.

The surface strengths were quantified by performing a penetration test using a rectangular bar attached to the pneumatic loading fixture of the ITTV. A 1.5 square-inch bar was forced into the ground at each test site and the pressure required to achieve a 1-inch penetration depth was recorded. This is quite similar to a commercially available device known as a Cone Penetrometer, and surface strength values are reported as a “cone index” (CI) which is the pressure in lbs. per square inch to achieve certain penetration depths. The hardest surface tested (EAFB1) had a CI of approximately 3000, the medium surface (EAFB2) had a CI of approximately 1000, and the softest surface (EAFB4, which is similar to a beach-like surface) had a CI of about 500. It had been reported that the “average” soil strength picked at random on the Earth’s surface is much more likely to resemble that of the medium surface (EAFB2) as opposed to a surface that is significantly harder or softer.

Bearing Pressure: All of the above surface strengths, in terms of pressure, would appear to be able to support any of the skid specimens tested. Table 3 lists the approximate bearing pressure each skid specimen would impart to the surface under a vertical load of 5000 lbs., and includes a value for a redesigned nose gear skid discussed later.

Table 3. Calculated bearing pressure for each skid at 5000 lb. load.

Skid Specimen	Calculated Bearing Pressure
201N (full-scale nose)	21.4 psi
201NS (sub-scale nose)	85.6 psi
201M (full-scale main)	14.5 psi
201MS (sub-scale main)	90.4 psi
210NR (redesigned nose)	21.4 to 48.3 psi depending on skid penetration level

None of the specimens have a bearing pressure that even comes close to the CI values that were measured using the bar described in the previous section. Based on a bearing pressure comparison only, it would appear that all of the surfaces, including the beach-like EAFB4, could support any of these skids. However, as soon as testing commenced on the medium-strength surface EAFB2, it was found that the sub-scale V201 nose and main gear skids buried themselves deeply in that surface even though the ratio of surface strength to bearing pressure was nearly a factor of 11. Extrapolating this result revealed that there was no chance of the sub-scale V201 nose and main gear skids being adequately supported on EAFB4. Clearly, other factors are more determinative of adequate skid flotation than the bearing pressure alone. The following section describes the geometry effects that cause this phenomenon and explains why skid geometry is apparently a much more important consideration for adequate behavior than is the bearing pressure.

Skid Geometry Effects

Skid geometry heavily influences the dynamic behavior of the skid. The most important geometry factors are as follows:

- The geometry of the skid center of load relative to its center of ground contact
- The geometry of the skid leading edge

Recalling from figure 9, the drag force is not necessarily parallel to the velocity vector. If the skid leading edge were completely flat (i.e. a square-edged skid) then perhaps the drag force would be parallel to the velocity vector. Figure 11 shows a sketch of a skid similar to that in figure 9 but with a leading edge having a much larger radius.

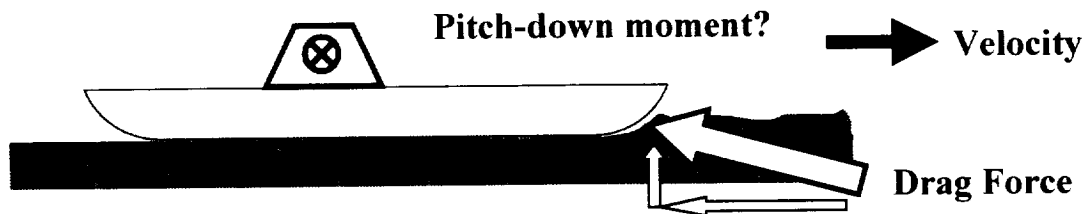


Figure 11. Sketch showing the effect of leading edge curvature on the pitch-down moment.

Depending on the curvature of the leading edge and the angle of incidence of the total drag force, there may or may not be a nose-down pitching moment for this configuration. However, it is clear that the behavior of the relatively square-edged skid shown in figure 9 would be drastically improved by adopting the leading edge curvature shown in figure 11. Testing on medium-strength soil (denoted in Appendix B as EAFB2) showed that the originally-proposed V201 nose gear skid basically behaved satisfactorily (i.e. non-divergent plowing) until the crab angle rose above 30 degrees. When this skid was tested at a 45-degree crab angle on this medium-strength surface, it dug in severely as previously discussed. While the proposed V201 main gear skid had a somewhat larger edge radius, it was felt that it would behave in essentially the same way as the nose gear skid. This appears to be a result of the interaction between the drag force incident angle and the skid geometry with particular reference to the pivot point and center of pressure on the skid. Figure 12 shows a sketch of a skid and the general orientation and position of the forces acting upon it.

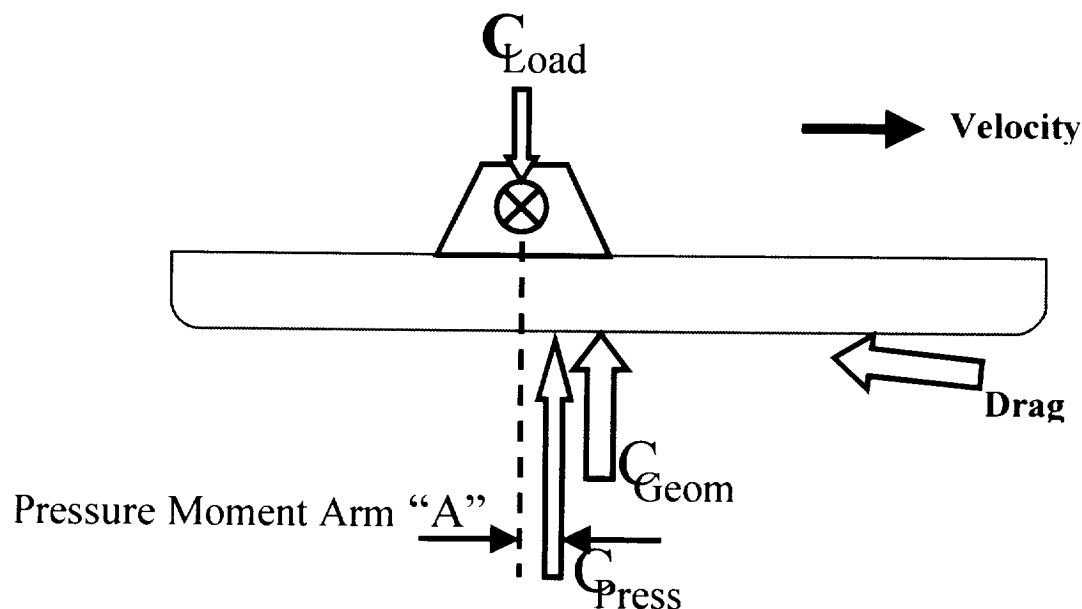


Figure 12. Free body diagram of typical skid forces.

Figure 12 depicts the important relationship between the vertical loading point (center of load), the drag force, and two other points in the skid footprint: the center of geometry and the center of pressure. If the skid were motionless, the center of pressure would be coincident with the center of geometry. However, as soon as the skid attains forward motion, the center of pressure (i.e. where the effective ground vertical load reaction is located) must move aft of the center of geometry. Thus, to obtain a stable skid design, one must design the pivot point (or center of load) to be aft of the geometric center. Further, the center of pressure (a difficult point to positionally define) needs to be forward of the center of load as well. The reason for this is to provide a restoring pitching moment to counteract the effect of any negative pitching moment produced by the drag force.

For the present testing, it was desirable to conduct tests with the skid specimens at crab angles simulating the possible attitudes of V201. For certain off-nominal conditions, crab angles at landing could range above 45 degrees and, in fact, could conceivably reach 180 degrees denoting a landing in which the wind speed exceeds the V201 forward flight trim speed. The sketches in figures 13 and 14 (views from above the skid) describe the relationship between the center of pressure and the center of load as crab angle is increased.

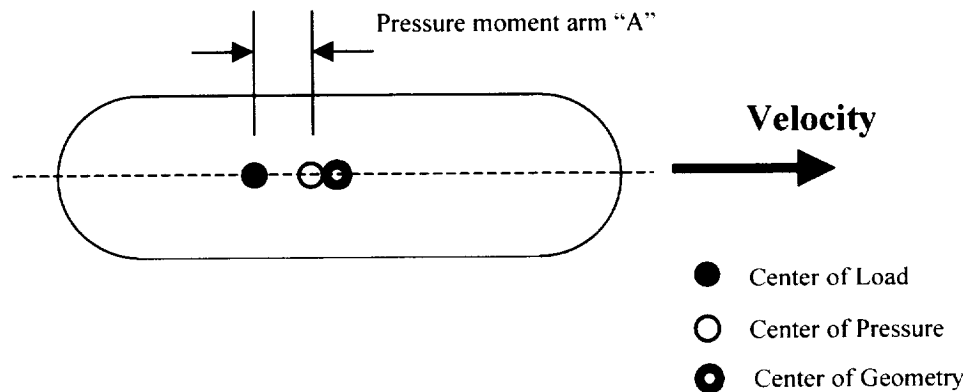


Figure 13. Sketch of relative positions of geometric variables at zero crab or yaw angle.

In figure 13, the pressure moment arm "A" multiplied by the vertical load can be assumed to be sufficient to counter the nose-down pitching moment due to drag.

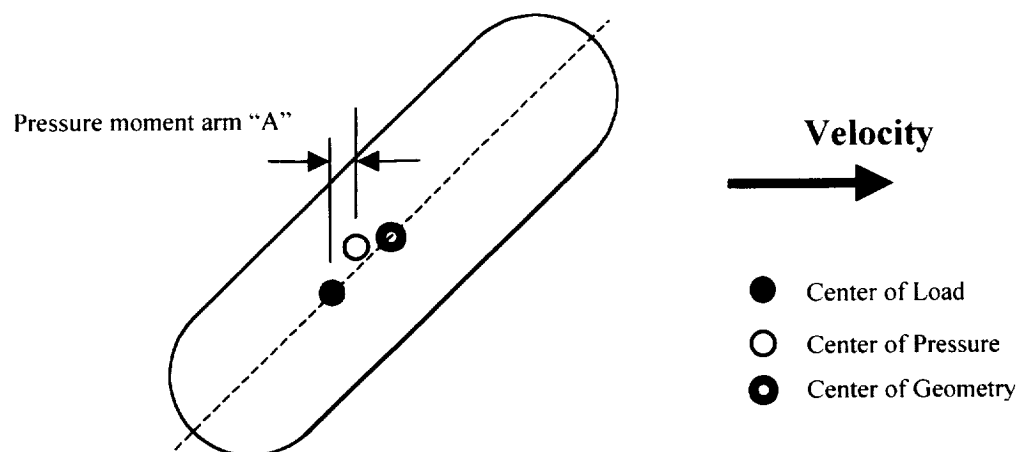


Figure 14. Sketch of relative positions of geometric variables at large crab or yaw angles.

In figure 14, the pressure moment arm “A” is now decreased by a factor of the sine of crab angle. Multiplying this shorter length by the vertical load obviously produces a smaller moment to counter nose-down pitching moment due to drag than that shown for the zero crab or yaw case. Thus, as shown in figures 13 and 14, there may exist a crab angle (even for an otherwise “stable” skid) beyond which the positive pitching moment created by the forward (in the velocity vector) center of pressure is overcome by the negative pitching moment caused by the drag force. The actual value of this angle is specific to each skid design, leading edge curvature, and surface strength. The surface strength plays a part as described previously because it tends to determine much about the true direction and elevation of the effective drag force. It is this phenomenon that caused the originally-proposed V201 nose skid design to act satisfactorily up to 30 degrees crab angle. However, between 30 and 45 degrees crab angle for that skid design on the medium strength soil tested, the pressure moment arm “A” decreased (figure 14) to the point where the moment balance switched directions and the negative moment created by the drag force was greater than the positive moment due to the forward center of pressure. This resulted in the divergent nose-dive behavior observed. A photograph of the originally-proposed V201 nose gear skid after this test is shown in figure 15. This reasoning, extended to 90-degree crab angles and above, suggests that a positive pitching moment cannot be achieved and digging in is quite likely. In fact, even a slow-speed, zero-degree crab test performed on the V131 main gear skid specimen showed unacceptable and dangerous nose-down pitching moment behavior because the center of load was forward of the geometric center of the footprint. Figure 16 shows photographs of this configuration and figure 6b shows a close-up view of the result of that test. This unfavorable skid geometry found on the V131/V132 main gear skid produced nose-dive plowing even on a hard surface (see figure 6b). The plowing loads tend to rise in an incredibly steep fashion and can rapidly destroy any attachment hardware (as was the case with the ITTV) unless the vertical loads are reduced in an equally rapid fashion. Hints of this nose-dive behavior are visible after actual V131/V132 flight test landings on the hard region of the lakebed. The initial touchdown marks for the main gear skids are reported to be quite similar to that shown in figure 6b with the exception that the actual marks are not as deep. So, why then do the V131/V132 skids not fail similarly during flight test landings? The answer lies in the two primary differences between the V131/V132 flight configuration and the current test configuration. First, remember for the test configuration, the skids are mounted in a “pedestal” configuration with one attach point / pivot point. The V131/V132 flight Landing Attenuation System (LAS) has a forward drag link which attaches to the skid up near the leading edge, limiting nose-dive motion. Second, during actual V131/V132 flight test landings, the belly of the vehicle hits as soon as the main gear strokes (on the order of tenths of a second after initial skid contact). This effectively unloads the main gear skids, limiting surface penetration and limiting the overall drag loads on the skid. If this were not the case, the V131/V132 LAS would likely experience catastrophic hardware failure during each landing along with the likelihood of damage to the vehicle itself. Furthermore, the core differences between the current test and the flight configurations, made it impossible to test V131/V132 skids as originally planned (denoted with a “ * “ in the chart in Appendix C).

It should be noted that a test such as that shown in figure 6b proved to be a fairly reliable indicator of the basic skid behavior. This quasi-static test consisted of applying load to a skid specimen and then slowly dragging the specimen forward and provided much insight about how that skid would behave in a high-speed test. Many tests, such as those planned using the sub-scale V201 nose and main skid specimens on the medium and soft surfaces were abandoned after realizing, with this type of quasi-static test, that they would behave poorly and dig into the surface. Such tests are shown in Appendix C and are denoted by “not done due to test/hardware safety or surface cannot support skid at all”.

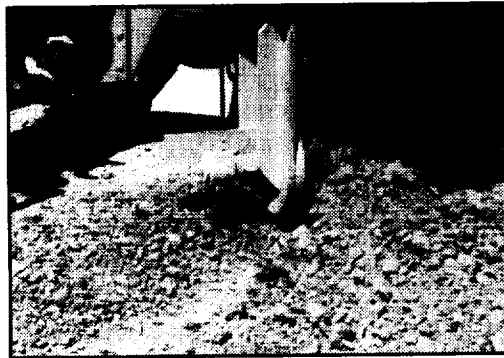


Figure 15. Originally-proposed V201 nose gear skid (201N) buried after divergent behavior.

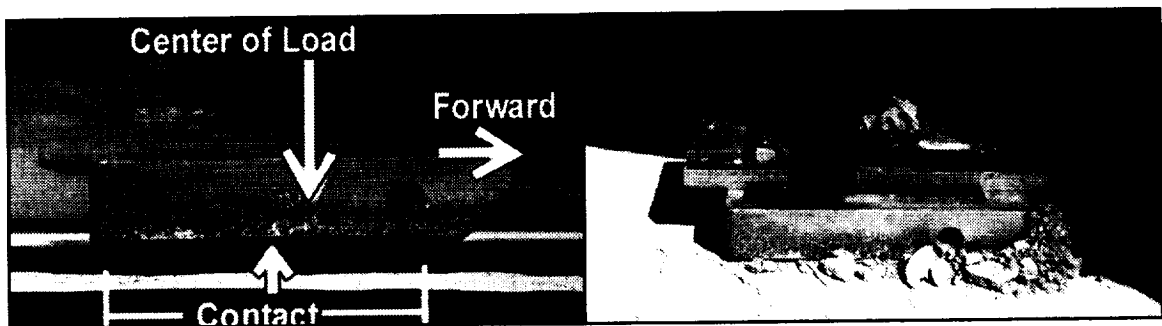


Figure 16. V131 main gear skid design is unstable.

As a result of these findings, it appears to be unwise to land a skid-equipped vehicle at high crab angles. Even fully symmetrical skids (i.e. a round pad) would at best provide neutrally stable or unstable results, since it would not be possible to ensure that the center of load is behind the center of pressure. Based on this, landings at crab angles greater than 30 degrees should be avoided at all costs. In particular, a landing with a headwind greater than the trimmed flight speed of the vehicle under the parafoil is a situation that should not be taken lightly. It may well be better to land the vehicle downwind at a higher overall energy than to land backwards which invites unstable skid behavior and possibly destructive drag loads.

Skid Redesign

After having described the required relationships between the center of load, pressure, and geometry of the skid, consideration was given to an alternate full-scale V201 skid design to alleviate some of the poor performance, especially at high crab angles and soft surfaces. Because changing the center of load for the proposed V201 skid involves other considerations such as stowage, etc., and the center of geometry was not likely to change for the same reason (no overall shape change or size growth for the skid), changing the skid's performance at high crab angles and on soft surfaces could only be achieved through changing the incident angle of the overall drag forces. The center of pressure, while possibly being affected through changing the drag force incident angle, could not be directly changed, nor is it known how to effect such a change. The incident angle of the overall drag forces appears to involve an interaction between the skid's leading edge curvature and the soil characteristics. Therefore, skid leading edge curvature was the one avenue open for modification, and it was apparent that the change in edge curvature needed to be a dramatic one. The full-scale edge curvatures on the originally proposed V201 nose and main gear skids both appeared to be extremely "sharp" and gave the impression that the skid performance would be no different than if the edge had no curvature. The full-scale V201 nose skid (201N) was then modified as described earlier with a 3.25-inch radius curvature on all sides (denoted as 201NR) and is pictured above the softest surface tested (EAFB4) in figure 17.

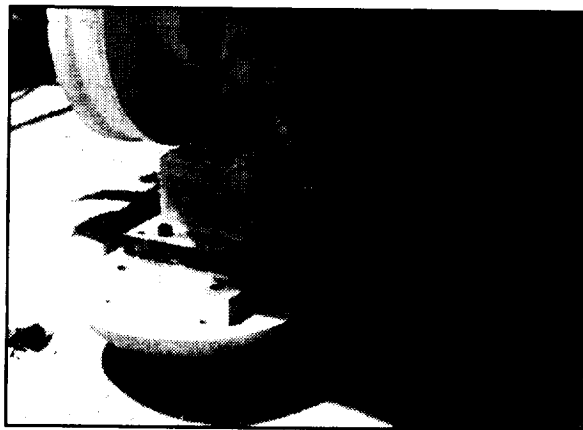


Figure 17. Modified full-scale nose gear skid (201NR).

The sketches in figures 9 and 11 are, in fact, scale drawings of the originally-proposed V201 nose gear skid (201N, figure 9, which has a radius of curvature of about 0.75 inches) and the newly modified version of that skid with a 3.25 inch radius of curvature on all edges (201NR, figure 11). The intention of the increased curvature was to force the tangent of the "stagnation" point of the soil being displaced on medium and soft surfaces to an angle other than essentially vertical as it was on the originally-proposed V201 nose gear skid design. This would then produce an upward component of the drag force as sketched in figure 11. On the hardest of surfaces, since no appreciable surface

penetration was present, this modification has no real effect whatsoever. Any upward drag component at the nose of the skid would translate into reduced (or possibly eliminated) pitch-down moment, contributing to a more stable skid behavior and/or increased crab angle that could be achieved before the pitch-up moment created by the center of pressure was overcome by the pitch-down moment created by the drag force. It may actually be possible that the angle of incidence of the drag force could be directed above the skid pivot point, insuring positive pitch-up moments. However, as the skid crab angle is increased, because of the relative narrowness of the skid at some point the line of action of the drag force would most likely act below the pivot point. It was also expected that the modified skid would allow flotation on the softest of surfaces, since the beneficial curvature would still be present even though the skid penetrates the surface more deeply and exhibits the horizontal plowing, but stable, behavior. All of these expectations were realized with this modification. Figure 18 presents a plot of the behavior of the originally-proposed V201 nose gear skid versus the newly-modified V201 nose gear skid design at high speed on the medium-strength surface.

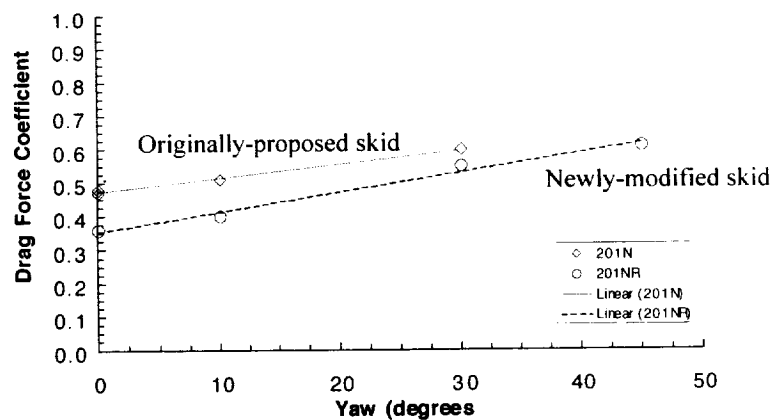


Figure 18. Modified nose skid design produces lower overall drag forces on EAFB2.

Tests as shown above were conducted on the medium strength surface (EAFB2) and the modified nose gear skid (201NR) exhibited excellent stability and flotation behavior, with no apparent tendency to dig-in even at a 45-degree crab angle, a condition that was totally unacceptable with the nose gear skid as originally designed. Finally, tests were conducted on surface EAFB4, a dirt/sand road in the EAFB "PIRA" area on Photo Resolution Road. Based on the prior testing experience, each member of the test team was confident that none of the originally-proposed V201 skids (either full- or sub-scale) had even a remote chance of providing adequate, stable flotation on this extremely soft surface. Three tests of the newly redesigned V201 nose gear skid (210NR) were conducted at initial speeds of 20 mph. The surface was so soft and narrow that it was dangerous to operate the ITTV at speeds greater than 20 mph. Figure 19 shows a blown-

up portion of figure 7b and the plowing, but stable nature of the skid can be seen more clearly.

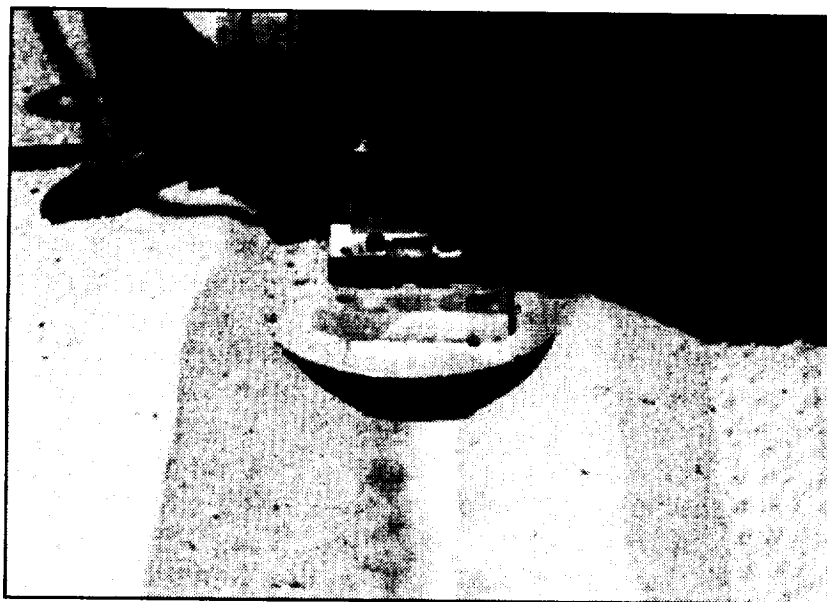


Figure 19. Redesigned nose gear skid provides floatation on soft surface.

Figure 19 shows the appearance of the surface after a zero-degree crab angle test. Subsequent testing at 30- and 45-degree crab angles had virtually identical appearances except that the path was wider because of the crab angle. In each case very satisfactory skid performance was noted, with sand being thrown laterally in a significant side plume. Referring back to figure 10, one can see that the drag forces associated with operating on this soft surface were higher than for the medium or hard surfaces, indicating that more energy is being expended into creating the side plume than for the other surfaces.

Conclusions and Recommendations

A series of tests was conducted to determine the drag force coefficients and dynamic behavior of various X-38 landing gear skids (atmospheric test flight vehicles 131/132 and space test vehicle 201) on surfaces of varying hardness. The tests were conducted on lakebed surfaces at the Edwards Air Force Base dry lakebed and surrounding area. Approximately 121 tests were conducted using six different specimens. The specimens included:

- V131/V132 main gear (actual flight hardware),
- the current V201 nose gear design,
- the current V201 main gear design,
- a sub-scale of the current V201 nose gear design (50% scale),
- a sub-scale of the current V201 main gear design (40% scale).

- ***a newly modified, full-scale V201 nose gear skid with substantially increased edge curvature than its original design (3.25-inch edge radius versus approximately 0.75-inch radius).***

The testing concentrated on three different surfaces with soil strengths ranging from very soft to very hard, with a medium-strength surface in the approximate hardness range of a randomly selected point on the Earth. The following are conclusions and recommendations reached as a result of this testing:

- The V131/V132 main gear skid design is unstable in the current test configuration. It has a center of load (pivot point) forward of the geometric center of its ground contact area. This causes the nose of the skid to tend to dig-in and create destructive drag loads on the test fixture and attachment hardware. For the flight configuration, vehicle belly contact during landing coupled with the forward drag link prevents excessive drag loads on the skid and, therefore, the LAS. This is accomplished both by limiting the vertical load on the skid and by keeping the “nose” of the skid up. However, landing gear damage caused to date from flight tests may have been caused by this inherently unstable skid behavior.
- Skid landings on the hardest portion of the lakebed are insensitive to bearing pressure, skid edge curvature, vertical load, and skid scale, resulting in relatively consistent drag results. However, skid behavior remains extremely sensitive to center of load versus center of pressure positioning even on the hardest of surfaces.
- The originally-proposed V201 skid designs provide adequate flotation and stability at crab angles up to 45 degrees, but ONLY on the hardest of lakebed surfaces. Unstable skid behavior was observed for the nose skid and should be expected for the main skid at higher crab angles on this hard surface.
- Landings on soft surfaces with the originally-proposed V201 skid designs should not be attempted.
- Landings on medium and hard surfaces at extremely large crab or yaw angles (i.e. greater than 45 degrees), including backwards landings (i.e. 180 degree crab angles), should be expected to exhibit unstable, destructive skid behavior and possibly produce enough drag force to overturn the vehicle. Landings with crab angles greater than 30 degrees, if using the originally-proposed V201 skids, should be avoided at all costs. Landings with crab angles greater than 45 degrees, if using the newly-modified skid design, should be avoided at all costs.
- Quasi-static skid testing (loading the skid at “zero horizontal velocity” and slowly dragging forward) offers a fairly reliable method of determining the overall skid stability and behavior.
- Skid drag forces are opposite the velocity vector and side forces transverse to the velocity vector are not produced even in the presence of a crab angle.
- Drag force coefficient increases linearly as speed decreases. Increasing crab angle increases drag force coefficient, though to a lesser extent than the speed effect.
- Bearing pressure values compared to surface strength measurements do not adequately describe the resistance of a skid to “digging-in.” Other parameters such as leading edge curvature and pivot point location versus center of geometry are far more important design considerations for stable skid behavior.

- Scale model testing for dynamic behavior appears to be unsatisfactory. A method to appropriately scale edge curvatures, bearing pressures, and skid geometry while the soil and surface characteristics remain un-scaled is currently unknown.
- Extremely large skid edge curvature (including the leading edge and sides if crabbed landings are desired) is probably the single most important design consideration after ensuring the center of load is sufficiently aft of the center of geometry.
- The originally-proposed V201 skid designs (both nose and main) have edge curvatures so sharp that it renders the skids unstable above 30 degrees crab on the type of surface that is most likely to be landed upon (medium strength surfaces).
- It is recommended that the originally-proposed V201 skid designs (both nose and main) be modified to have all edges with a radius of curvature of 3.25. This edge curvature allows stable behavior on soft, medium, and hard surfaces at up to 45 degrees crab angle.

Appendix A: V201 Skid Drawings

V-201 Full- and Sub-Scale Nose Gear Skid

DASH NO.	A	B	C	D	E	F	G	H	I	J	K	L	M	N	O	P	Q	R	S	T	U	V	W	X	Y	Z	AA	AB	AC	AD	AE	AF	AG	AH	AI	AJ	AK	AL	AM	AN	AO	AP	AQ	AR	AS	AT	AU	AV	AW	AX	AY	AZ	BA	BB	BC	BD	BE	BF	BG	BH	BI	BJ	BK	BL	BM	BN	BO	BP	BQ	BR	BS	BT	BU	BV	BW	BX	BY	BZ	CA	CB	CC	CD	CE	CF	CG	CH	CI	CJ	CK	CL	CM	CN	CO	CP	CQ	CR	CS	CT	CU	CV	CW	CX	CY	CZ	DA	DB	DC	DD	DE	DF	DG	DH	DI	DJ	DK	DL	DM	DN	DO	DP	DQ	DR	DS	DT	DU	DV	DW	DX	DY	DZ	EA	EB	EC	ED	EE	EF	EG	EH	EI	EJ	EK	EL	EM	EN	EO	EP	EQ	ER	ES	ET	EU	EV	EW	EX	EY	EZ	FA	FB	FC	FD	FE	FF	FG	FH	FI	FJ	FK	FL	FM	FN	FO	FP	FQ	FR	FS	FT	FU	FV	FW	FX	FY	FZ	GA	GB	GC	GD	GE	GF	GG	GH	GI	GJ	GK	GL	GM	GN	GO	GP	GQ	GR	GS	GT	GU	GV	GW	GX	GY	GZ	HA	HB	HC	HD	HE	HF	HG	HH	HI	HJ	HK	HL	HM	HN	HO	HP	HQ	HR	HS	HT	HU	HV	HW	HX	HY	HZ	IA	IB	IC	ID	IE	IF	IG	IH	II	IJ	IK	IL	IM	IN	IO	IP	IQ	IR	IS	IT	IU	IV	IW	IX	IY	IZ	JA	JB	JC	JD	JE	JF	JG	JH	JI	JJ	JK	JL	JM	JN	JO	JP	JQ	JR	JS	JT	JU	JV	JW	JX	JY	JZ	KA	KB	KC	KD	KE	KF	KG	KH	KI	KJ	KL	KM	KN	KO	KP	KQ	KR	KS	KT	KU	KV	KW	KX	KY	KZ	LA	LB	LC	LD	LE	LF	LG	LH	LI	LJ	LK	LL	LM	LN	LO	LP	LQ	LR	LS	LT	LU	LV	LW	LX	LY	LZ	MA	MB	MC	MD	ME	MF	MG	MH	MI	MJ	MK	ML	MM	MN	MO	MP	MQ	MR	MS	MT	MU	MV	MW	MX	MY	MZ	NA	NB	NC	ND	NE	NF	NG	NH	NI	NJ	NK	NL	NM	NN	NO	NP	NQ	NR	NS	NT	NU	NV	NW	NX	NY	NZ	OA	OB	OC	OD	OE	OF	OG	OH	OI	OJ	OK	OL	OM	ON	OO	OP	OQ	OR	OS	OT	OU	OV	OW	OX	OY	OZ	PA	PB	PC	PD	PE	PF	PG	PH	PI	PJ	PK	PL	PM	PN	PO	PP	PQ	PR	PS	PT	PU	PV	PW	PX	PY	PZ	QA	QB	QC	QD	QE	QF	QG	QH	QI	QJ	QK	QL	QM	QN	QO	QP	QQ	QR	QS	QT	QU	QV	QW	QX	QY	QZ	RA	RB	RC	RD	RE	RF	RG	RH	RI	RJ	RK	RL	RM	RN	RO	RP	RQ	RR	RS	RT	RU	RV	RW	RX	RY	RZ	SA	SB	SC	SD	SE	SF	SG	SH	SI	SJ	SK	SL	SM	SN	SO	SP	SQ	SR	SS	ST	SU	SV	SW	SX	SY	SZ	TA	TB	TC	TD	TE	TF	TG	TH	TI	TJ	TK	TL	TM	TN	TO	TP	TQ	TR	TS	TT	TU	TV	TW	TX	TY	TZ	UA	UB	UC	UD	UE	UF	UG	UH	UI	UJ	UK	UL	UM	UN	UO	UP	UQ	UR	US	UT	UU	UV	UW	UX	UY	UZ	VA	VB	VC	VD	VE	VF	VG	VH	VI	VJ	VK	VL	VM	VN	VO	VP	VQ	VR	VS	VT	VU	VV	VW	VX	VY	VZ	WA	WB	WC	WD	WE	WF	WG	WH	WI	WJ	WK	WL	WM	WN	WO	WP	WQ	WR	WS	WT	WU	WV	WW	WX	WY	WZ	XA	XB	XC	XD	XE	XF	YG	YH	YI	YJ	YK	YL	YM	YN	YO	YP	YQ	YR	YS	YT	YU	YV	YW	YX	YY	YZ	ZA	ZB	ZC	ZD	ZE	ZF	ZG	ZH	ZI	ZJ	ZK	ZL	ZM	ZN	ZO	ZP	ZQ	ZR	ZS	ZT	ZU	ZV
----------	---	---	---	---	---	---	---	---	---	---	---	---	---	---	---	---	---	---	---	---	---	---	---	---	---	---	----	----	----	----	----	----	----	----	----	----	----	----	----	----	----	----	----	----	----	----	----	----	----	----	----	----	----	----	----	----	----	----	----	----	----	----	----	----	----	----	----	----	----	----	----	----	----	----	----	----	----	----	----	----	----	----	----	----	----	----	----	----	----	----	----	----	----	----	----	----	----	----	----	----	----	----	----	----	----	----	----	----	----	----	----	----	----	----	----	----	----	----	----	----	----	----	----	----	----	----	----	----	----	----	----	----	----	----	----	----	----	----	----	----	----	----	----	----	----	----	----	----	----	----	----	----	----	----	----	----	----	----	----	----	----	----	----	----	----	----	----	----	----	----	----	----	----	----	----	----	----	----	----	----	----	----	----	----	----	----	----	----	----	----	----	----	----	----	----	----	----	----	----	----	----	----	----	----	----	----	----	----	----	----	----	----	----	----	----	----	----	----	----	----	----	----	----	----	----	----	----	----	----	----	----	----	----	----	----	----	----	----	----	----	----	----	----	----	----	----	----	----	----	----	----	----	----	----	----	----	----	----	----	----	----	----	----	----	----	----	----	----	----	----	----	----	----	----	----	----	----	----	----	----	----	----	----	----	----	----	----	----	----	----	----	----	----	----	----	----	----	----	----	----	----	----	----	----	----	----	----	----	----	----	----	----	----	----	----	----	----	----	----	----	----	----	----	----	----	----	----	----	----	----	----	----	----	----	----	----	----	----	----	----	----	----	----	----	----	----	----	----	----	----	----	----	----	----	----	----	----	----	----	----	----	----	----	----	----	----	----	----	----	----	----	----	----	----	----	----	----	----	----	----	----	----	----	----	----	----	----	----	----	----	----	----	----	----	----	----	----	----	----	----	----	----	----	----	----	----	----	----	----	----	----	----	----	----	----	----	----	----	----	----	----	----	----	----	----	----	----	----	----	----	----	----	----	----	----	----	----	----	----	----	----	----	----	----	----	----	----	----	----	----	----	----	----	----	----	----	----	----	----	----	----	----	----	----	----	----	----	----	----	----	----	----	----	----	----	----	----	----	----	----	----	----	----	----	----	----	----	----	----	----	----	----	----	----	----	----	----	----	----	----	----	----	----	----	----	----	----	----	----	----	----	----	----	----	----	----	----	----	----	----	----	----	----	----	----	----	----	----	----	----	----	----	----	----	----	----	----	----	----	----	----	----	----	----	----	----	----	----	----	----	----	----	----	----	----	----	----	----	----	----	----	----	----	----	----	----	----	----	----	----	----	----	----	----	----	----	----	----	----	----	----	----	----	----	----	----	----	----	----	----	----	----	----	----	----	----	----	----	----	----	----	----	----	----	----	----	----	----	----	----	----	----	----	----	----	----	----	----	----	----	----	----	----	----	----	----	----	----	----	----	----	----	----	----	----	----	----	----	----	----	----	----	----	----	----	----	----	----	----	----	----	----	----	----	----	----	----	----	----	----	----	----	----	----	----	----	----	----	----	----	----

DASH NO	A (REF)	B	C	D (RAD US)	E (RAD US)	F PIVOT POINT
-001	9.449	7.333	989	0.78"	4.74	11.220
-003	4.03	6.56	989	0.394	2.362	5.610

REFERENCE V: EN

0-22	0-23	0-24	0-25	0-26	0-27	0-28	0-29	0-30	0-31	0-32	0-33	0-34	0-35	0-36	0-37	0-38	0-39	0-40	0-41	0-42	0-43	0-44	0-45	0-46	0-47	0-48	0-49	0-50	0-51	0-52	0-53	0-54	0-55	0-56	0-57	0-58	0-59	0-60	0-61	0-62	0-63	0-64	0-65	0-66	0-67	0-68	0-69	0-70	0-71	0-72	0-73	0-74	0-75	0-76	0-77	0-78	0-79	0-80	0-81	0-82	0-83	0-84	0-85	0-86	0-87	0-88	0-89	0-90	0-91	0-92	0-93	0-94	0-95	0-96	0-97	0-98	0-99
0-22	0-23	0-24	0-25	0-26	0-27	0-28	0-29	0-30	0-31	0-32	0-33	0-34	0-35	0-36	0-37	0-38	0-39	0-40	0-41	0-42	0-43	0-44	0-45	0-46	0-47	0-48	0-49	0-50	0-51	0-52	0-53	0-54	0-55	0-56	0-57	0-58	0-59	0-60	0-61	0-62	0-63	0-64	0-65	0-66	0-67	0-68	0-69	0-70	0-71	0-72	0-73	0-74	0-75	0-76	0-77	0-78	0-79	0-80	0-81	0-82	0-83	0-84	0-85	0-86	0-87	0-88	0-89	0-90	0-91	0-92	0-93	0-94	0-95	0-96	0-97	0-98	0-99

001 (SHOWN)
003 (AS NOTED)

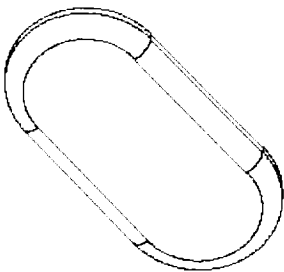
5. BRAP ALL SHARP EDGES AND ROUND ALL CORNERS TO .02 - .04 R.
4. ALL DIMENSIONS ARE IN INCHES-POUNDS.
3. CLEAN TO LEVEL 2C PER MIL-STD-883C.
2. FABRICATION TOLERANCES AND DIMENSIONS PER MIL-STD-883C.
1. MICROBET PER JES-550C 4.

NOTES: UNLESS OTHERWISE SPECIFIED

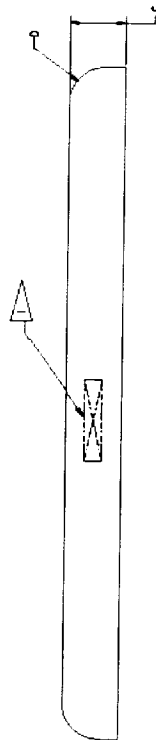
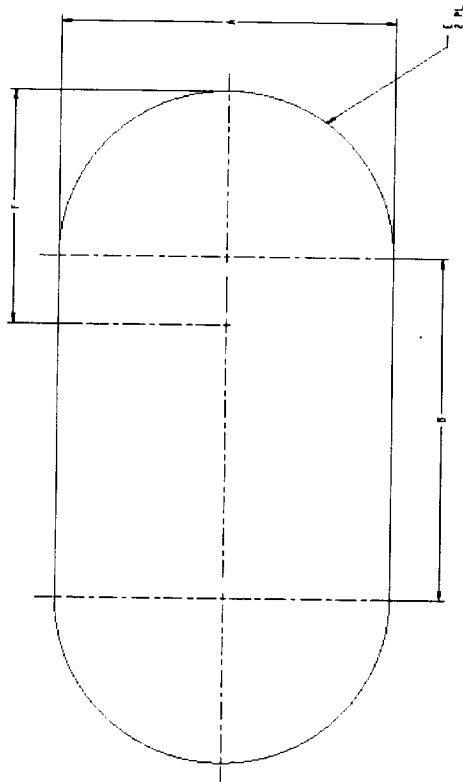
FLAG NOTES

206-D-9002 206-D-9001 206-D-9000
 CHARLES AND KSA - SC 402-4000 4000 4000
 RUBBER STAMP PART NUMBER AND SIZE. NUMBER IN THE HIGH 50-100

DASH NO	A (IN.)	B	C	D (INCHES)	E (INCHES)	F PIVOT POINT
-101	13.169	14.252	2.302	1.575	0.080	9.724
-103	5.512	5.761	2.000	0.650	2.754	3.080



REFERENCE VIEW



-001 (SHOWN)
-003 (AS NOTED)

5. BREAK ALL SHARP EDGES AND ROUND ALL CORNERS TO .02 - .04 R.
4. ALL DIMENSIONS ARE IN INCHES/POUNDS.
3. CLEAN TO LEVEL EC PER NASA/JSC PNC-5001.
2. FABRICATION TOLERANCES AND PRACTICES PER BZX 34103755.
INTERPRET PER JPC 8500 4.

NOTES: UNLESS OTHERWISE SPECIFIED

△ RUBBER STAMP PART NUMBER AND SERIAL NUMBER IN 1/8 HIGH GOTHIC CHARACTERS PER NASH/JSC PRC-8002 LOCATE APPROXIMATELY AS SHOWN

FLAG NOTES

[illegible]

Appendix B: Planned and Actual Test Runs

Revision D 9/23/99		Appendix B	
<div>K-28/CPI/Skid Tests</div>			
Notes	Specimen Designation	Comments	ITTV Run Number
	131 = V131 main	All tests begin at 55 mph and decel to 0 unless otherwise noted	
	201M = V201 main full scale		
	201MS = V201 main sub scale		
	201N = V201 nose full scale		
	201NS = V201 nose sub scale		
Run #	Specimen	Surface	Vertical Load (lbs)
			Yaw (deg)
1	201N	EAFB 1	1000
2	201N	EAFB 1	2000
3	201N	EAFB 1	3000
4	201N	EAFB 1	4000
5	201N	EAFB 1	5000
6	201N	EAFB 1	5000
7	201N	EAFB 1	5000
8	201N	EAFB 1	5000
9	201N	EAFB 1	5000
10	201N	EAFB 1	5000
11	201N	EAFB 1	5000
12	201N	EAFB 1	5000
13	201N	EAFB 1	5000
14	201N	EAFB 1	5000
15	201N	EAFB 1	5000
16	201N	EAFB 1	5000
17	201N	EAFB 1	3000
18	201N	EAFB 1	3000
19	201N	EAFB 1	3000
20	201N	EAFB 1	3000
21	201N	EAFB 1	3000
22	201N	EAFB 1	3000


23	201M	EAFB 1	3000	0				Appendix B.
24	201M	EAFB 1	3000	10				
25	201M	EAFB 1	3000	30				
26	201M	EAFB 1	3000	45				
27	201M	EAFB 1	5000	0			Run27	
28	201M	EAFB 1	5000	0	Test for repeatability		Run28	
29	201M	EAFB 1	5000	10			Run29	
30	201M	EAFB 1	5000	30			Run30	
31	201M	EAFB 1	5000	30	Test for repeatability		Run31	
32	201M	EAFB 1	5000	45			Run32	
33	201NS	EAFB 1	5000	0	Switch to scaled specimens		Run33	
34	201NS	EAFB 1	5000	0	Test for repeatability			
35	201NS	EAFB 1	5000	10			Run35	
36	201NS	EAFB 1	5000	30			Run36	
37	201NS	EAFB 1	1250	0	Switch to scaled loads on scaled nose specimen		Run37	
38	201NS	EAFB 1	1250	10			Run38	
39	201NS	EAFB 1	1250	10	Test for repeatability		Run39	
40	201NS	EAFB 1	1250	30			Run40	
41	201NS	EAFB 1	1250	45				
42	201MS	EAFB 1	800	0	Switch to scaled loads on scaled main specimen			
43	201MS	EAFB 1	800	10				
44	201MS	EAFB 1	800	10	Test for repeatability			
45	201MS	EAFB 1	800	30				
46	201MS	EAFB 1	800	45				
47	201MS	EAFB 1	5000	0			Run47	
48	201MS	EAFB 1	5000	10			Run48	
49	201MS	EAFB 1	5000	30			Run49	
50	131	EAFB 1	5000	0				
51	131	EAFB 1	5000	10				
52	131	EAFB 1	5000	30				
53	131	EAFB 1	5000	45				
54	131	EAFB 1	3000	0			Run54	
55	131	EAFB 1	3000	10				
56	131	EAFB 1	3000	30				
57	131	EAFB 1	3000	45				
58	131	EAFB 2	5000	0	Switch to EAFB 2 for spot checks			
59	131	EAFB 2	5000	10				
60	131	EAFB 2	5000	30				
61	201N	EAFB 2	5000	0			Run61	
62	201N	EAFB 2	5000	0	Test for repeatability		Run62	

63	201N	EA FB 2	5000	10		Run63	Appendix B.
64	201N	EA FB 2	5000	30		Run64	
65	201M	EA FB 2	5000	0		Run65	
66	201M	EA FB 2	5000	10		Run66	
67	201M	EA FB 2	5000	30		Run67	
68	201M	EA FB 2	5000	30	Test for repeatability		
69	201N	EA FB 1	5000	90	Look at high yaw angles	Run69	
70	201N	EA FB 1	5000	135			
71	201N	EA FB 1	5000	180			
72	201N	EA FB 1	3000	90			
73	201N	EA FB 1	3000	135			
74	201N	EA FB 1	3000	180			
75	201NS	EA FB 1	1250	90			
76	201NS	EA FB 1	1250	135			
77	201NS	EA FB 1	1250	180			
78	201NS	EA FB 1	5000	45			
79	201NS	EA FB 1	5000	90			
80	201NS	EA FB 1	5000	135			
81	201NS	EA FB 1	5000	180			
82	201NS	EA FB 1	3000	0		Run82	
83	201NS	EA FB 1	3000	10		Run83	
84	201NS	EA FB 1	3000	30		Run84	
85	201NS	EA FB 1	3000	45			
86	201N	EA FB 1	5000	0		Run86	
87	201N	EA FB 1	5000	0		Run87	
88	201NS	EA FB 1	500	0		Run88	
89	201NS	EA FB 1	1250	0		Run89	
90	201NS	EA FB 1	3000	0		Run90	
91	201NS	EA FB 1	5000	0		Run91	
92	201N	EA FB2	3000	0		Run92	
93	201N	EA FB2	5000	45		Run93	
94	201M	EA FB2	5000	45			
95	201NS	EA FB2	3000	0		Run95	
96	201NS	EA FB2	5000	0			
97	201NS	EA FB2	5000	10			
98	201NS	EA FB2	5000	30			
99	201MS	EA FB2	5000	0			
100	201MS	EA FB2	5000	10			
101	201MS	EA FB2	5000	30			
102	201M	EA FB3	3000	0		Run102	

103	201M	EAFB3	3000	30			Appendix B:
104	201M	EAFB3	5000	0		Run104	
105	201M	EAFB3	5000	10			
106	201M	EAFB3	5000	30		Run106	
107	201M	EAFB3	5000	30		Run107	
108	201NR	EAFB2	5000	0	Test redesigned nose skid	Run108	
109	201NR	EAFB2	5000	10		Run109	
110	201NR	EAFB2	5000	30		Run110	
111	201NR	EAFB2	5000	45		Run111	
112	201NR	EAFB2	5000	10		Run112	
113	201NR	EAFB2	5000	45		Run113	
114	201NR	EAFB2	5000	90			
115	V131	EAFB1	3000	0	Attempt to match V131 landings	Run115	
116	V131	EAFB1	5000	0			
117	201NR	EAFB1	5000	45		Run117	
118	201NR	EAFB4	3000	0	Test on extremely soft surface	Run118	
119	201NR	EAFB4	5000	0		Run119	
120	201NR	EAFB4	5000	30		Run120	
121	201NR	EAFB4	5000	45		Run121	

Appendix C: Graphical Depiction of Test Matrix

<i>Skid Hardware</i>																			
V131 Main, Flight				V201 Nose, Scaled				V201 Nose, Full				V201 Main, Full				V201 Nose, Full, Redesign			
Yaw Angle				Yaw Angle				Yaw Angle				Yaw Angle				Yaw Angle			
0	10	30	45	0	10	30	45	0	10	30	45	0	10	30	45	0	10	30	45
Test Site																			
EAFB 1	*			0.38	0.38	0.42		0.38	0.42	0.43	0.46	0.37	0.40	0.37		0.46	0.42	0.45	0.45
HARD	*			0.44	0.50	0.49		0.53	0.55	0.54	0.61	0.54	0.50	0.48		0.58	0.57	0.57	0.59
CI = 3000	*			0.59	0.64	0.65		0.66	0.66	0.64	0.70	0.65	0.53	0.62		0.69	0.65	0.66	0.64
EAFB 2				Dig				0.47	0.51	0.60									
MED-SOFT				Dig				0.64	0.59	0.65	0.60								
CI = 1000				Dig				0.72	0.73	0.69	0.65								
EAFB 3																			
MED																			
CI = 1300 (variable)																			
EAFB 4																0.66			0.69
VERY SOFT																0.67			0.73
CI = 400-600																0.62			0.54
																			0.72

	<ul style="list-style-type: none"> = full speed range of 48, 12, and 3 mph respectively (vertically) = not done due to test/hardware safety or surface cannot support skid at all = lower speed range of 20, 12, and 3 mph respectively (vertically) = not done due to logic (no need to acquire data at this point) = unusable data and/or not done due to surface not homogeneous
---	--

Notes: The three vertically-arranged values are the drag force coefficients for each test site at each yaw angle at selected velocities

* = unable to accurately simulate vehicle configuration

CI is the Cone Index value in psi

All skid specimen vertical loads 5000 lb. regardless of skid scale

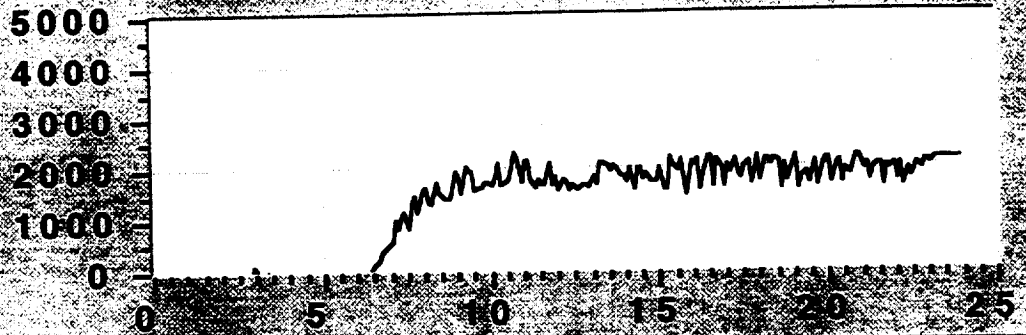
Appendix D: Raw Test Data

Edwards01

Plot A

Return

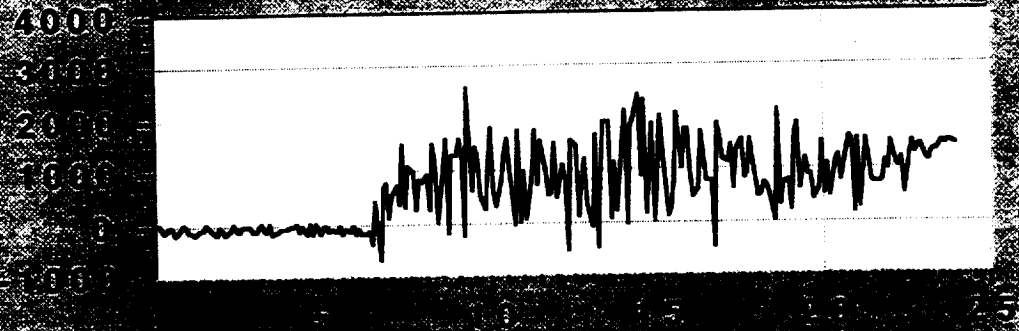
Vertical
Load, lb



Time, sec

Plot B

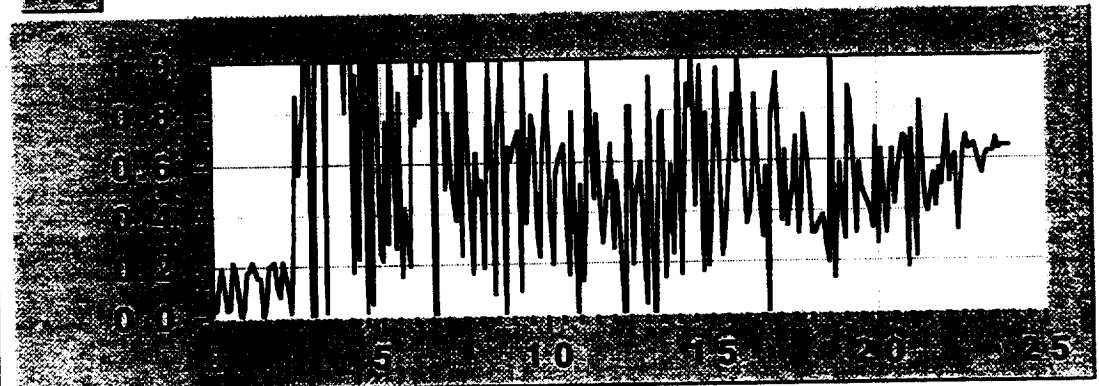
Drag Load
#1, lb



Time, sec

Plot C

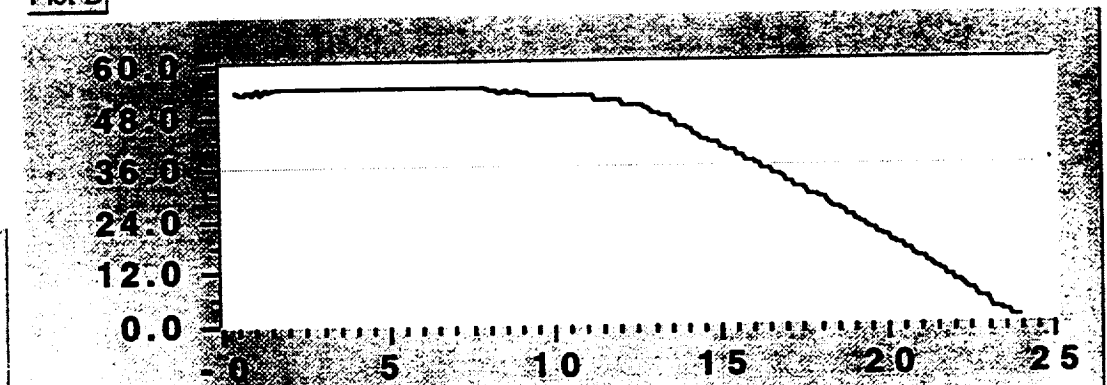
Drag
Friction
Coefficient



Time, sec

Plot D

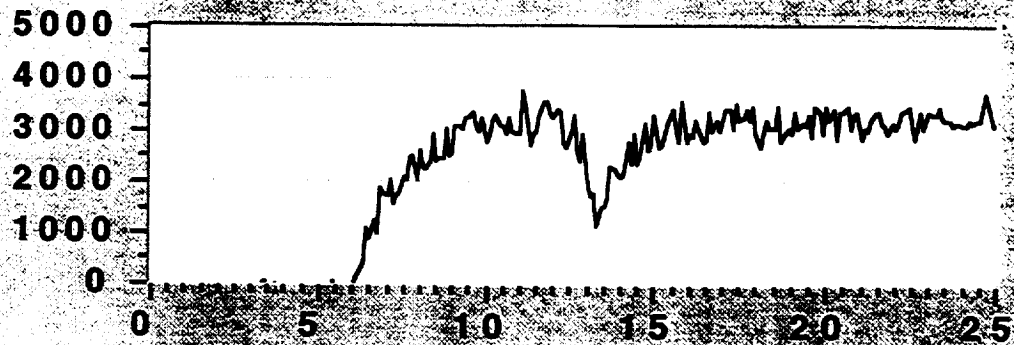
5th Wheel
Velocity,
mph



Time, sec

Run03

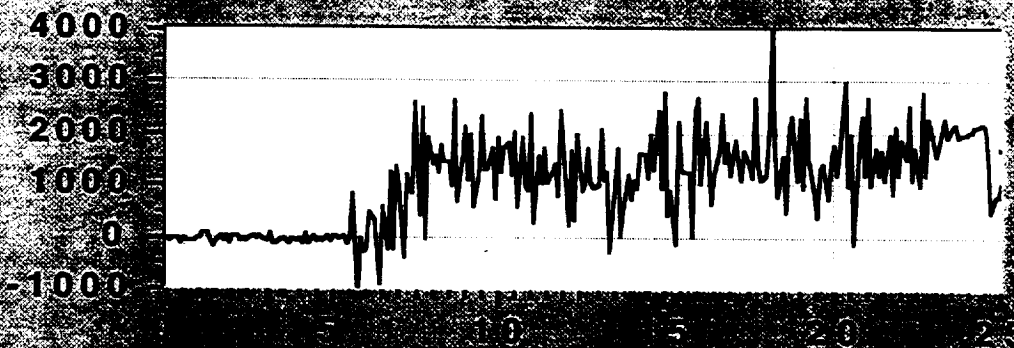
Plot A



Vertical
Load, lb

Plot B

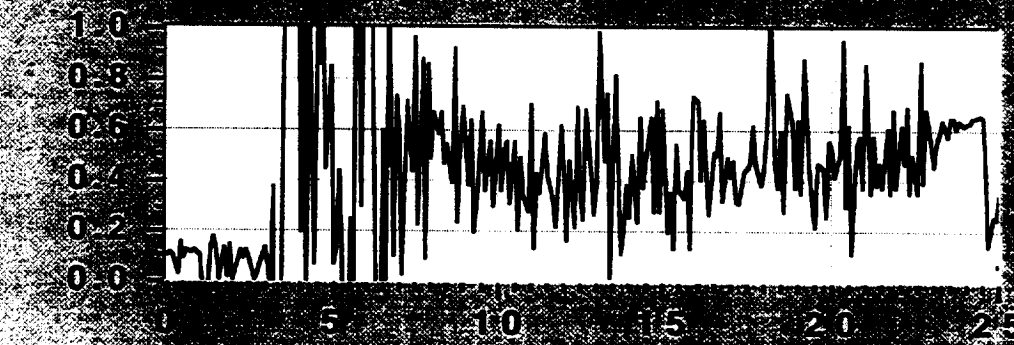
Time, sec



Drag Load
#1, lb

Plot C

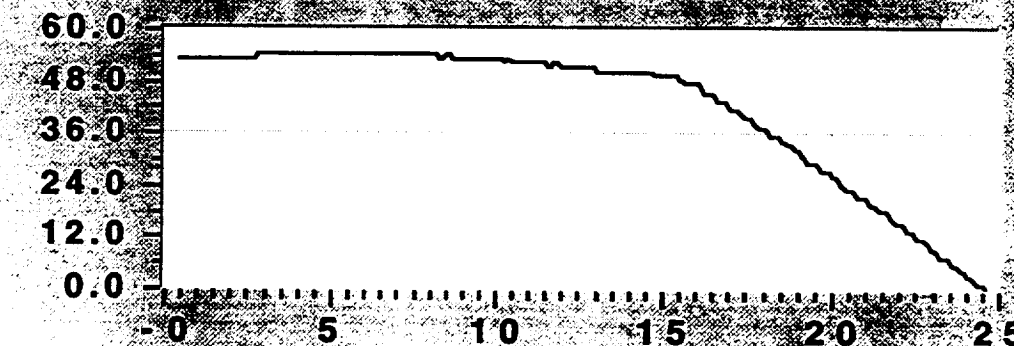
Time, sec



Drag
Friction
Coefficient

Plot D

Time, sec



5th Wheel
Velocity,
mph

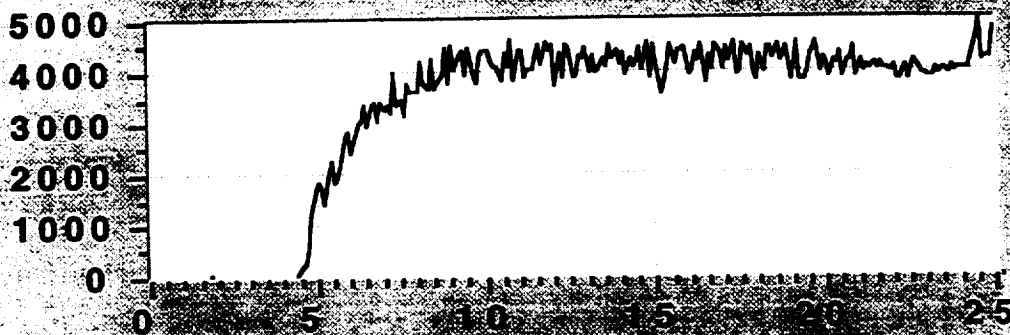
Time, sec

Run04

Plot A

Return

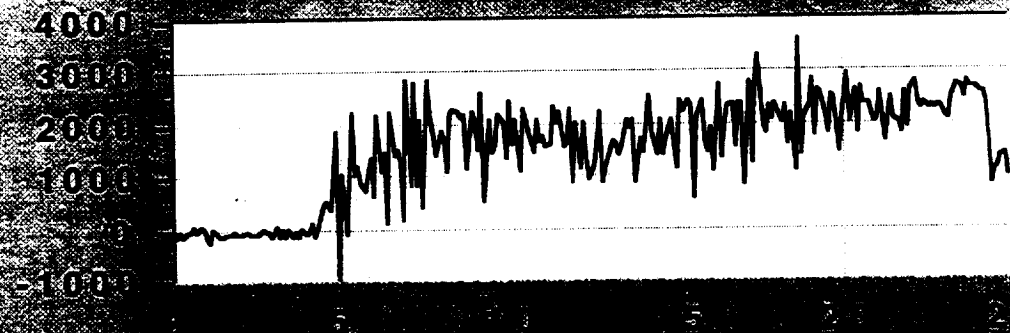
Vertical
Load, lb



Plot B

Time, sec

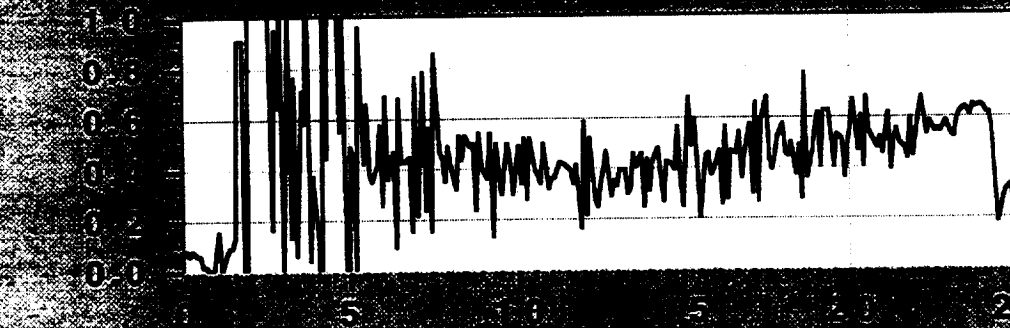
Drag Load
#1, lb



Plot C

Time, sec

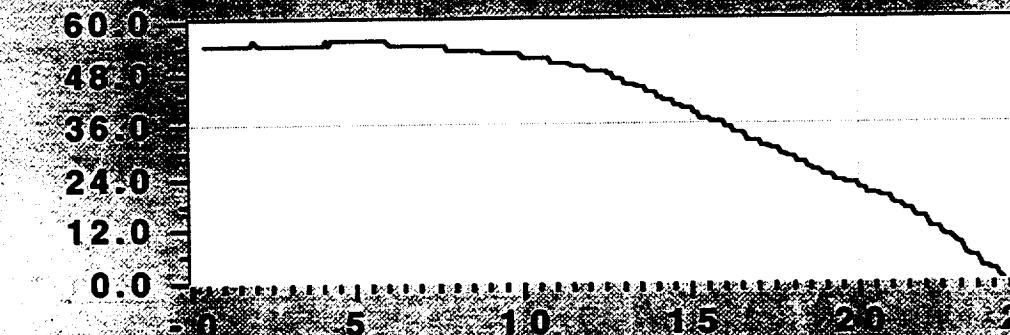
Drag
Friction
Coefficient



Plot D

Time, sec

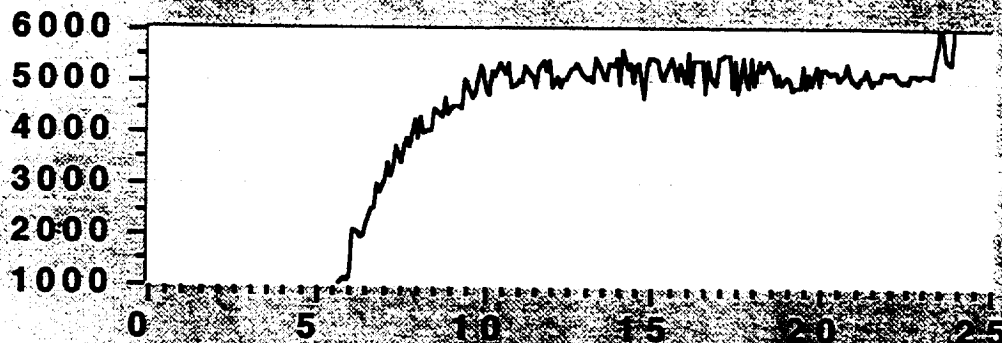
5th Wheel
Velocity,
mph



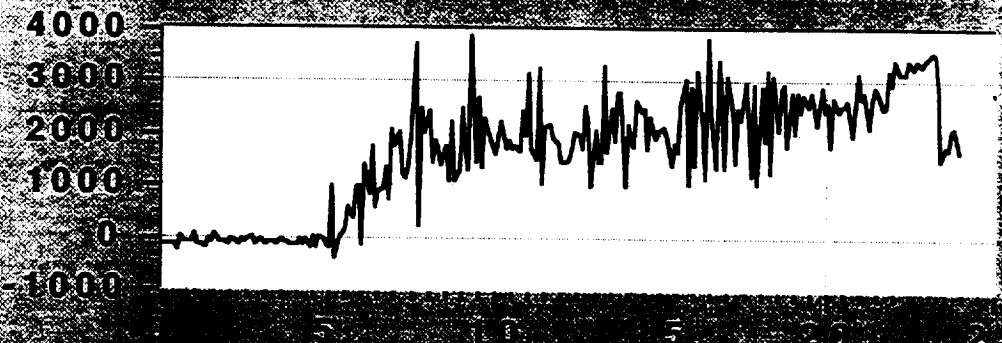
Time, sec

Run05

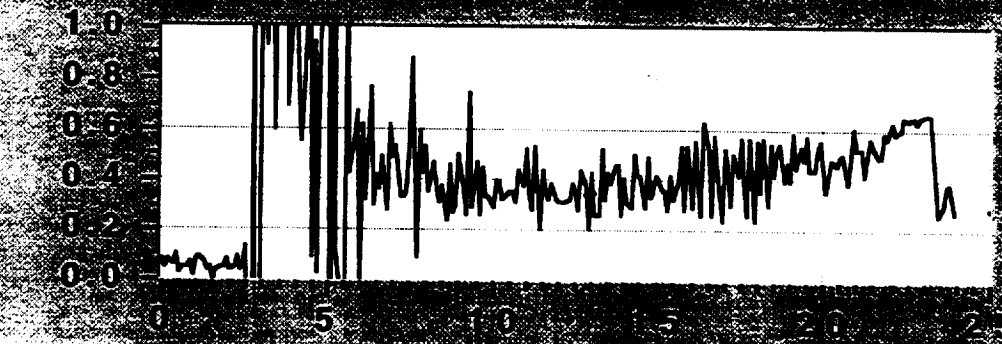
Plot A



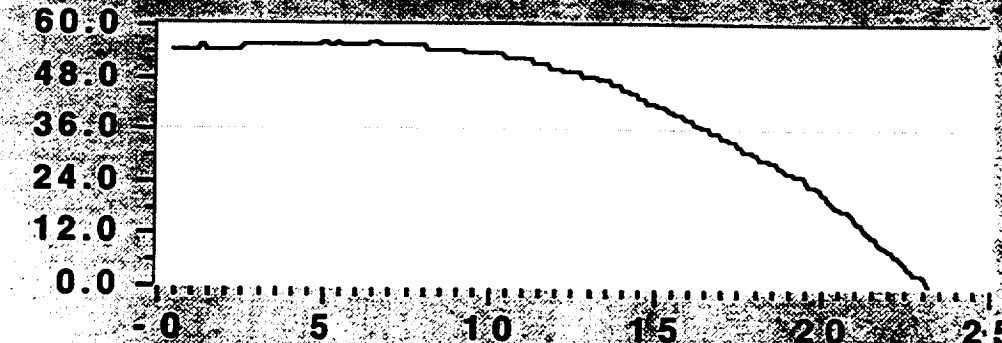
Plot B



Plot C



Plot D

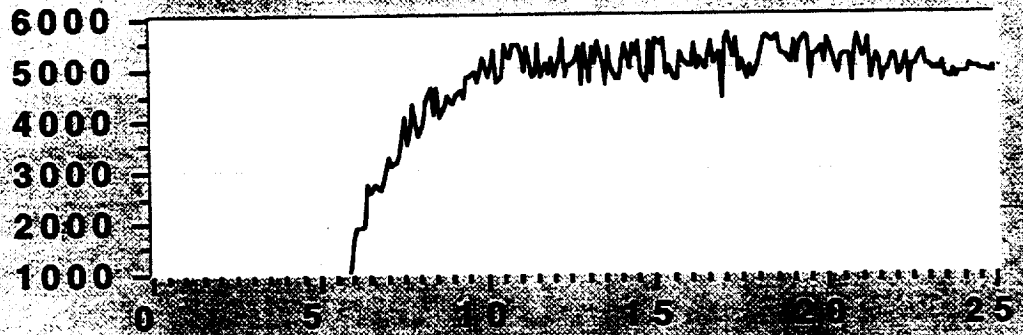


Run06

Plot A

Return

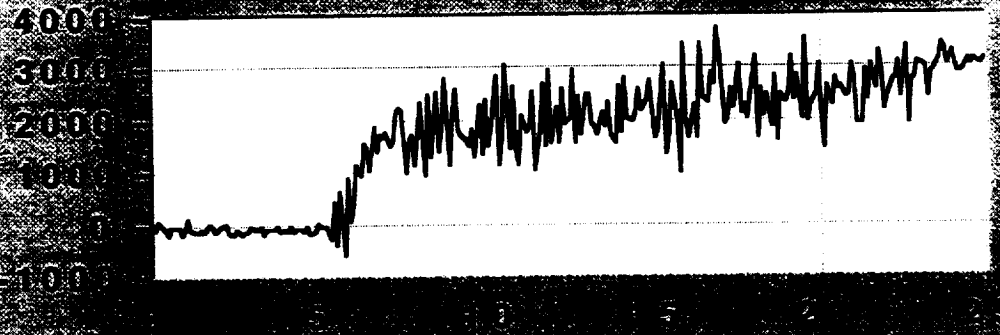
Vertical
Load, lb



Plot B

Time, sec

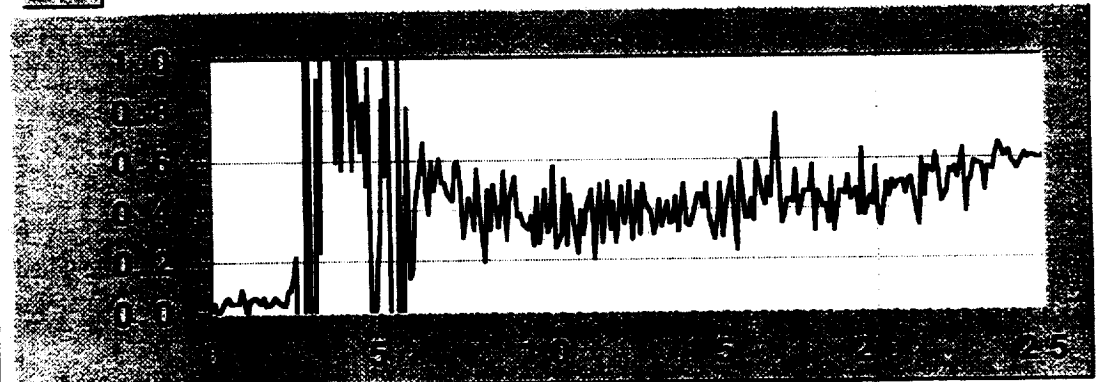
Drag Load
#1, lb



Plot C

Time, sec

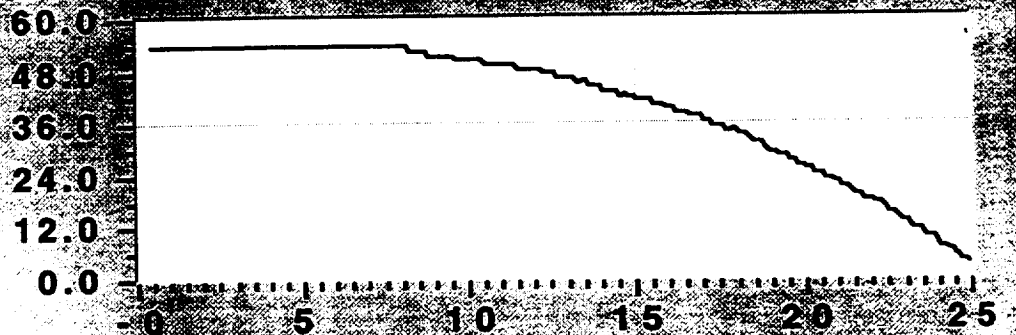
Drag
Friction
Coefficient



Plot D

Time, sec

5th Wheel
Velocity,
mph



Time, sec

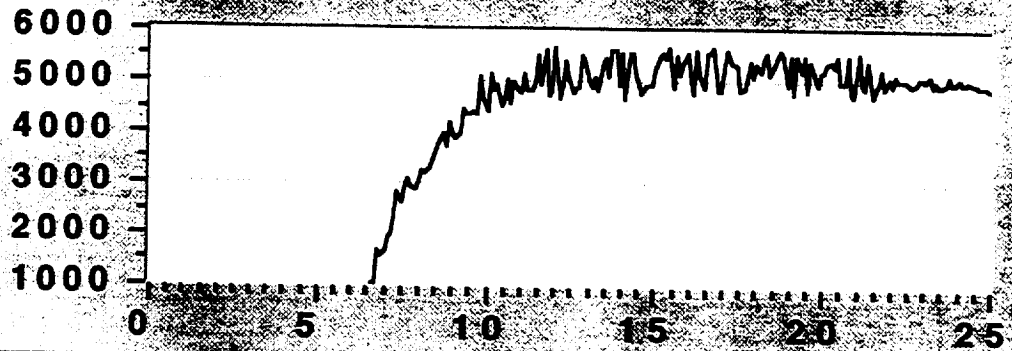


Return

Vertical
Load, lb

Plot A

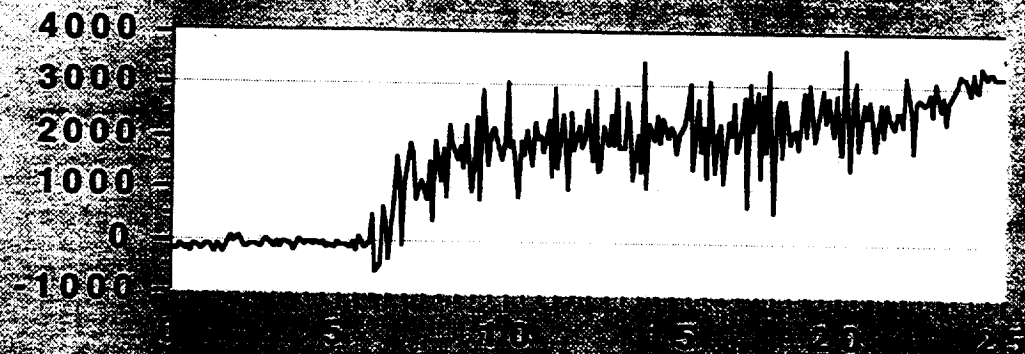
Run07



Plot B

Time, sec

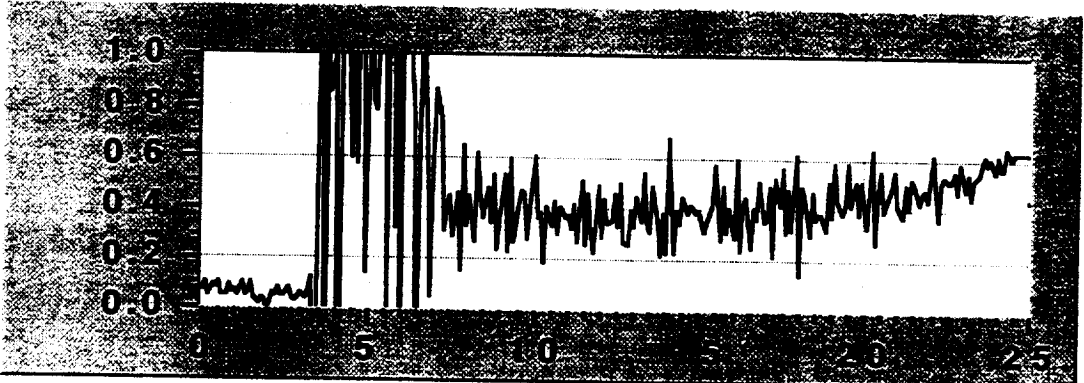
Drag Load
#1, lb



Plot C

Time, sec

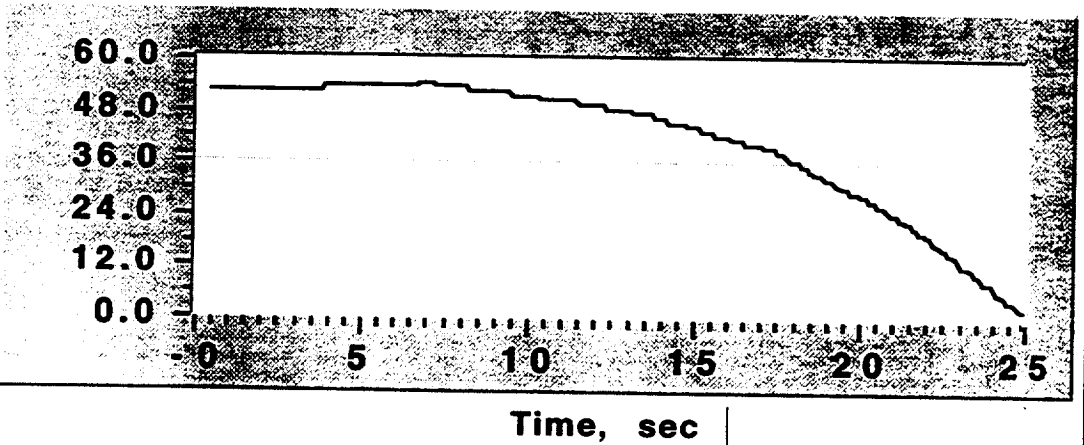
Drag
Friction
Coefficient



Plot D

Time, sec

5th Wheel
Velocity,
mph



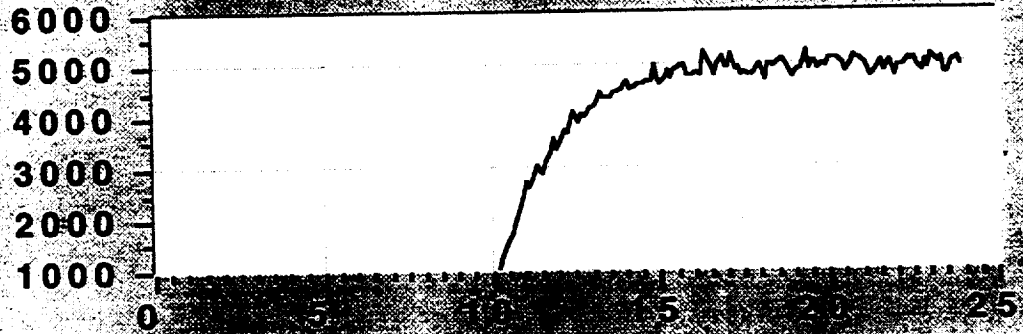
Run08

Plot A



Return

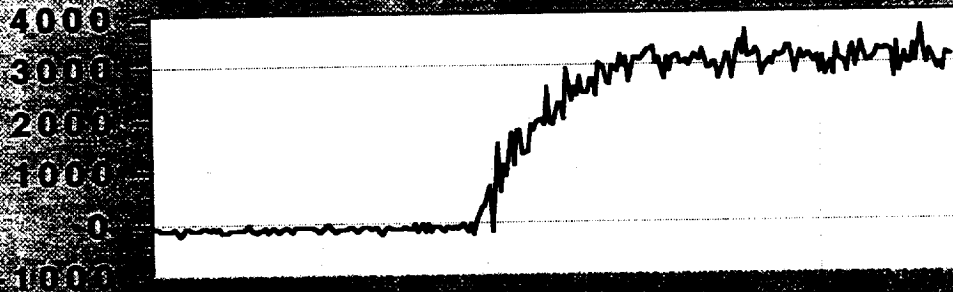
Vertical
Load, lb



Time, sec

Plot B

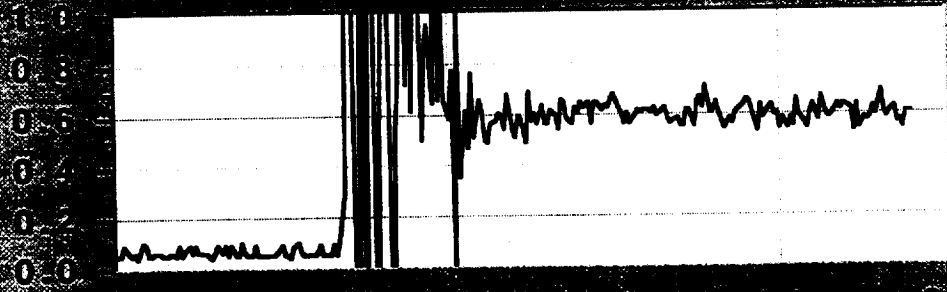
Drag Load
#1, lb



Time, sec

Plot C

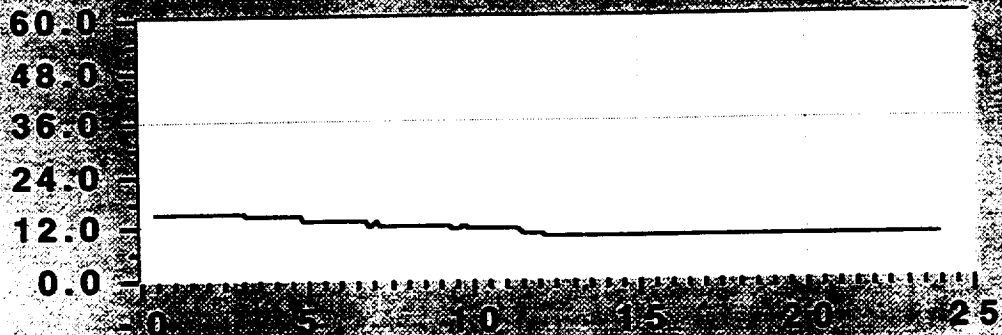
Drag
Friction
Coefficient



Time, sec

Plot D

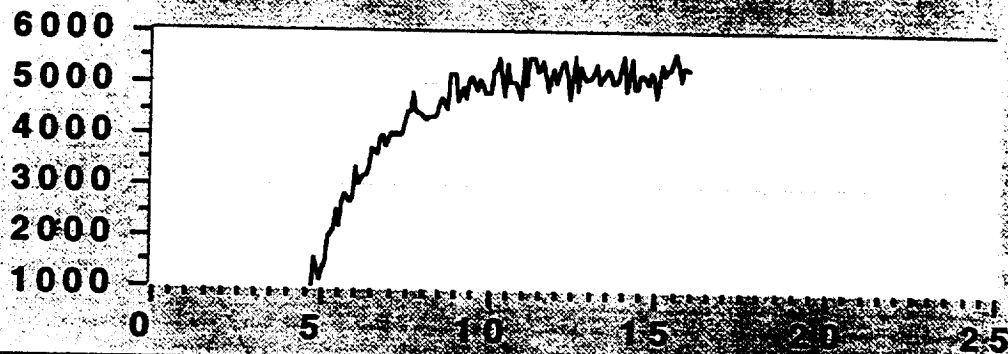
5th Wheel
Velocity,
mph



Time, sec

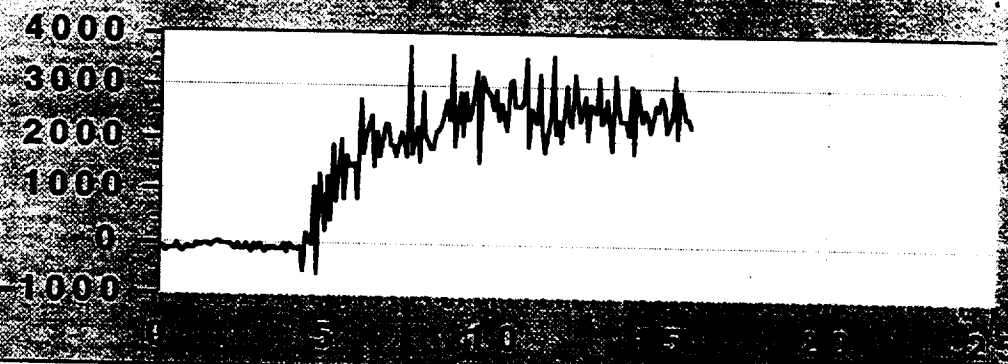
Run10

Plot A



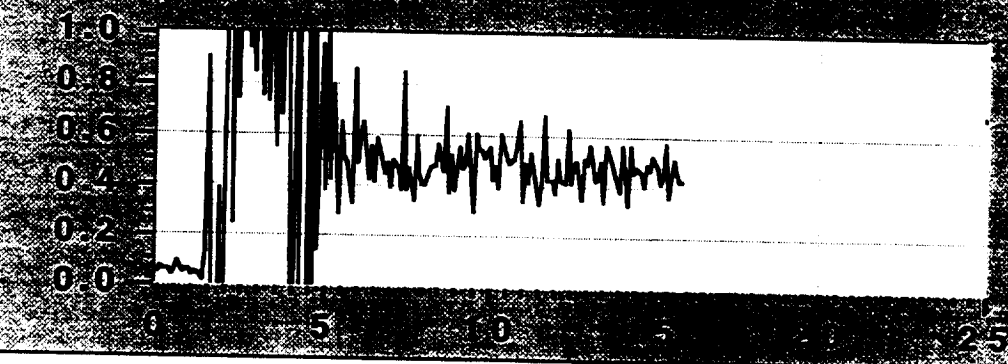
Plot B

Time, sec



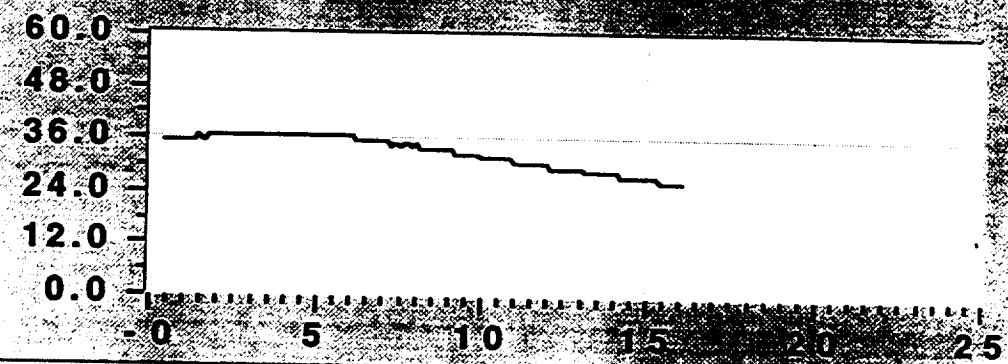
Plot C

Time, sec



Plot D

Time, sec



Time, sec

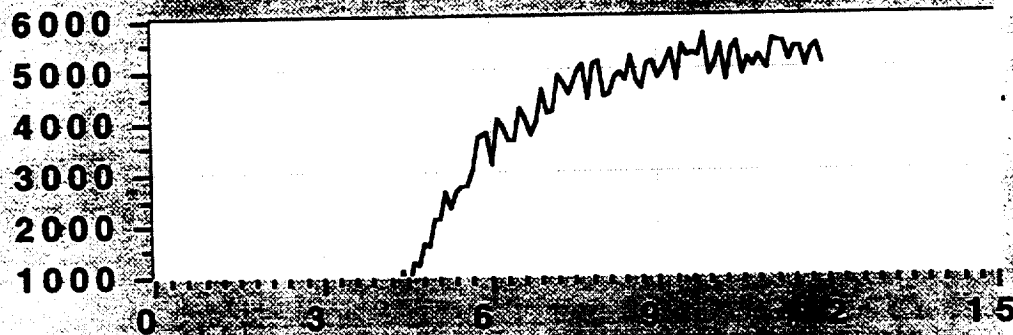
Run13



Return

Vertical
Load, lb

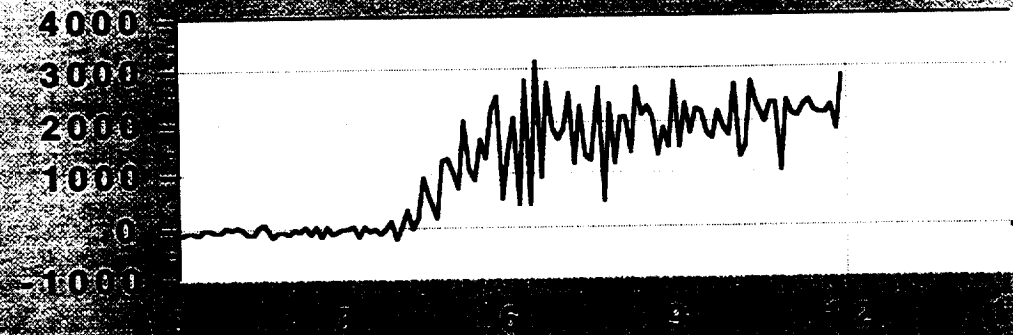
Plot A



Time, sec

Plot B

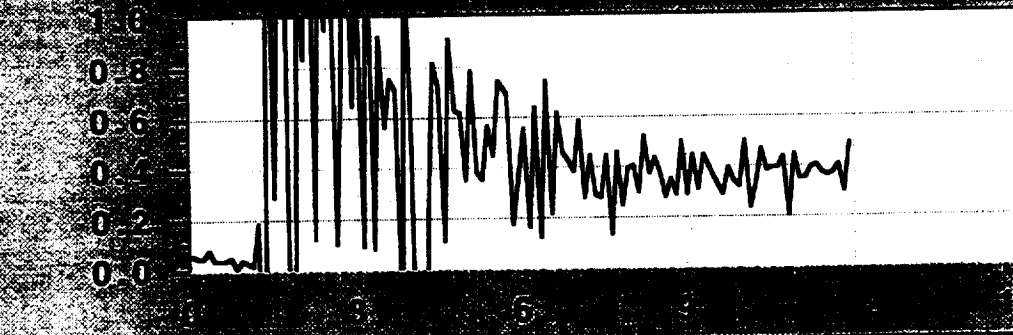
Drag Load
#1, lb



Time, sec

Plot C

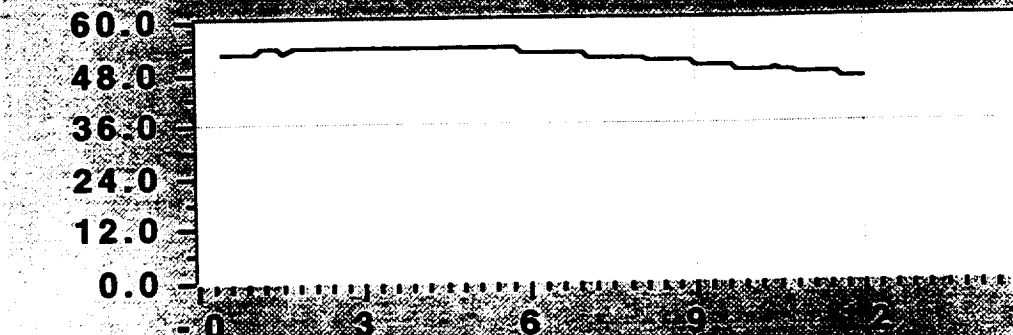
Drag
Friction
Coefficient



Time, sec

Plot D

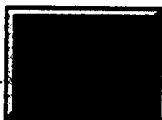
5th Wheel
Velocity,
mph



Time, sec

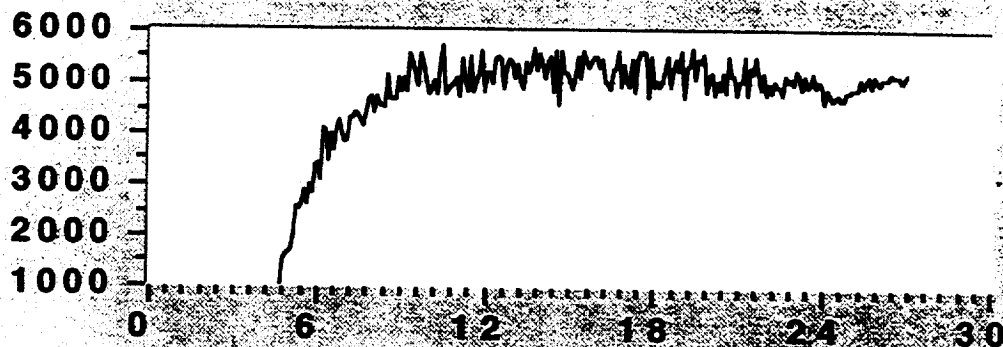
Run14

Plot A



Return

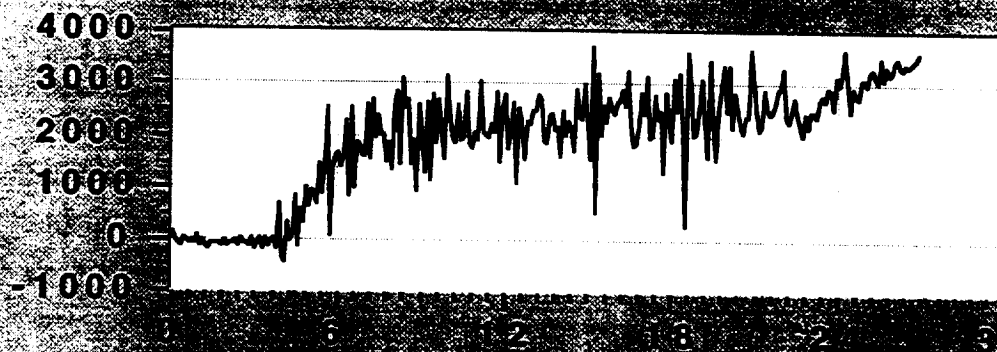
Vertical
Load, lb



Plot B

Time, sec

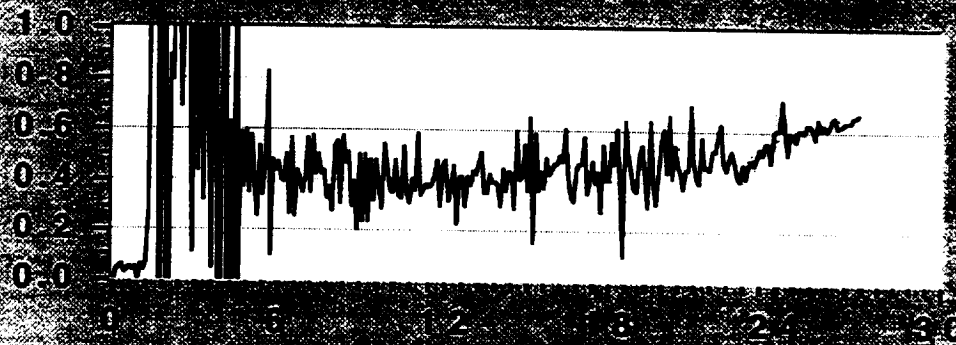
Drag Load
#1, lb



Plot C

Time, sec

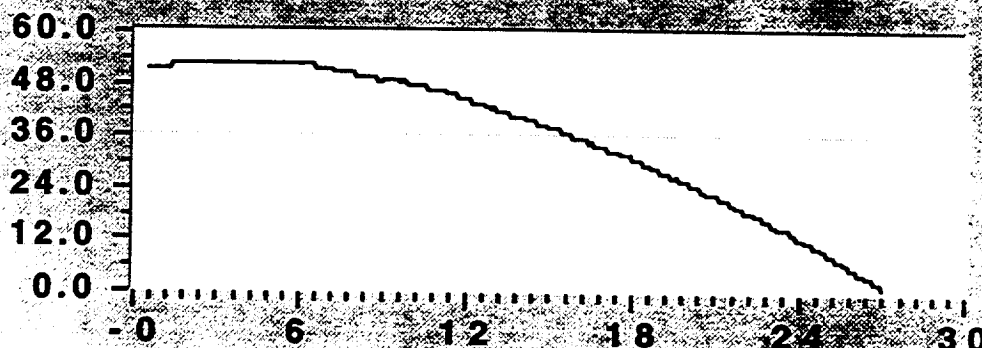
Drag
Friction
Coefficient



Plot D

Time, sec

5th Wheel
Velocity,
mph



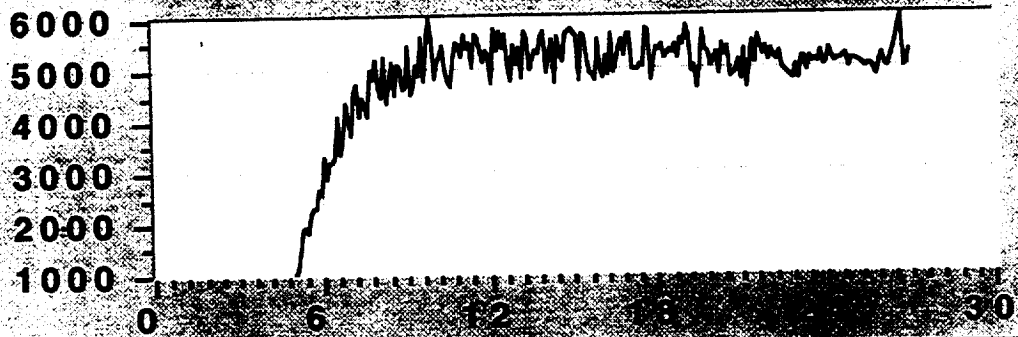
Time, sec

Run15

Plot A

Return

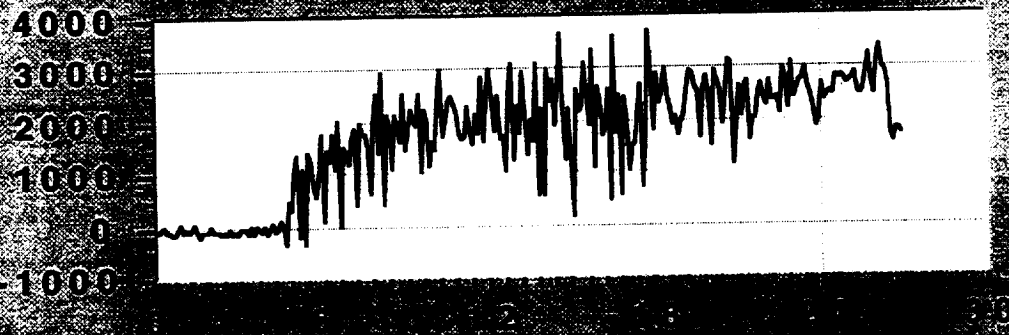
Vertical
Load, lb



Plot B

Time, sec

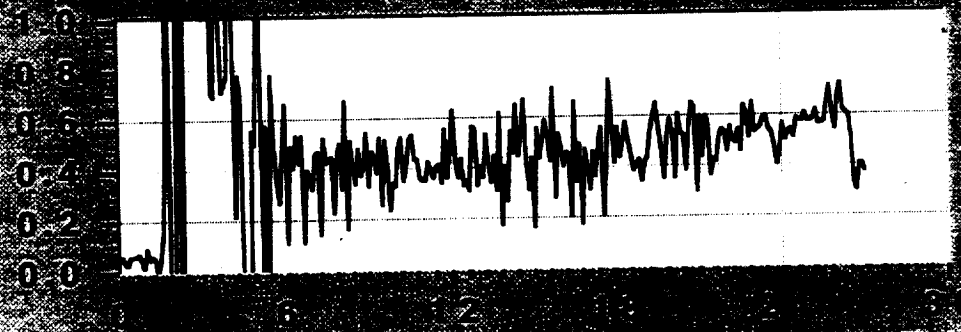
Drag Load
#1, lb



Plot C

Time, sec

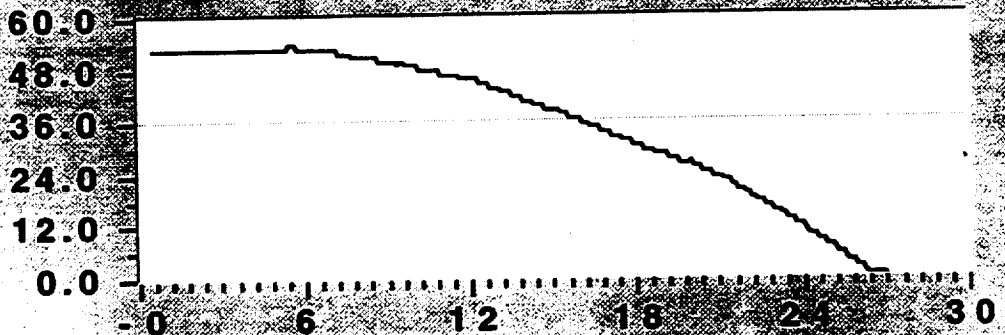
Drag
Friction
Coefficient



Plot D

Time, sec

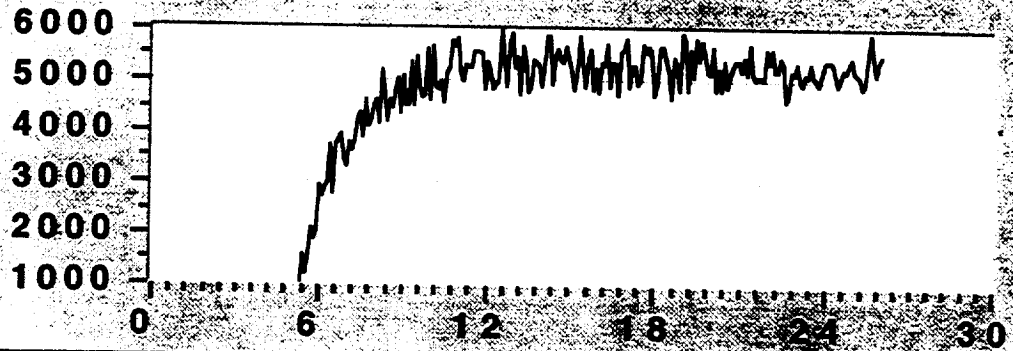
5th Wheel
Velocity,
mph



Time, sec

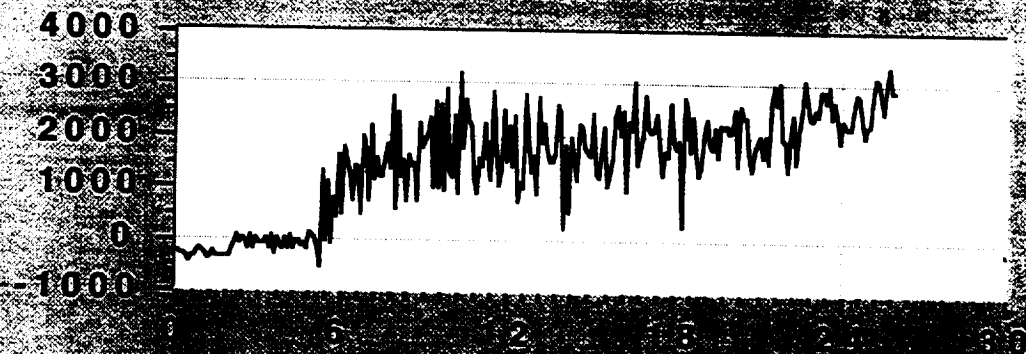
Run16

Plot A



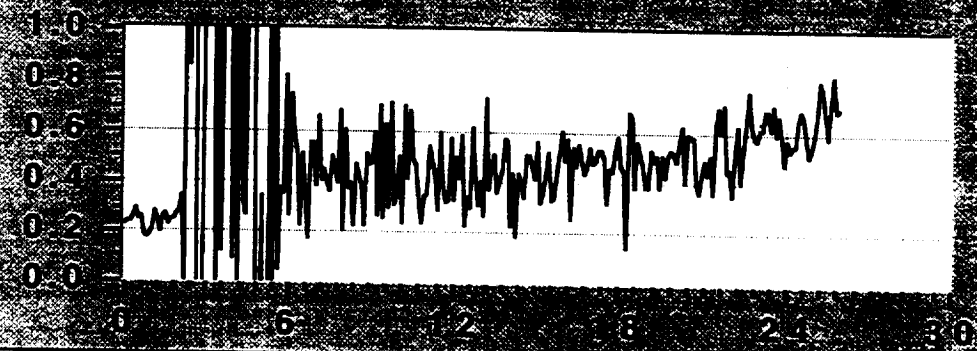
Plot B

Time, sec



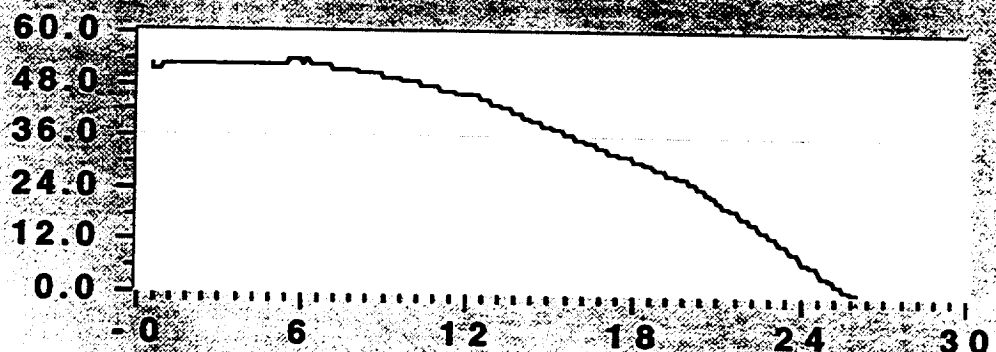
Plot C

Time, sec



Plot D

Time, sec



Time, sec

Return

Vertical
Load, lb

Drag Load
#1, lb

Drag
Friction
Coefficient

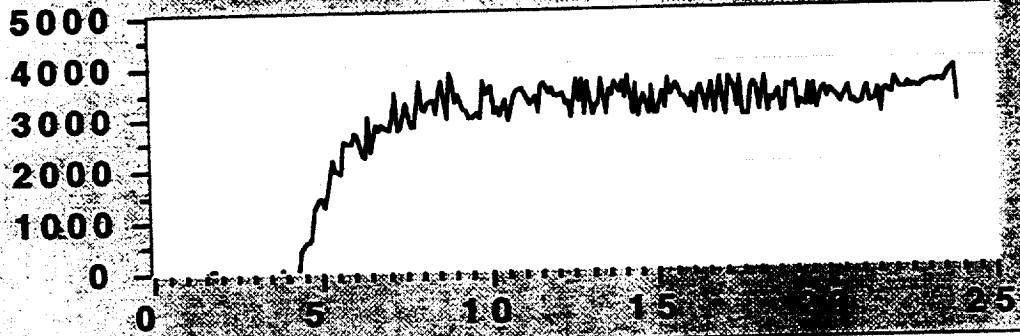
5th Wheel
Velocity,
mph

Run17

Plot A

Return

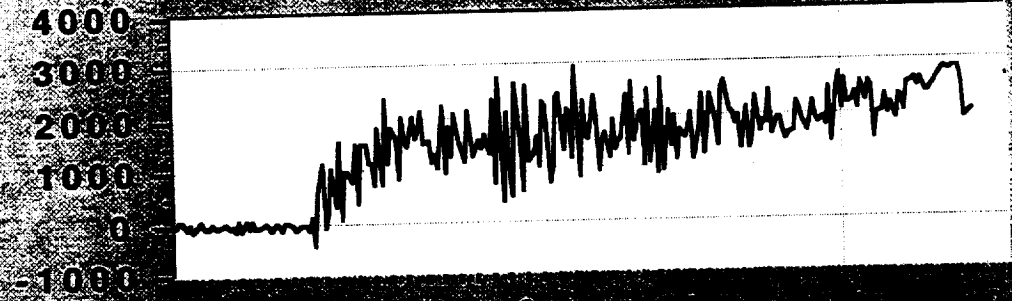
Vertical
Load, lb



Plot B

Time, sec

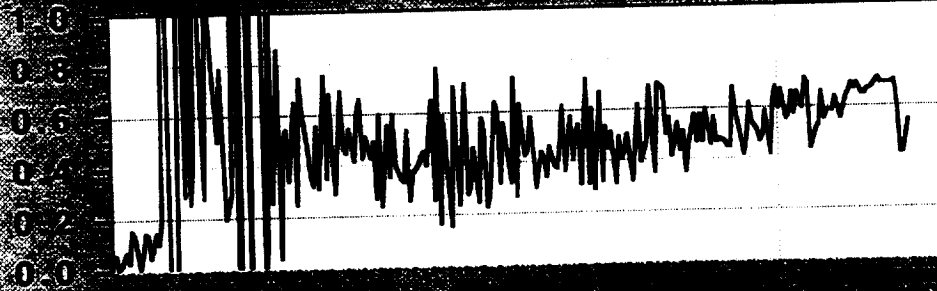
Drag Load
#1, lb



Plot C

Time, sec

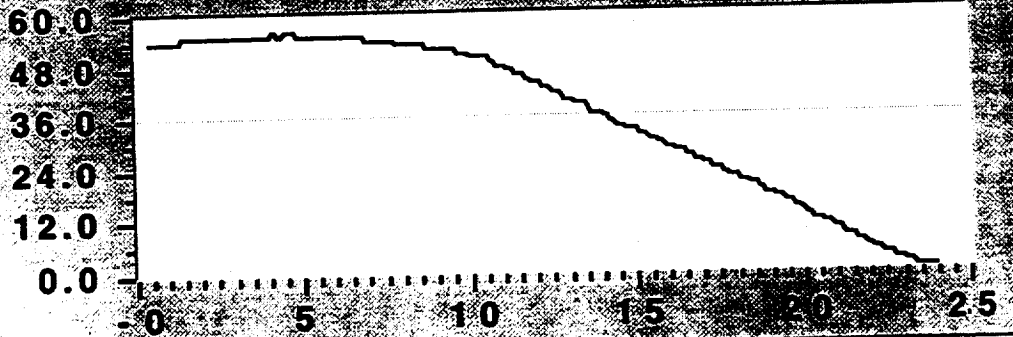
Drag
Friction
Coefficient



Plot D

Time, sec

5th Wheel
Velocity,
mph



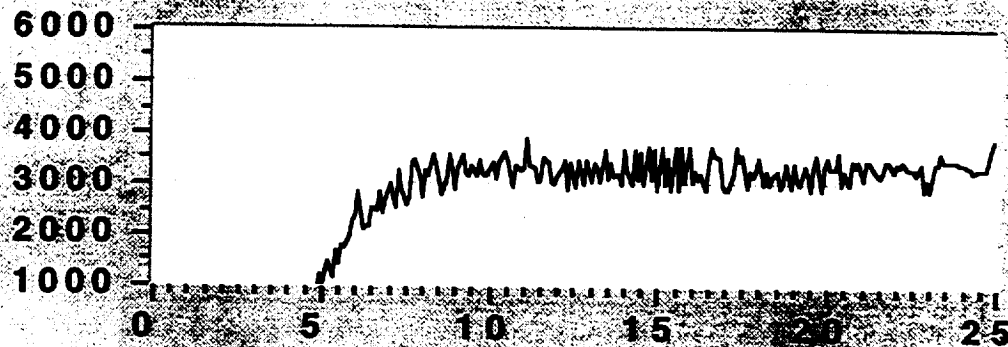
Time, sec

Run18

Plot A

Return

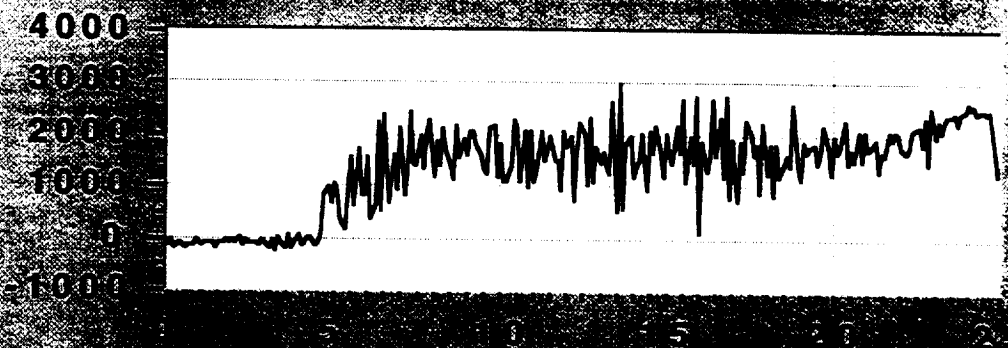
Vertical
Load, lb



Plot B

Time, sec

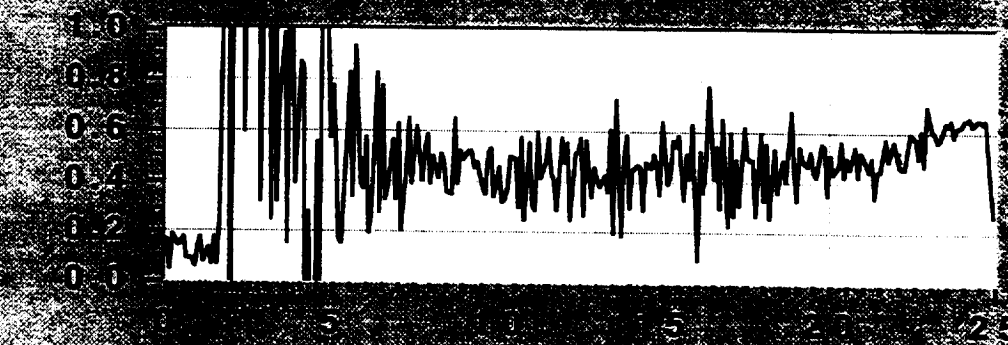
Drag Load
#1, lb



Plot C

Time, sec

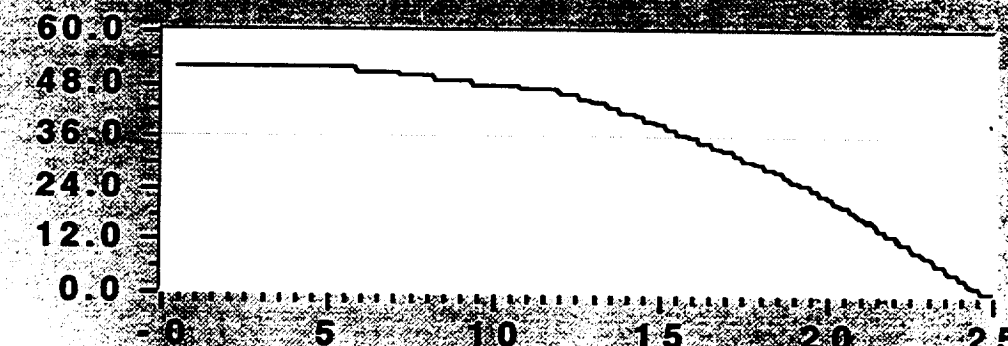
Drag
Friction
Coefficient



Plot D

Time, sec

5th Wheel
Velocity,
mph



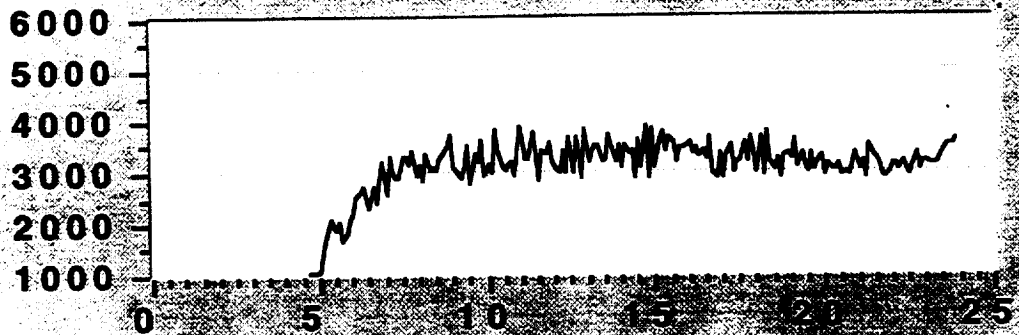
Time, sec

Run19

Plot A

Return

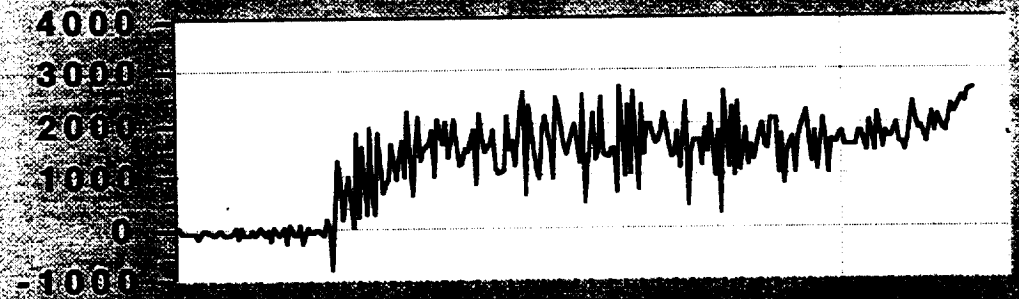
Vertical
Load, lb



Plot B

Time, sec

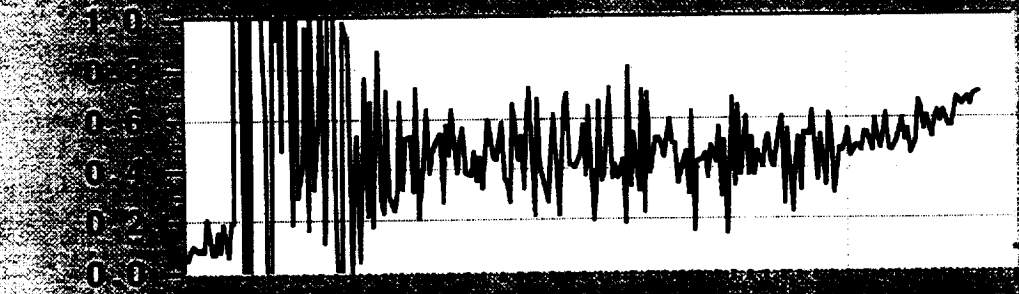
Drag Load
#1, lb



Plot C

Time, sec

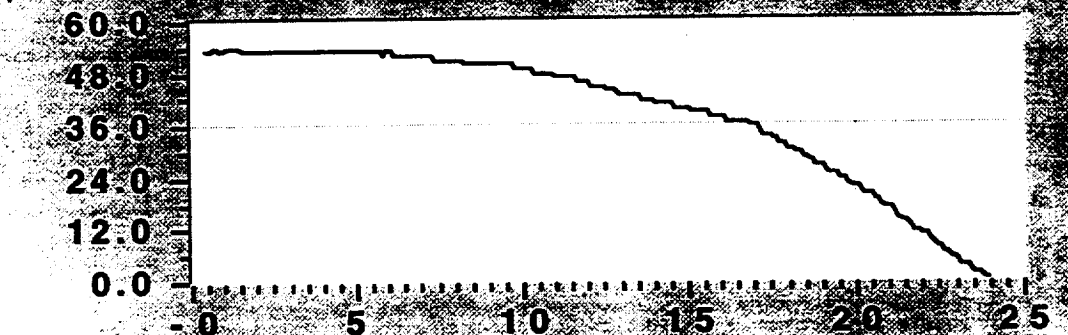
Drag
Friction
Coefficient



Plot D

Time, sec

5th Wheel
Velocity,
mph



Time, sec

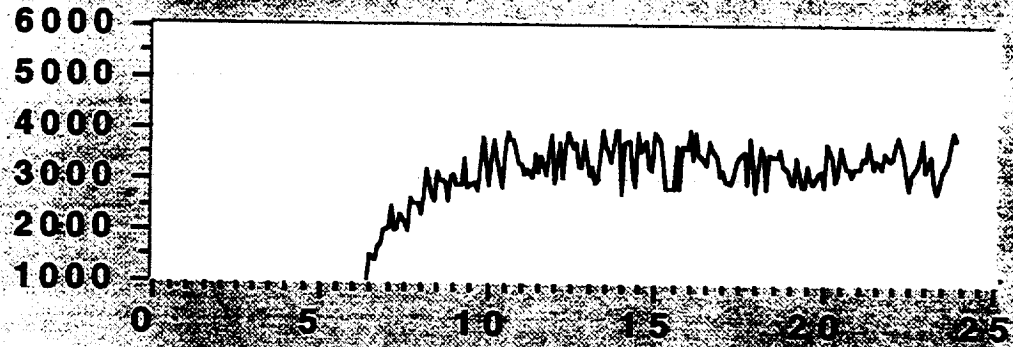
Run20

Plot A



Return

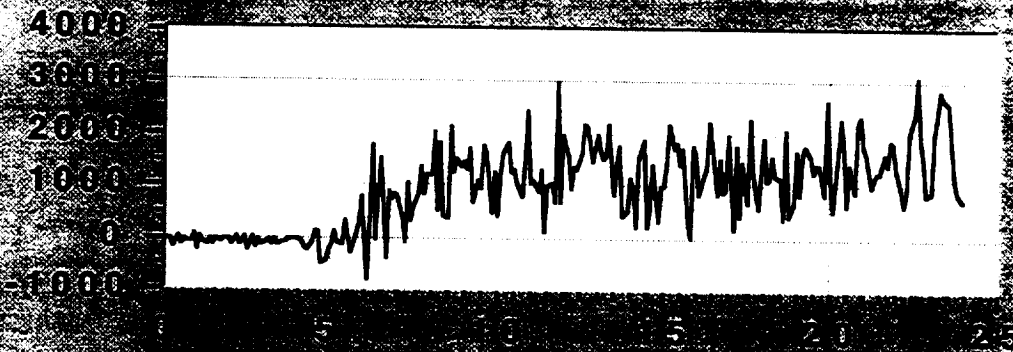
Vertical
Load, lb



Plot B

Time, sec

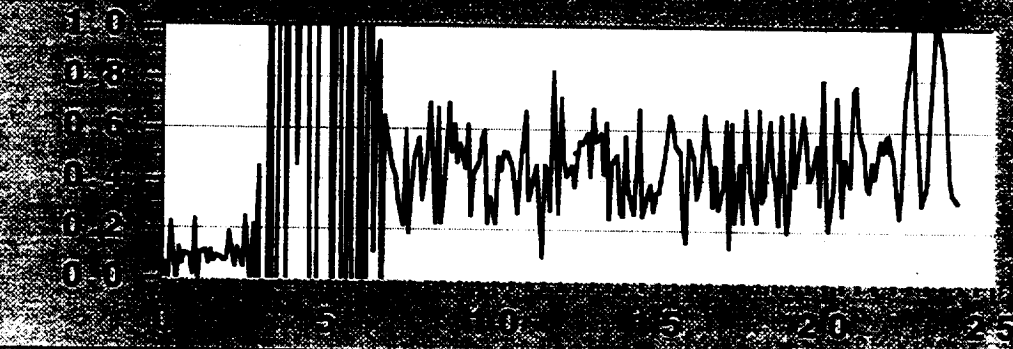
Drag Load
#1, lb



Plot C

Time, sec

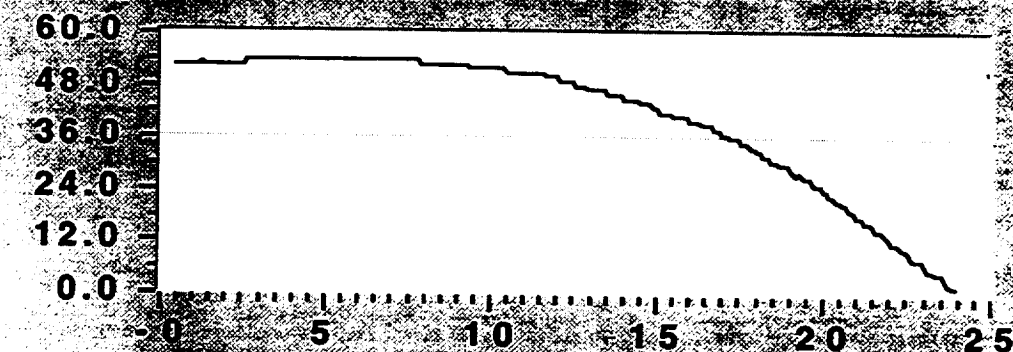
Drag
Friction
Coefficient



Plot D

Time, sec

5th Wheel
Velocity,
mph



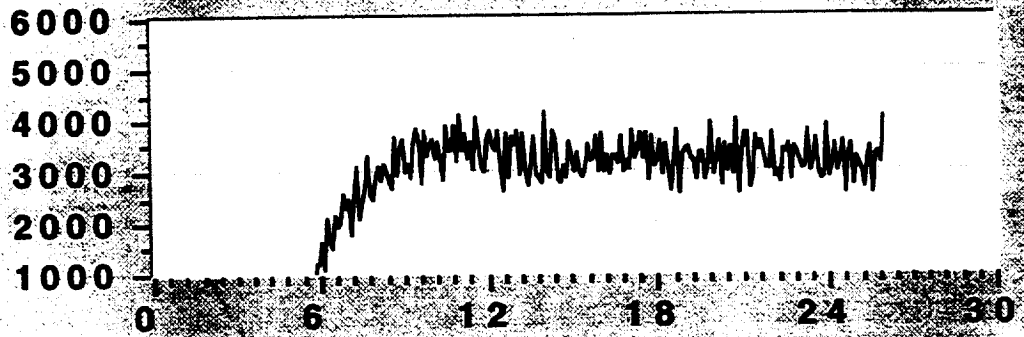
Time, sec

Run21

Plot A

Return

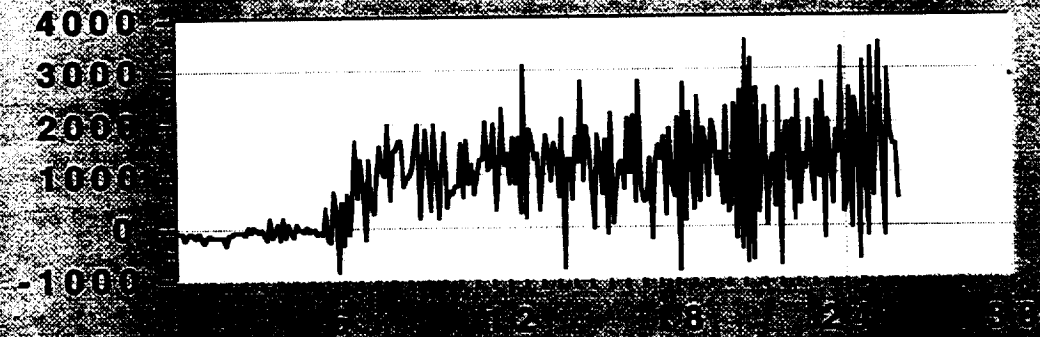
Vertical
Load, lb



Plot B

Time, sec

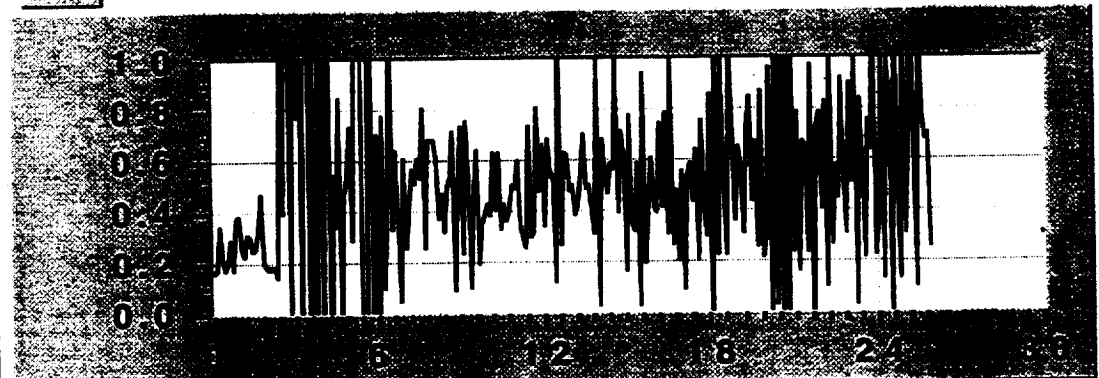
Drag Load
#1, lb



Plot C

Time, sec

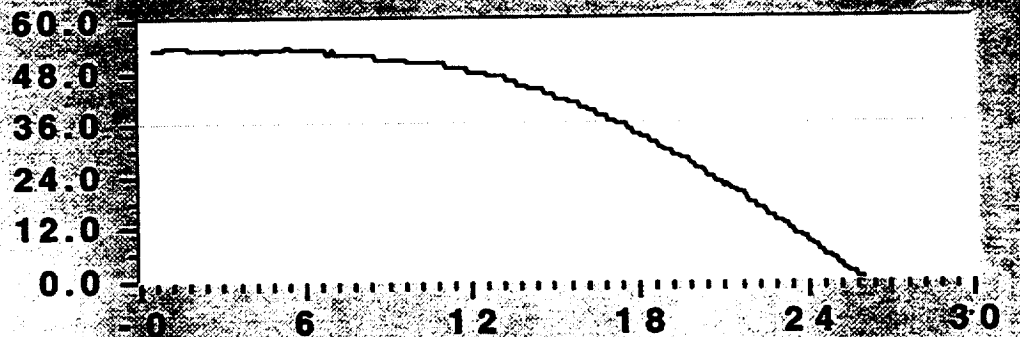
Drag
Friction
Coefficient



Plot D

Time, sec

5th Wheel
Velocity,
mph



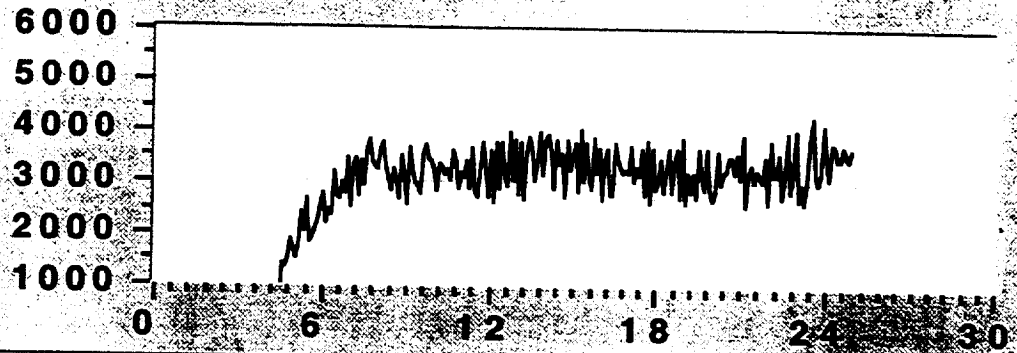
Time, sec

Run22

Plot A

Return

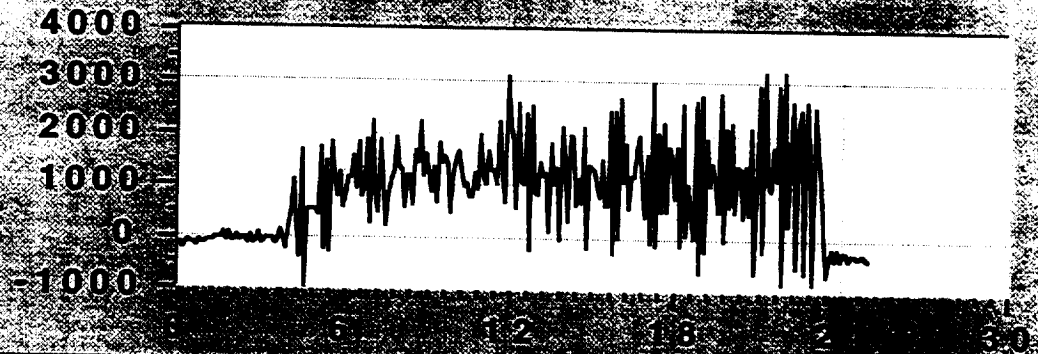
Vertical
Load, lb



Plot B

Time, sec

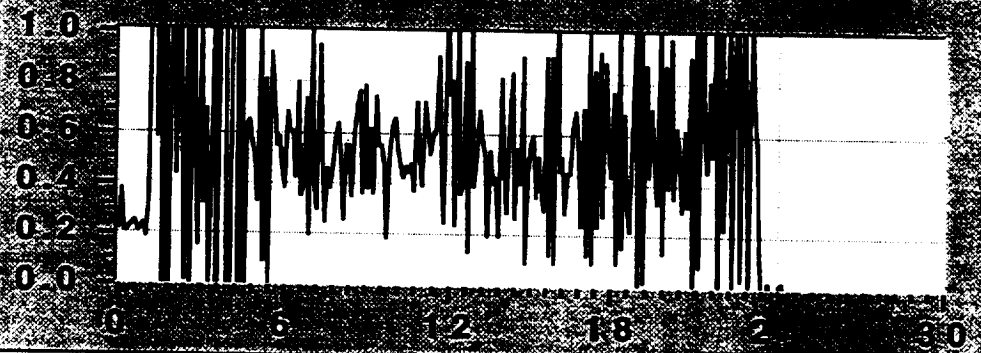
Drag Load
#1, lb



Plot C

Time, sec

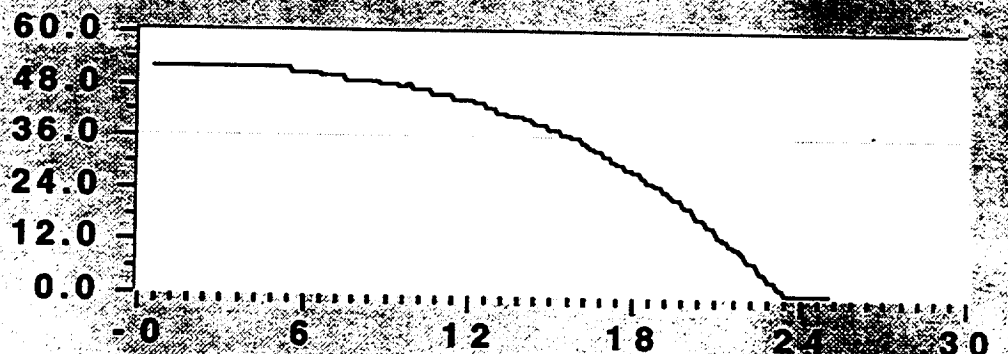
Drag
Friction
Coefficient



Plot D

Time, sec

5th Wheel
Velocity,
mph



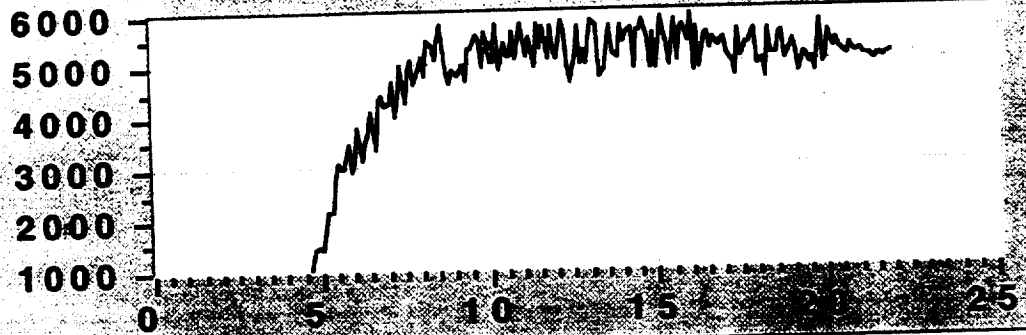
Time, sec

Run27

Plot A

Return

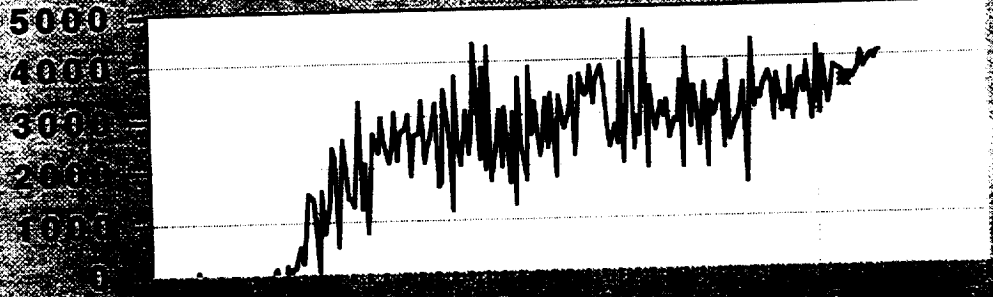
Vertical
Load, lb



Time, sec

Plot B

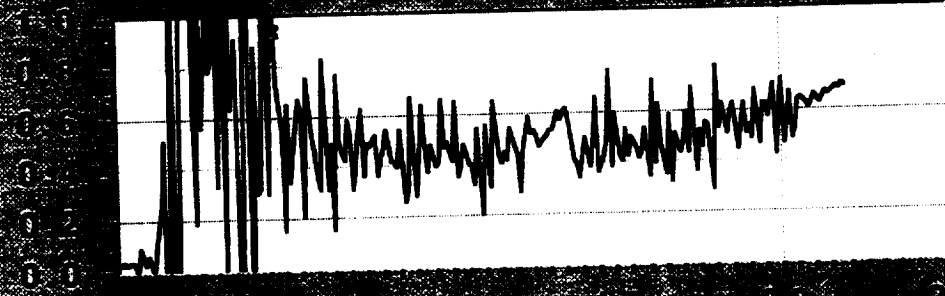
Drag Load
#1, lb



Time, sec

Plot C

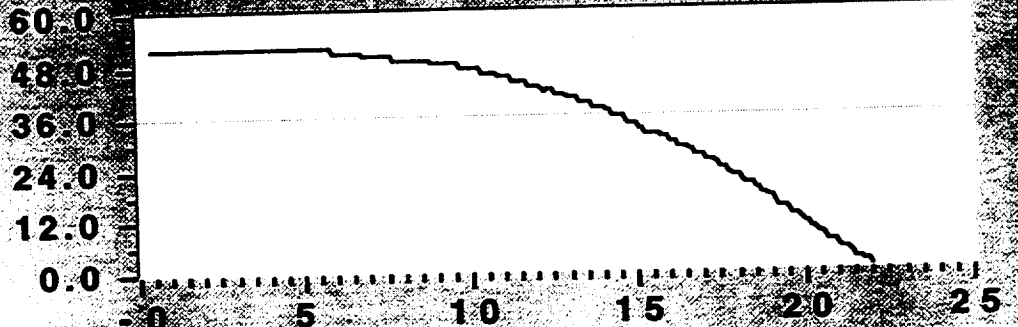
Drag
Friction
Coefficient



Time, sec

Plot D

5th Wheel
Velocity,
mph



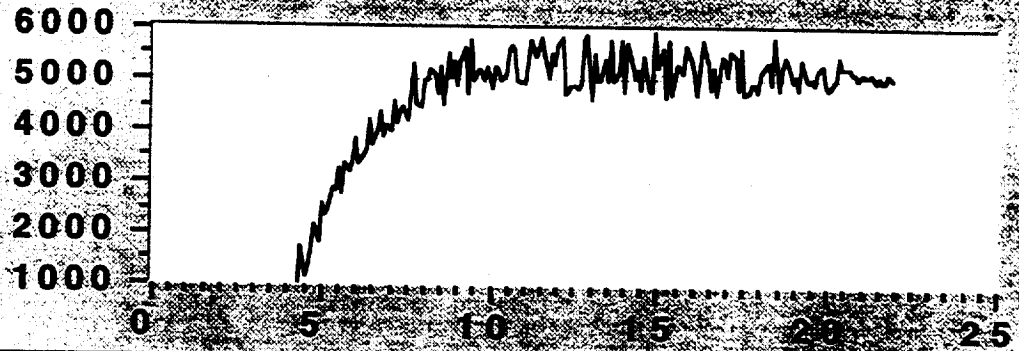
Time, sec

Run28

Plot A

Return

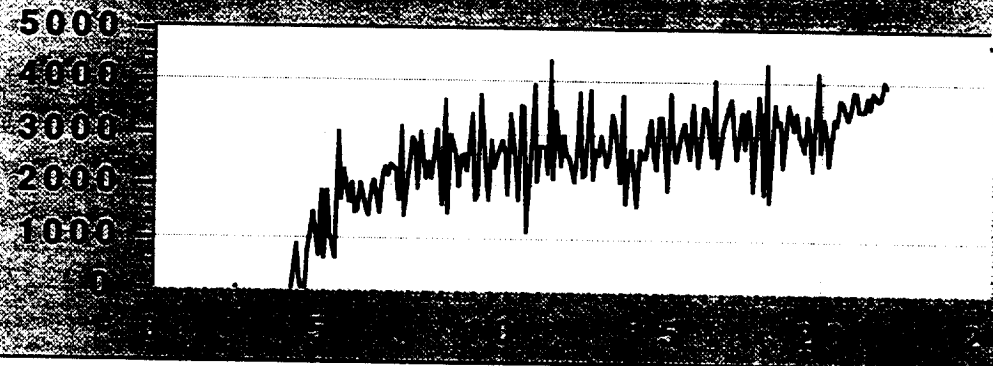
Vertical
Load, lb



Plot B

Time, sec

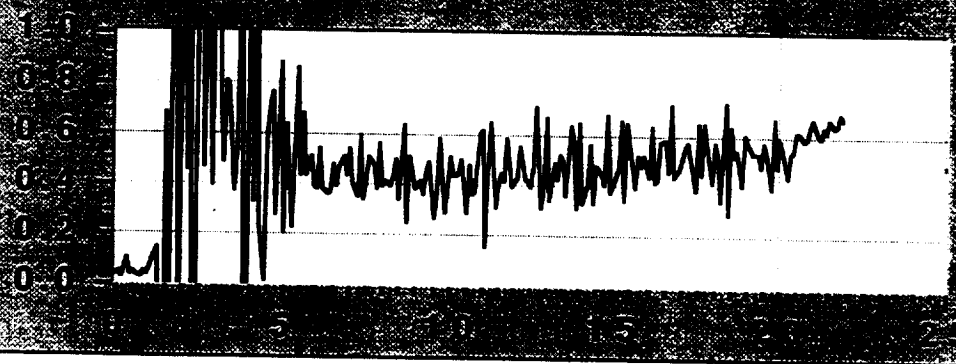
Drag Load
#1, lb



Plot C

Time, sec

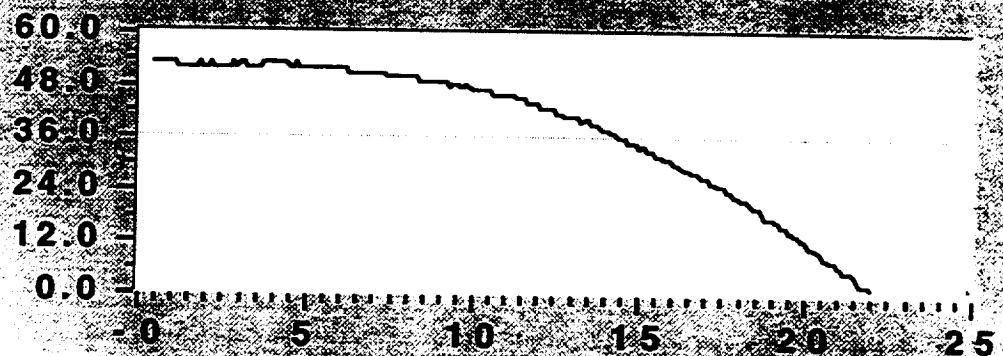
Drag
Friction
Coefficient



Plot D

Time, sec

5th Wheel
Velocity,
mph



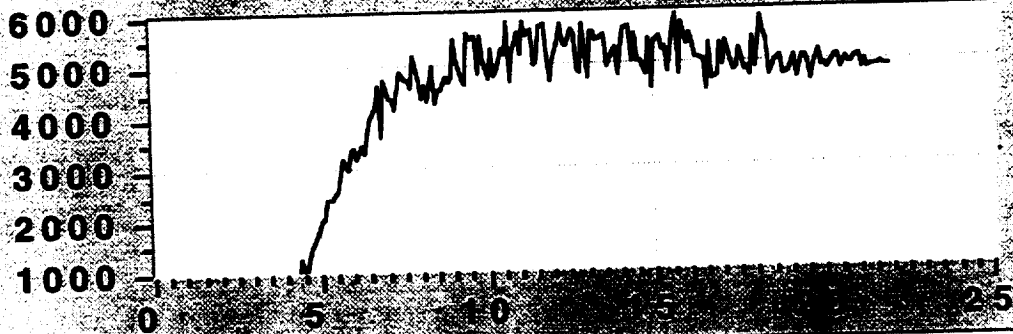
Time, sec

Run29

Plot A

Return

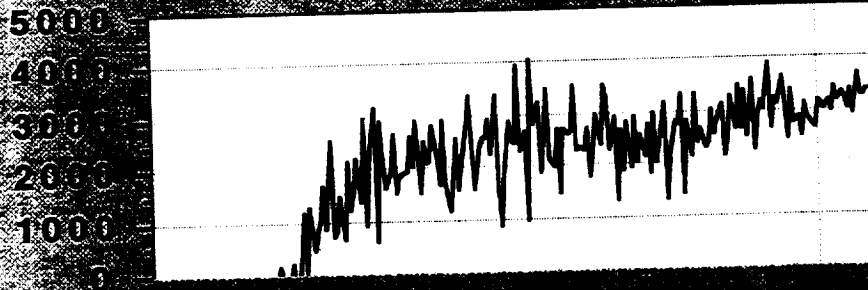
Vertical
Load, lb



Time, sec

Plot B

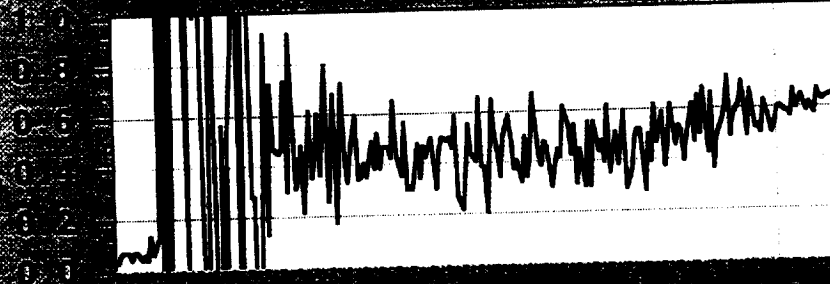
Drag Load
#1, lb



Time, sec

Plot C

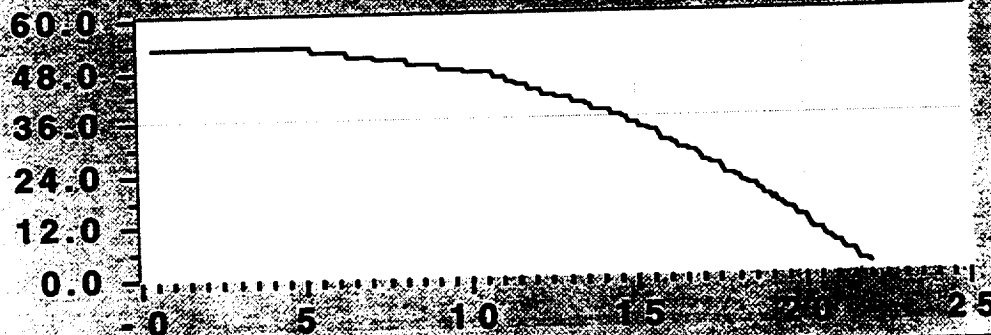
Drag
Friction
Coefficient



Time, sec

Plot D

5th Wheel
Velocity,
mph



Time, sec

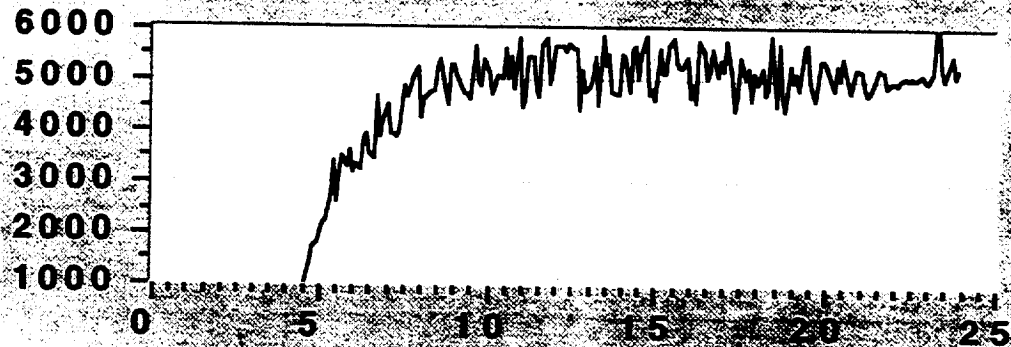
Run30

Plot A



Return

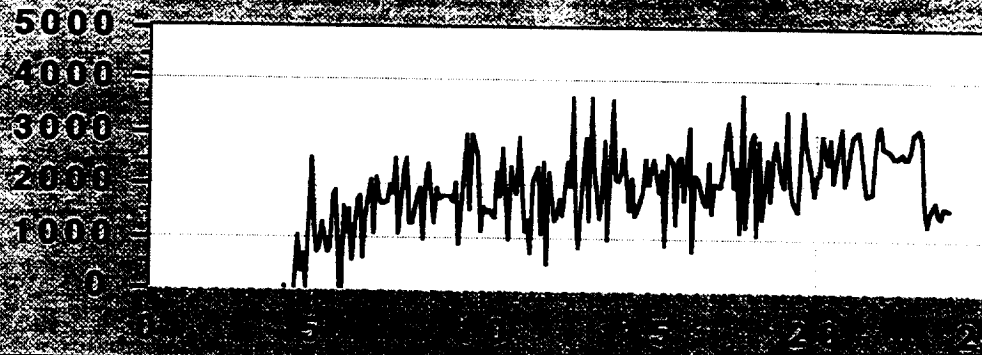
Vertical
Load, lb



Plot B

Time, sec

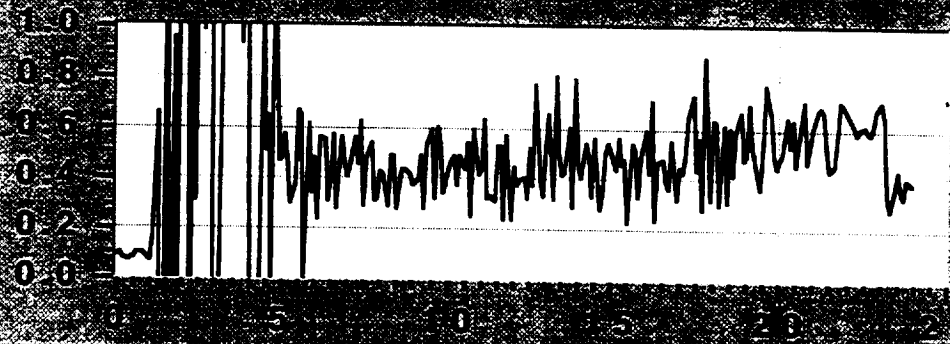
Drag Load
#1, lb



Plot C

Time, sec

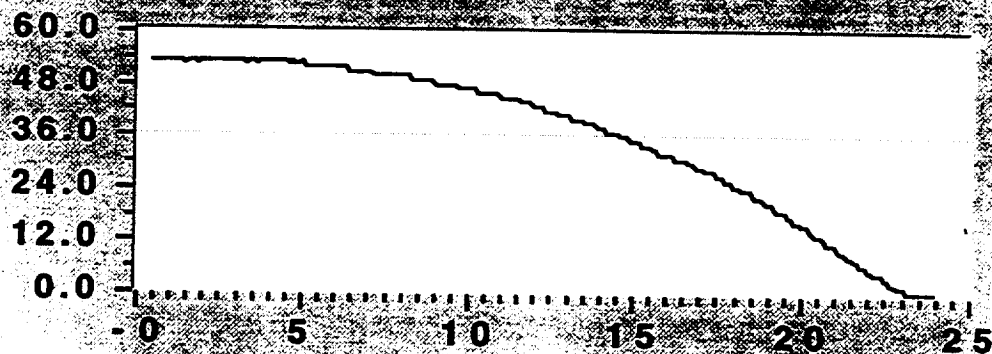
Drag
Friction
Coefficient



Plot D

Time, sec

5th Wheel
Velocity,
mph



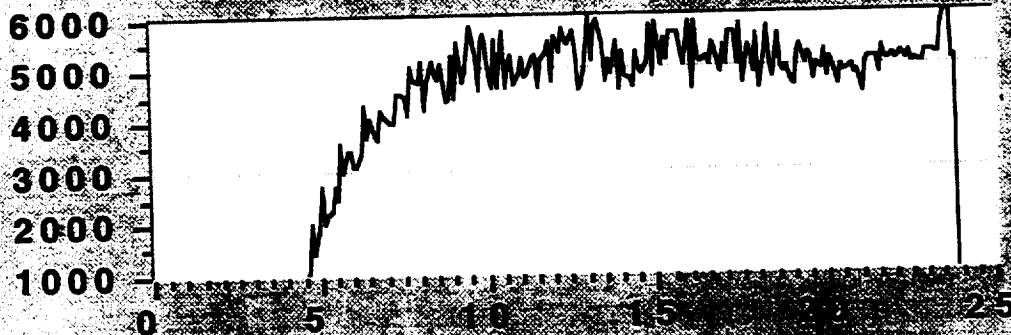
Time, sec

Run31

Plot A

Return

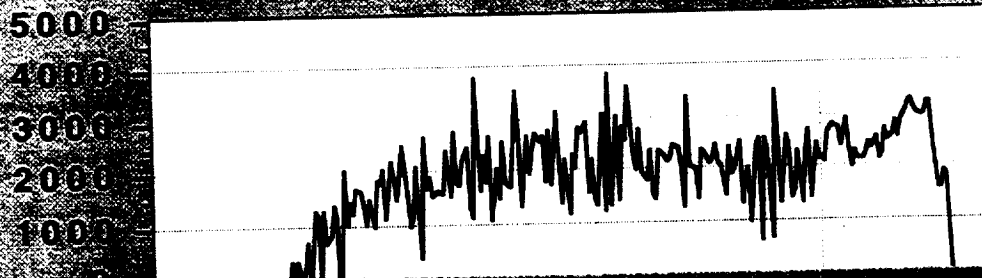
Vertical
Load, lb



Time, sec

Plot B

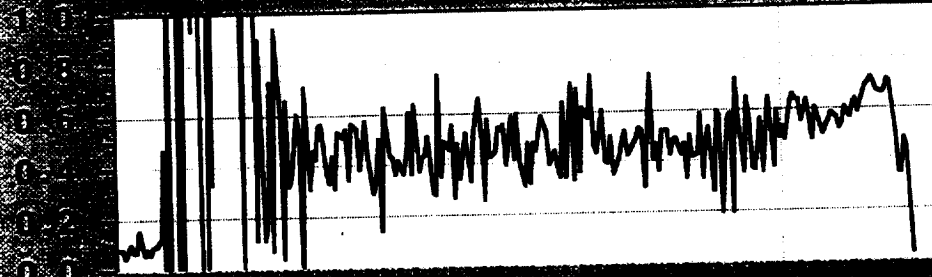
Drag Load
#1, lb



Time, sec

Plot C

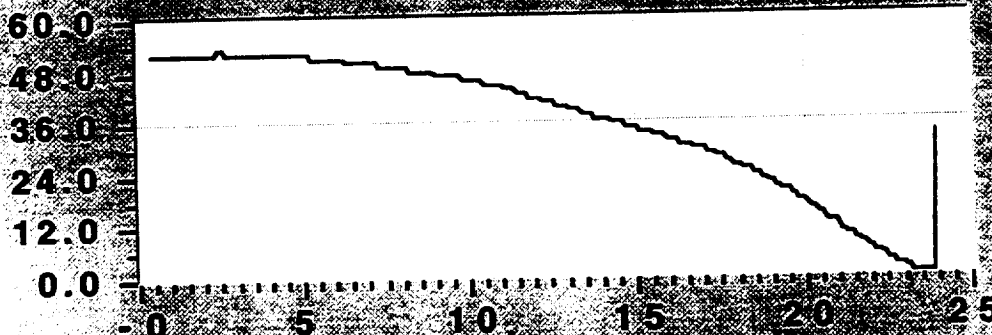
Drag
Friction
Coefficient



Time, sec

Plot D

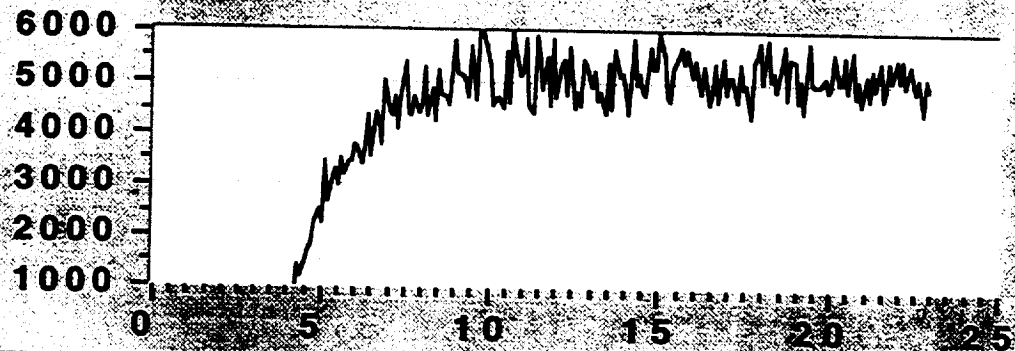
5th Wheel
Velocity,
mph



Time, sec

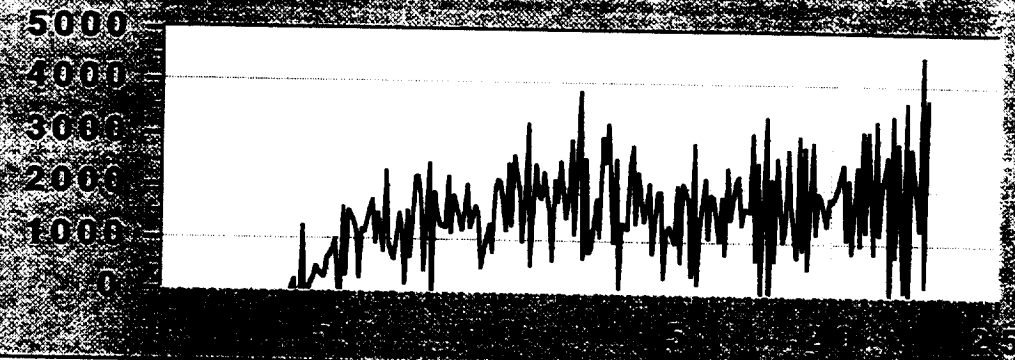
Run32

Plot A



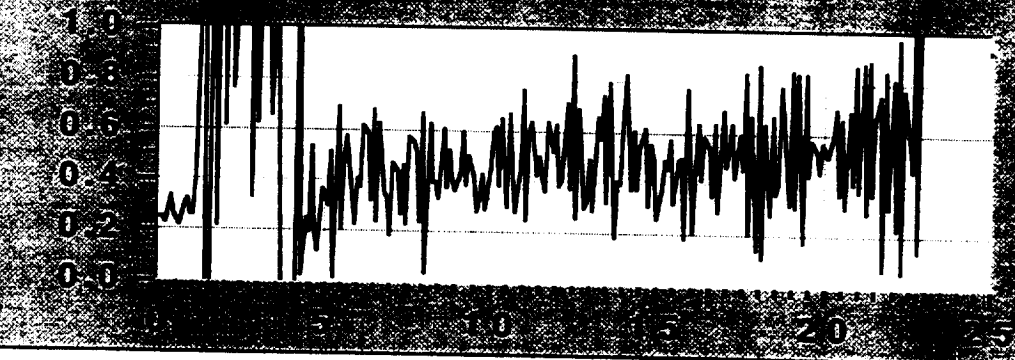
Plot B

Time, sec



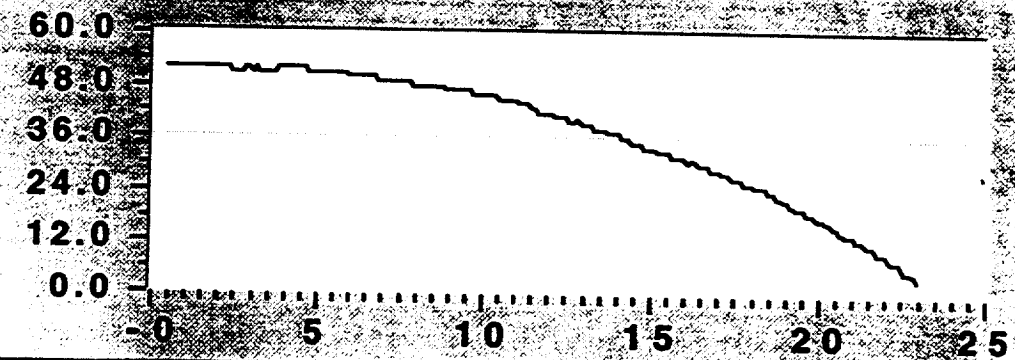
Plot C

Time, sec



Plot D

Time, sec



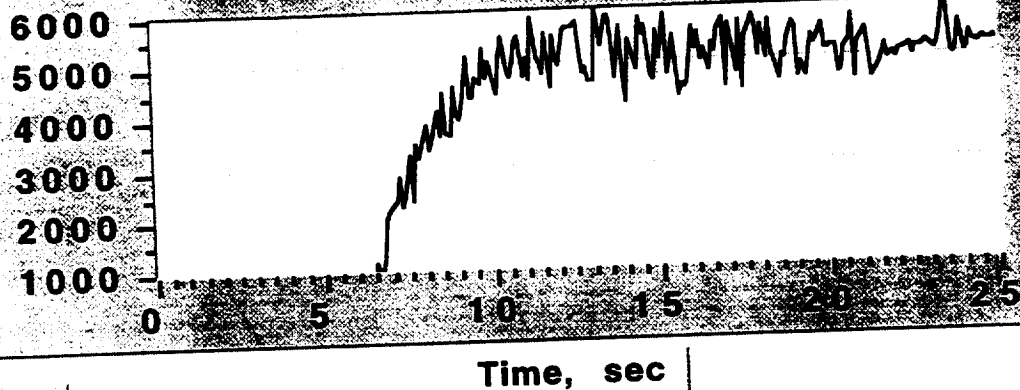
Time, sec

Run33

Plot A

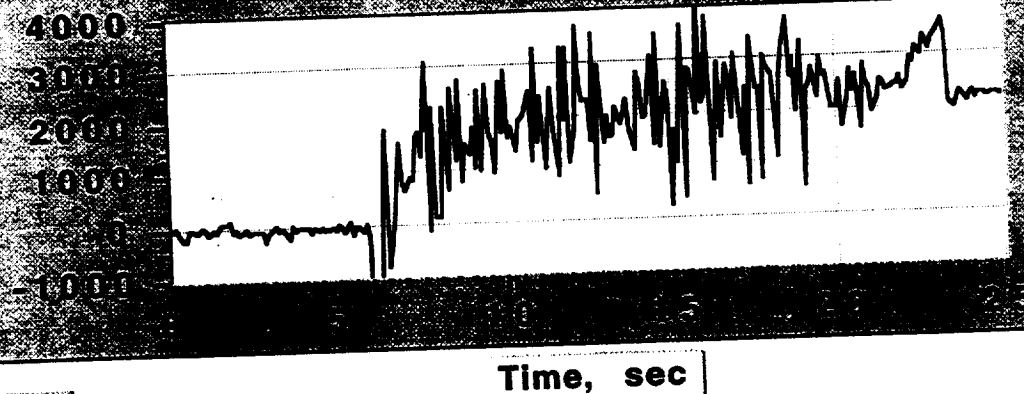
Return

Vertical
Load, lb



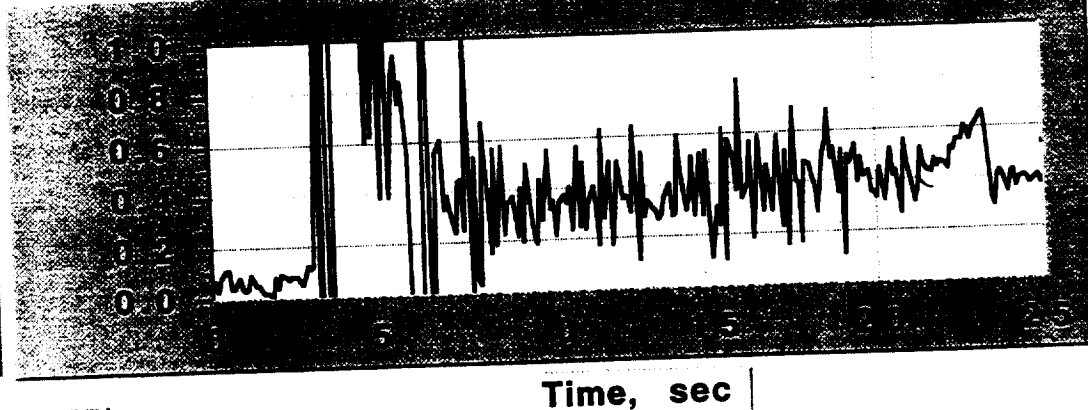
Plot B

Drag Load
#1, lb



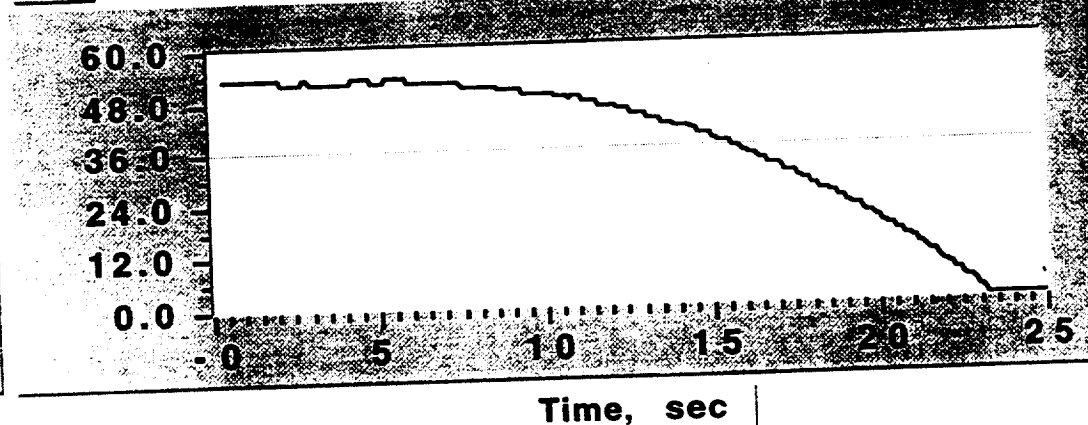
Plot C

Drag
Friction
Coefficient



Plot D

5th Wheel
Velocity,
mph



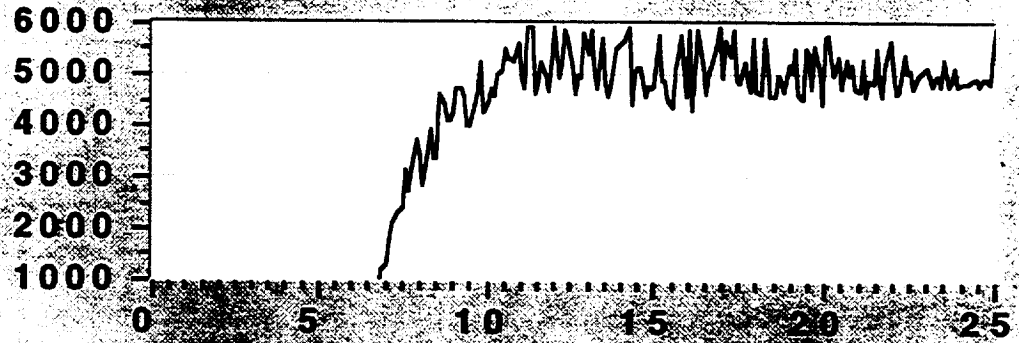
Run35

Plot A



Return

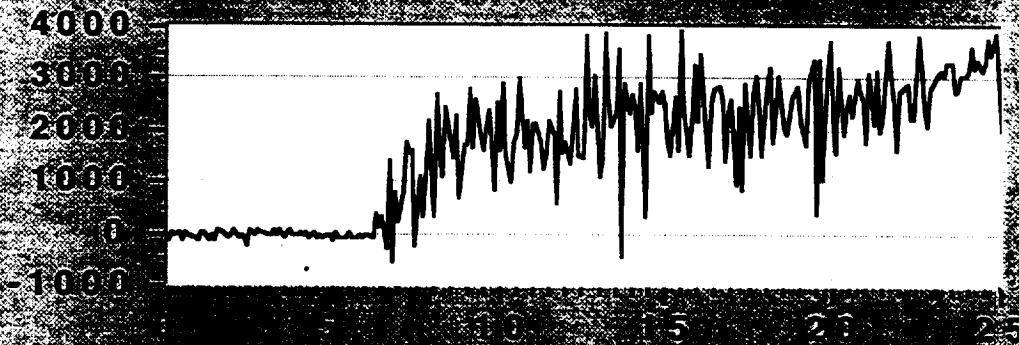
Vertical
Load, lb



Plot B

Time, sec

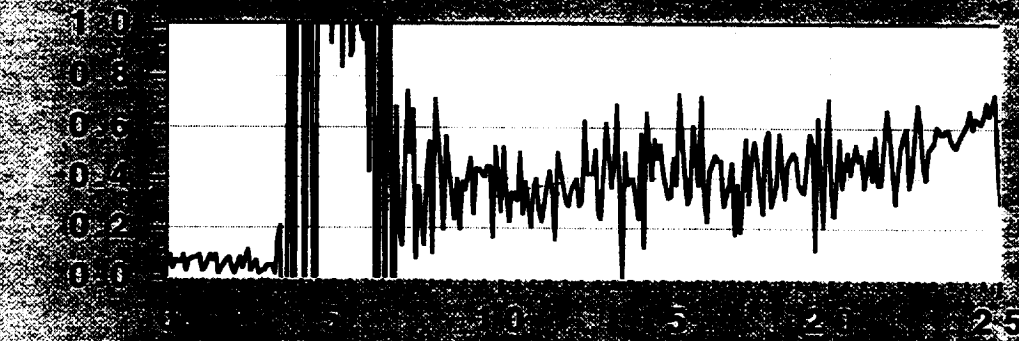
Drag Load
#1, lb



Plot C

Time, sec

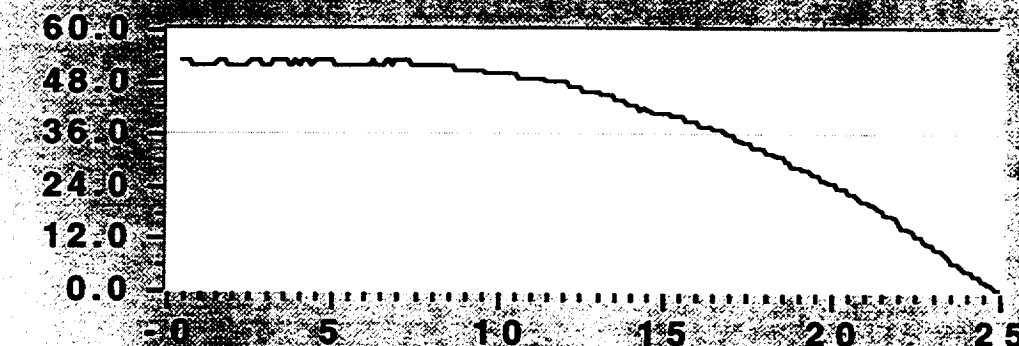
Drag
Friction
Coefficient



Plot D

Time, sec

5th Wheel
Velocity,
mph



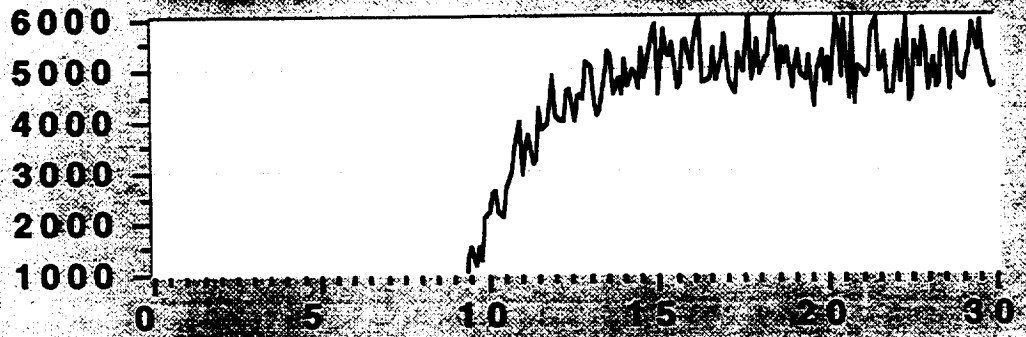
Time, sec

Run36

Plot A

Return

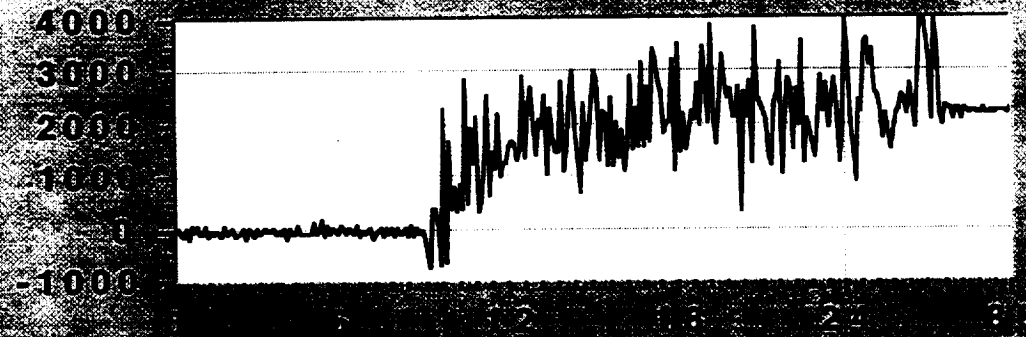
Vertical
Load, lb



Plot B

Time, sec

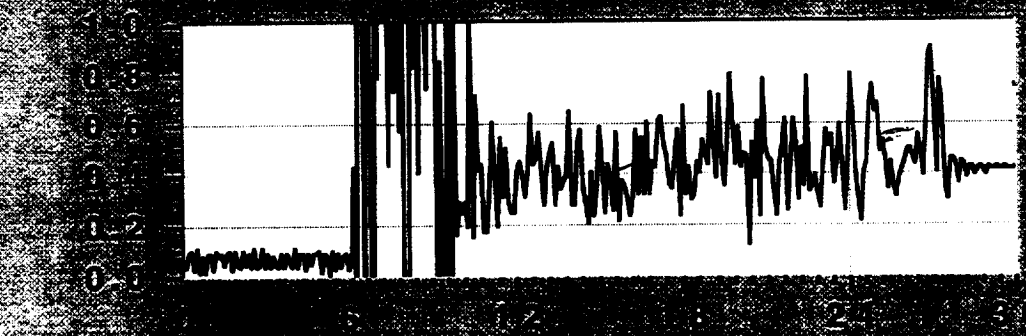
Drag Load
#1, lb



Plot C

Time, sec

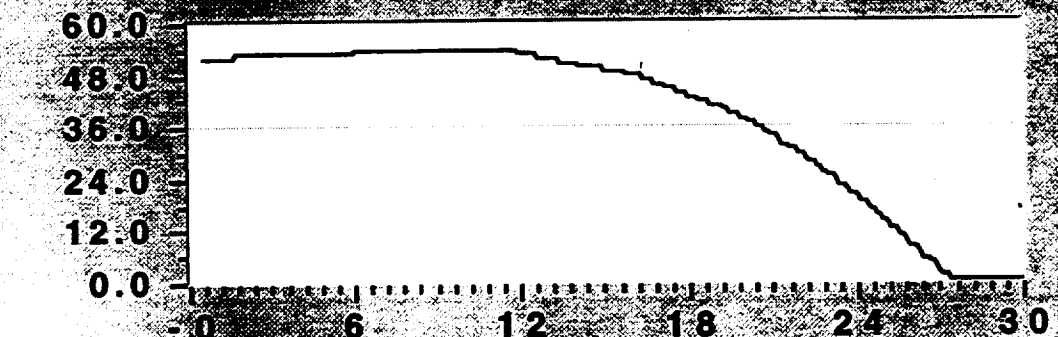
Drag
Friction
Coefficient



Plot D

Time, sec

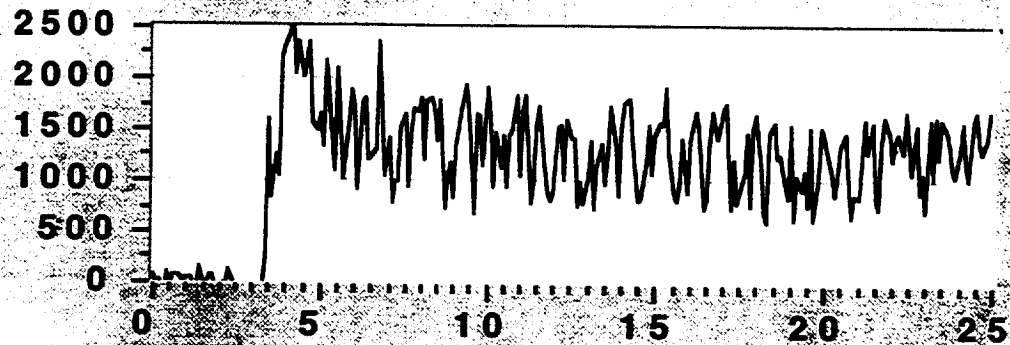
5th Wheel
Velocity,
mph



Time, sec

Run37

Plot A

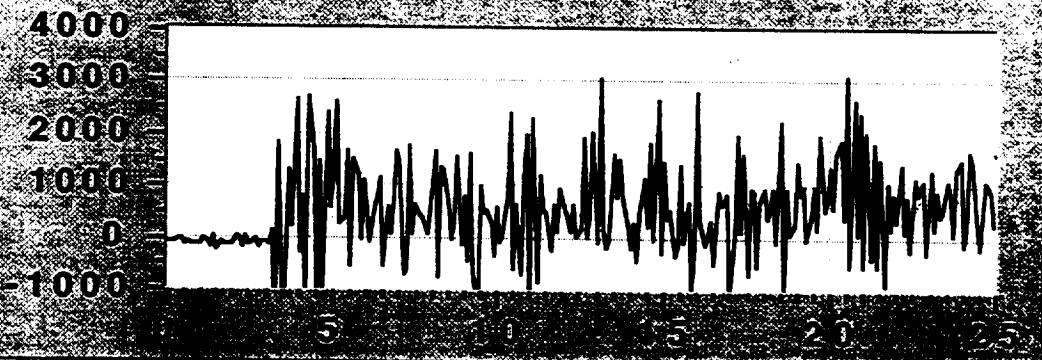


Return

Vertical
Load, lb

Plot B

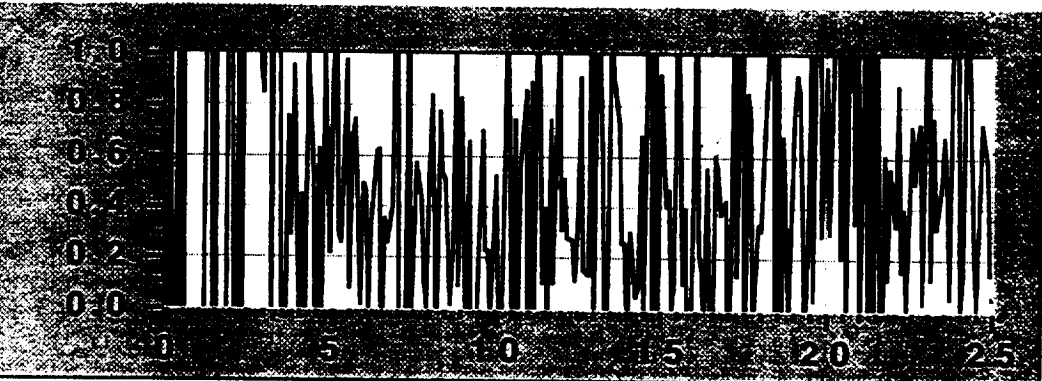
Time, sec



Drag Load
#1, lb

Plot C

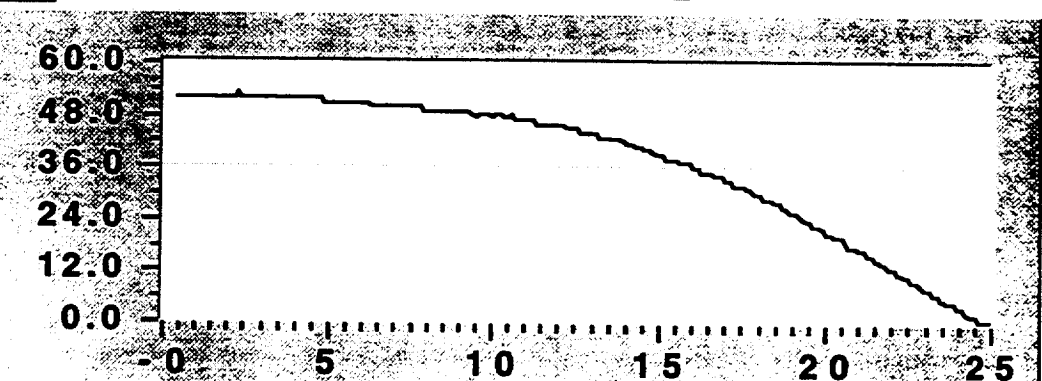
Time, sec



Drag
Friction
Coefficient

Plot D

Time, sec



5th Wheel
Velocity,
mph

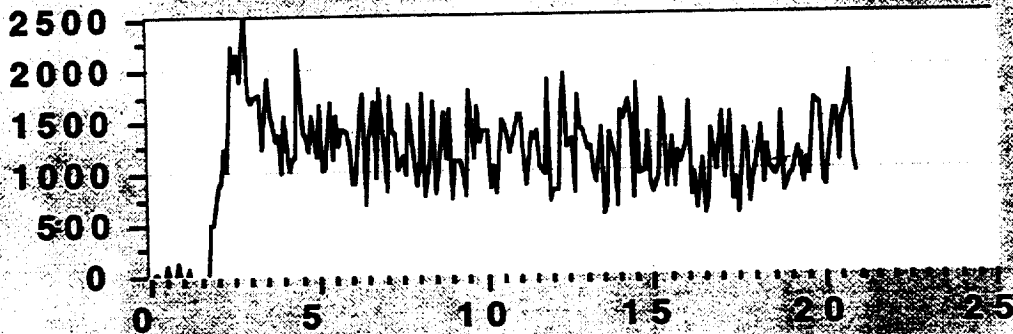
Time, sec

Run38

Plot A

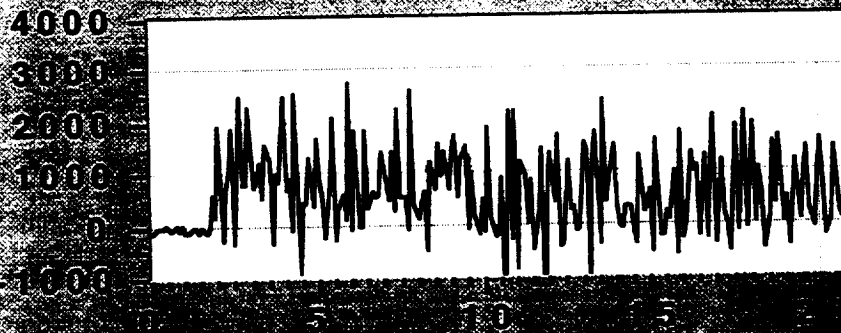
Return

Vertical
Load, lb



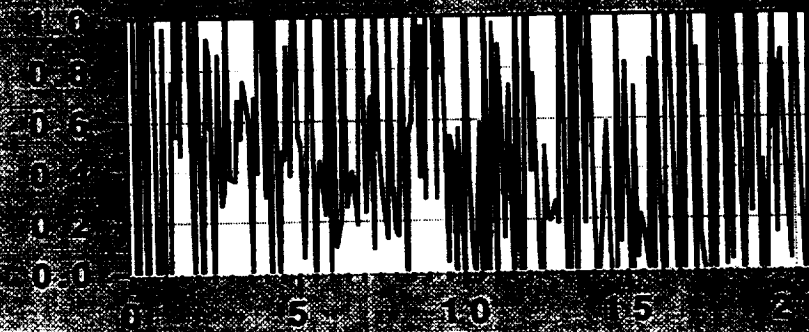
Plot B

Drag Load
#1, lb



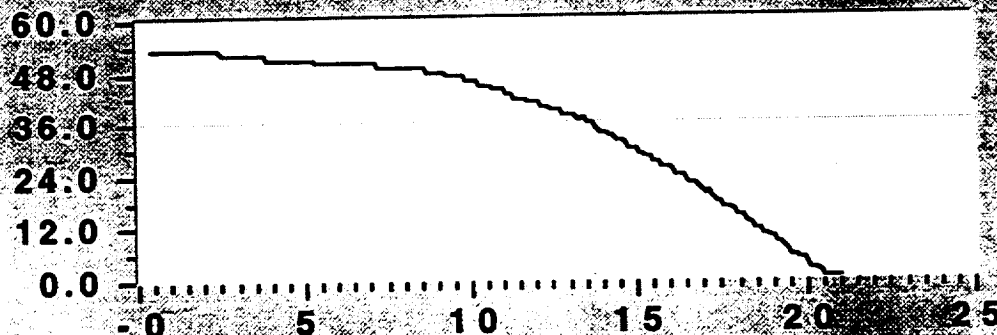
Plot C

Drag
Friction
Coefficient



Plot D

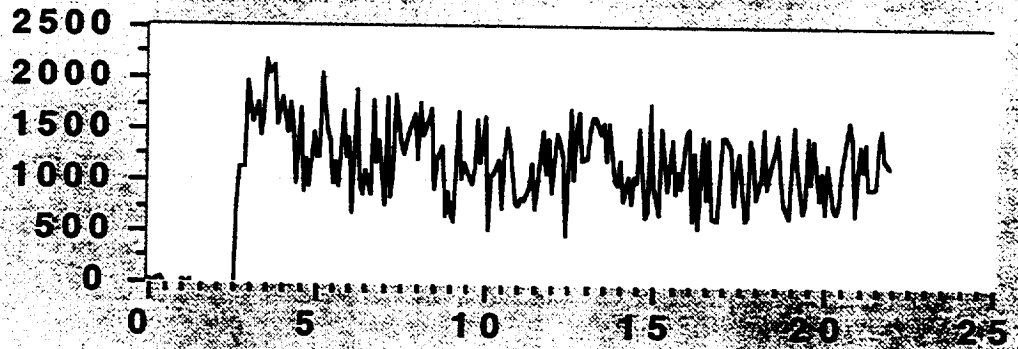
5th Wheel
Velocity,
mph



Time, sec

Run39

Plot A

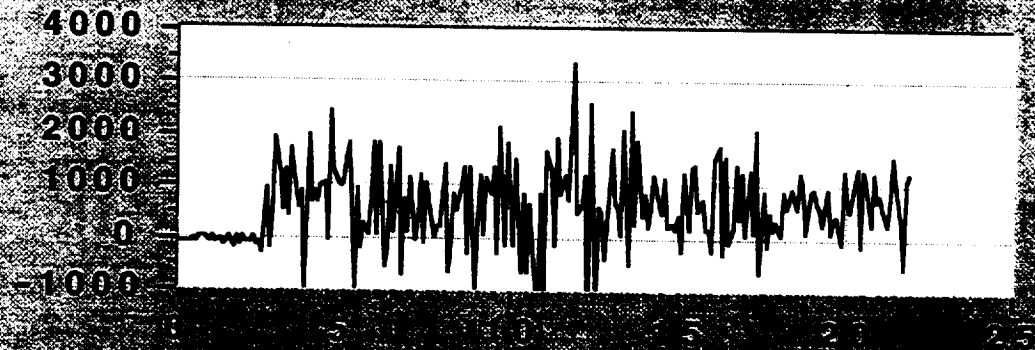


Return

Vertical
Load, lb

Plot B

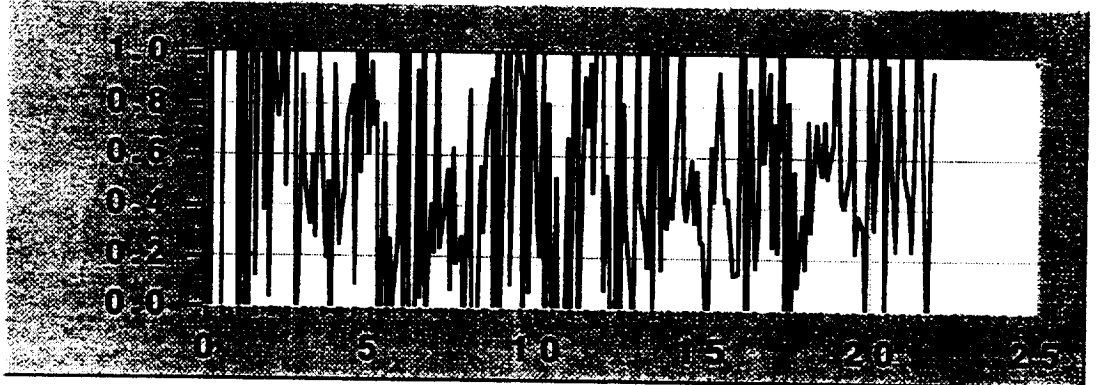
Time, sec



Drag Load
#1, lb

Plot C

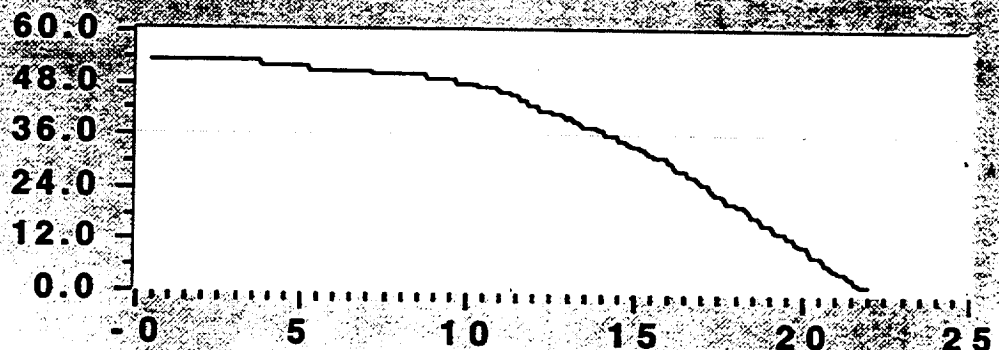
Time, sec



Drag
Friction
Coefficient

Plot D

Time, sec

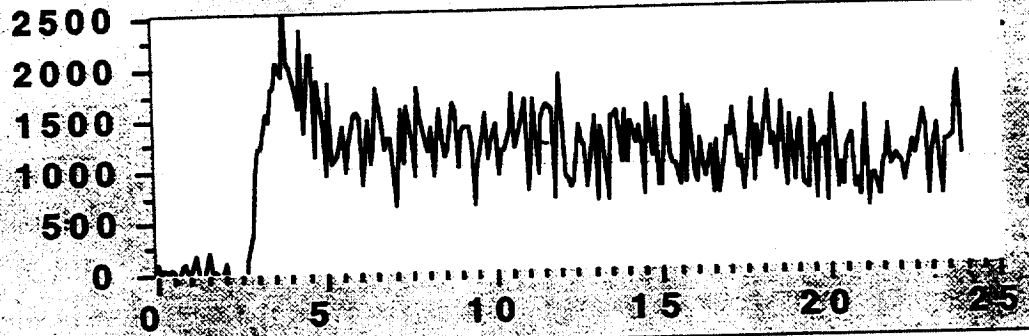


5th Wheel
Velocity,
mph

Time, sec

Run40

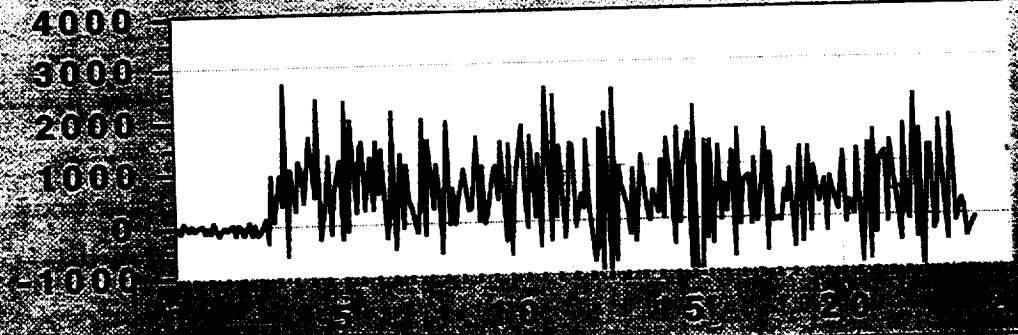
Plot A



Vertical
Load, lb

Return

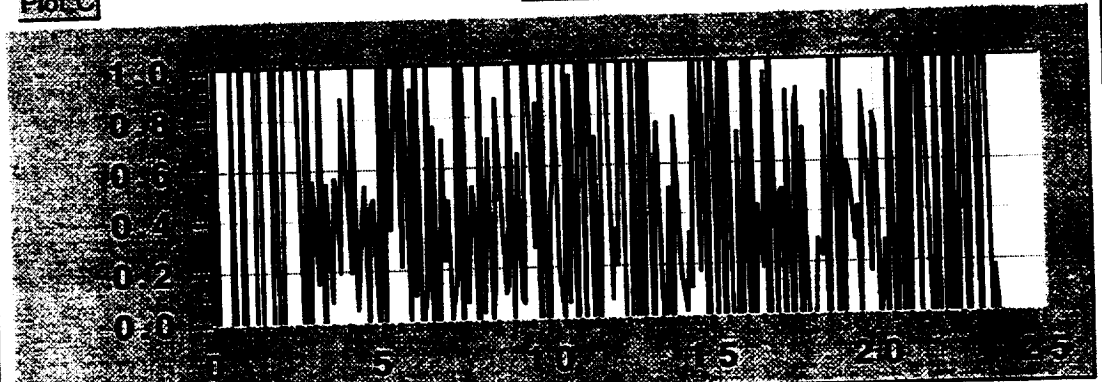
Plot B



Drag Load
#1, lb

Time, sec

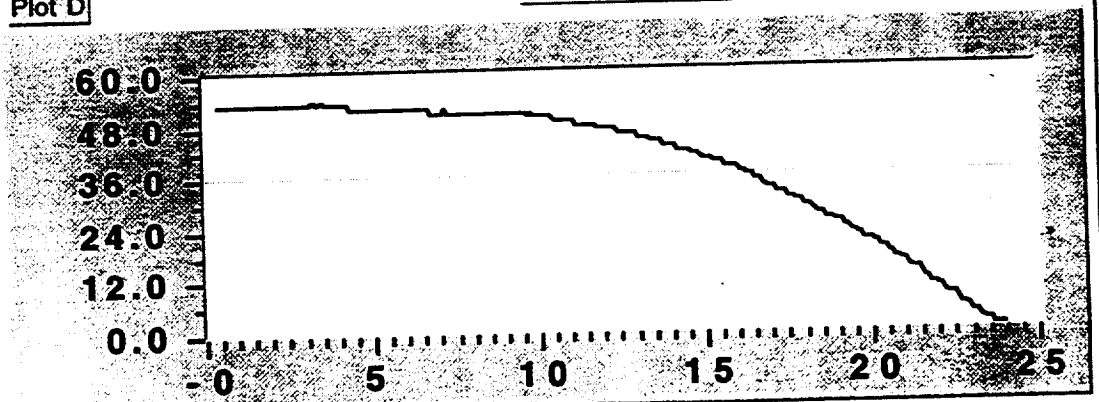
Plot C



Drag
Friction
Coefficient

Time, sec

Plot D

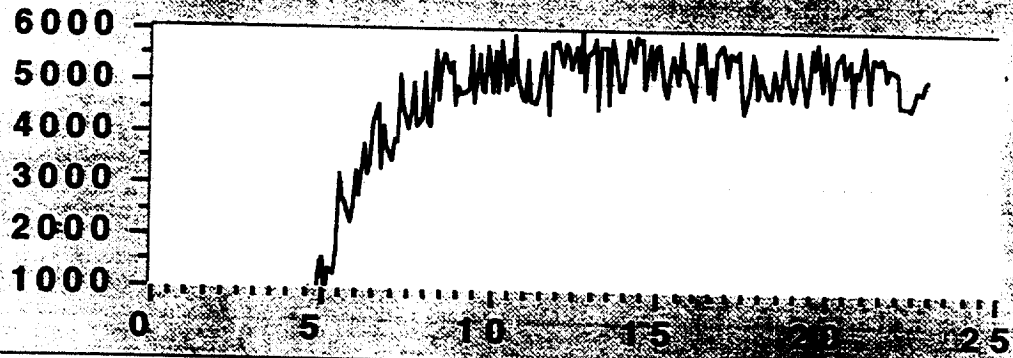


5th Wheel
Velocity,
mph

Time, sec

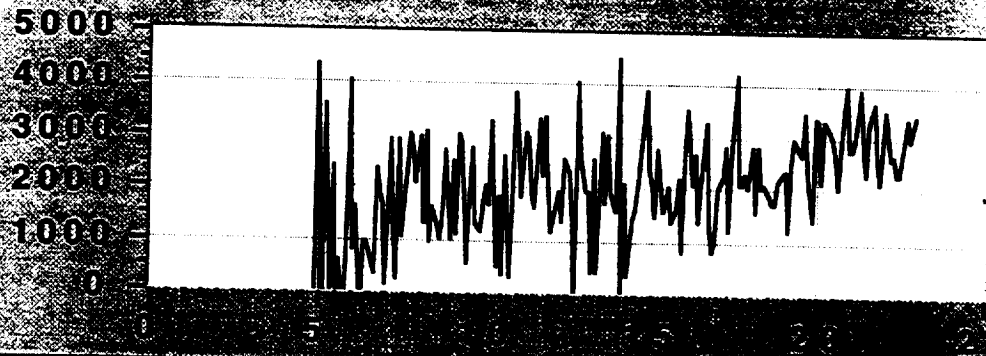
Run47

Plot A



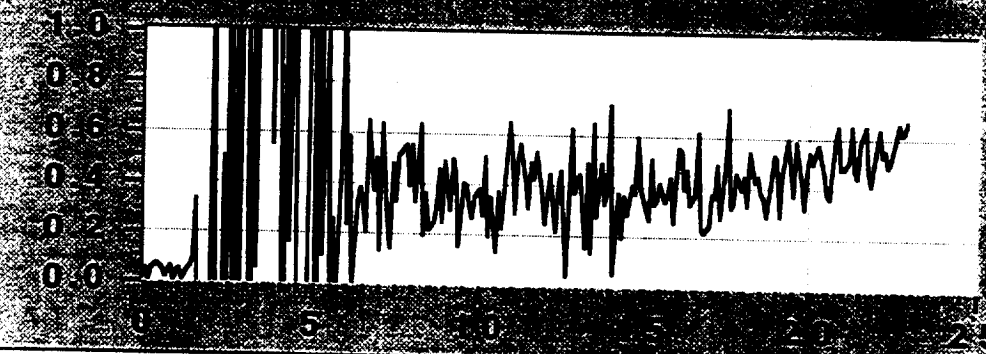
Plot B

Time, sec



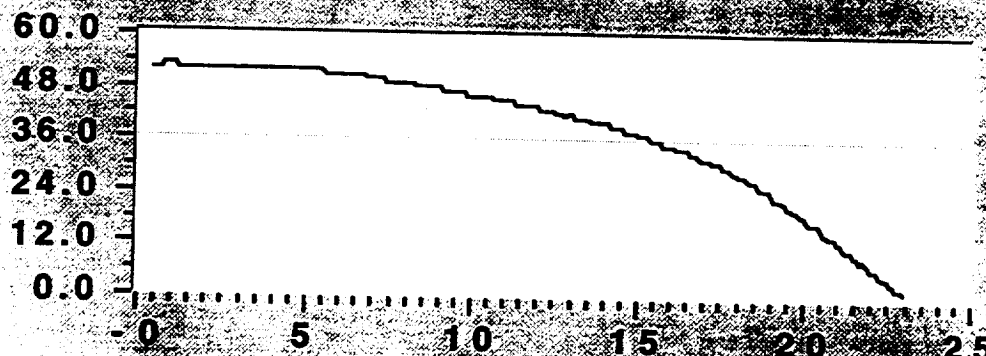
Plot C

Time, sec



Plot D

Time, sec



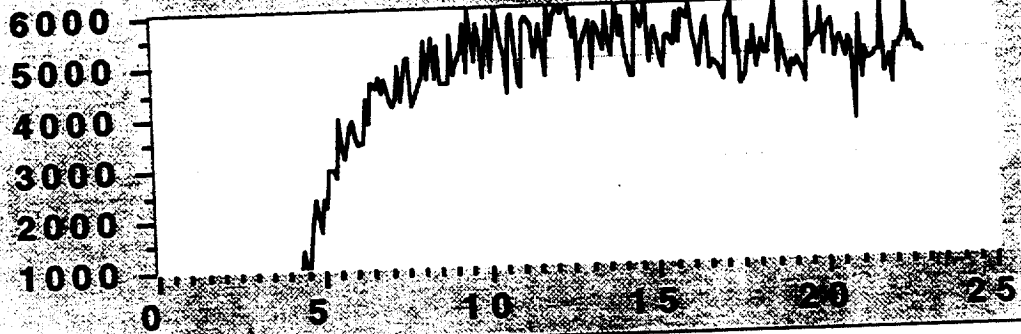
Run48

Plot A



Return

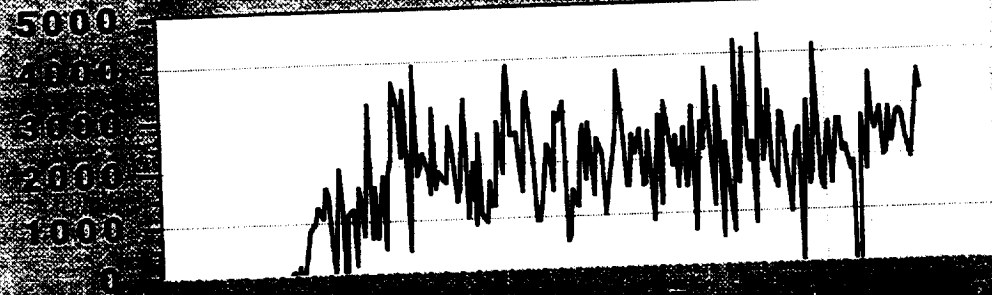
Vertical
Load, lb



Time, sec

Plot B

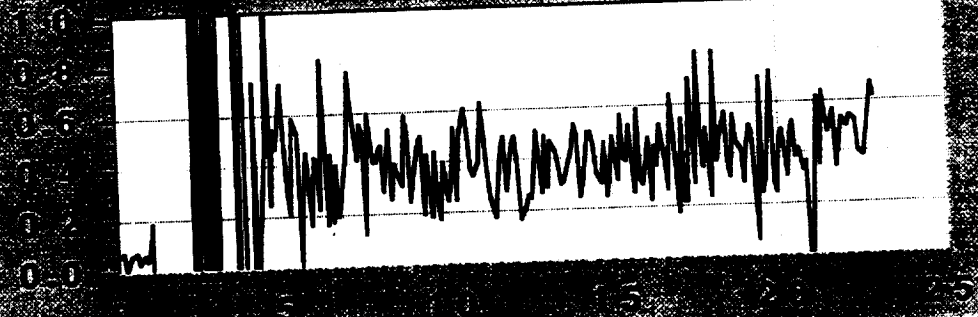
Drag Load
#1, lb



Time, sec

Plot C

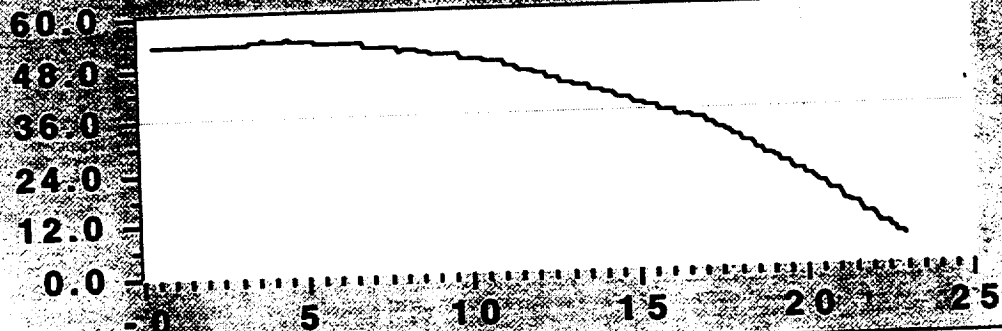
Drag
Friction
Coefficient



Time, sec

Plot D

5th Wheel
Velocity,
mph



Time, sec

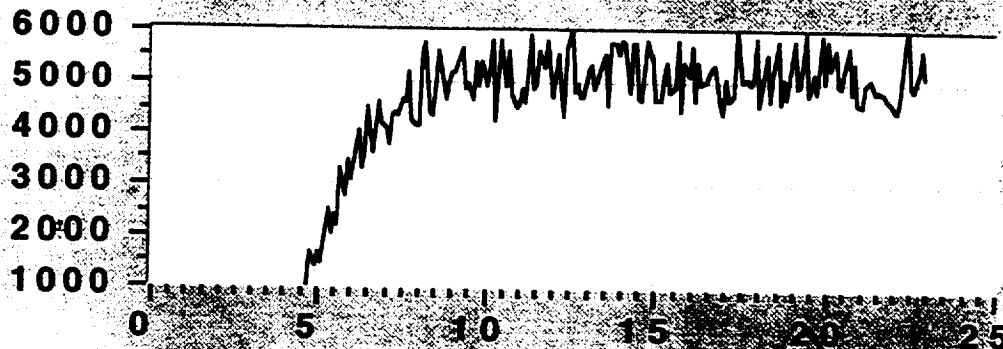
Run49

Plot A



Return

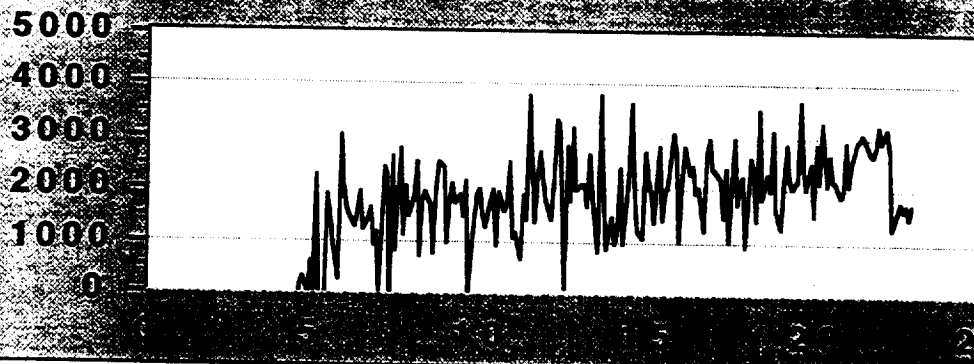
Vertical
Load, lb



Plot B

Time, sec

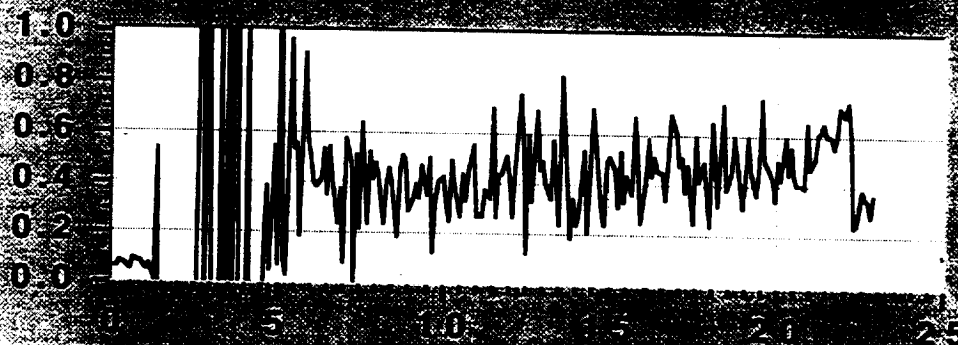
Drag Load
#1, lb



Plot C

Time, sec

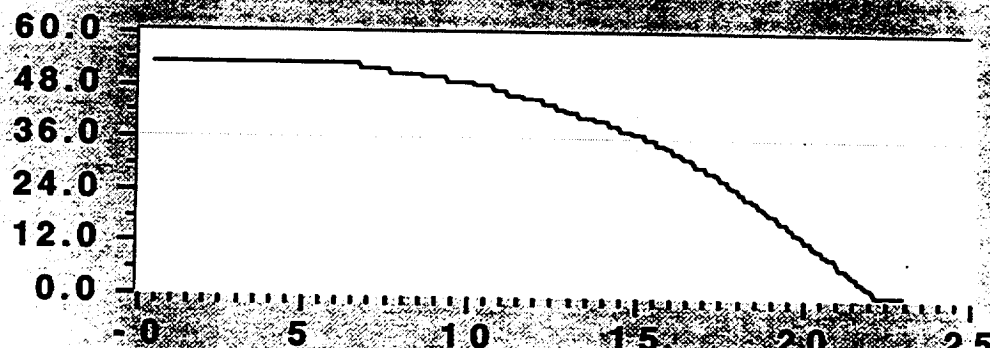
Drag
Friction
Coefficient



Plot D

Time, sec

5th Wheel
Velocity,
mph



Time, sec

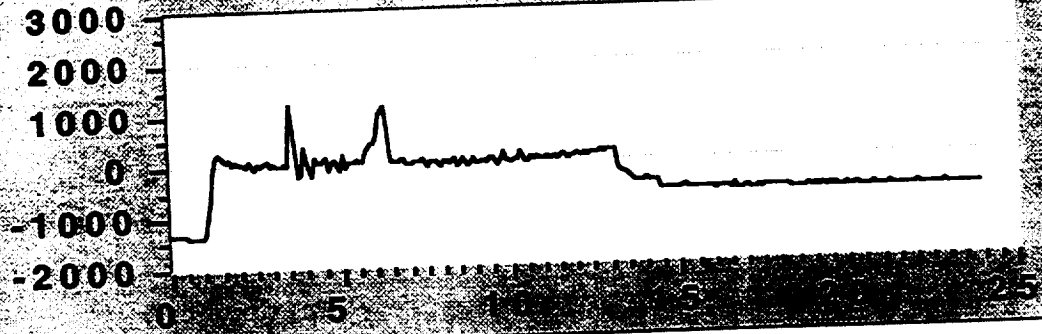
Run54

Plot A



Return

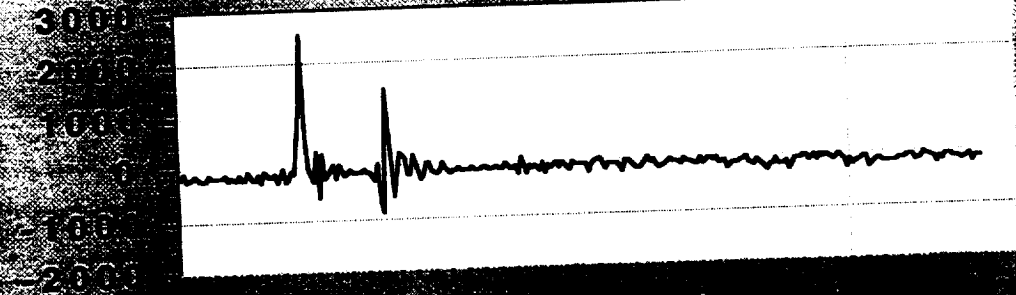
Vertical
Load, lb



Time, sec

Plot B

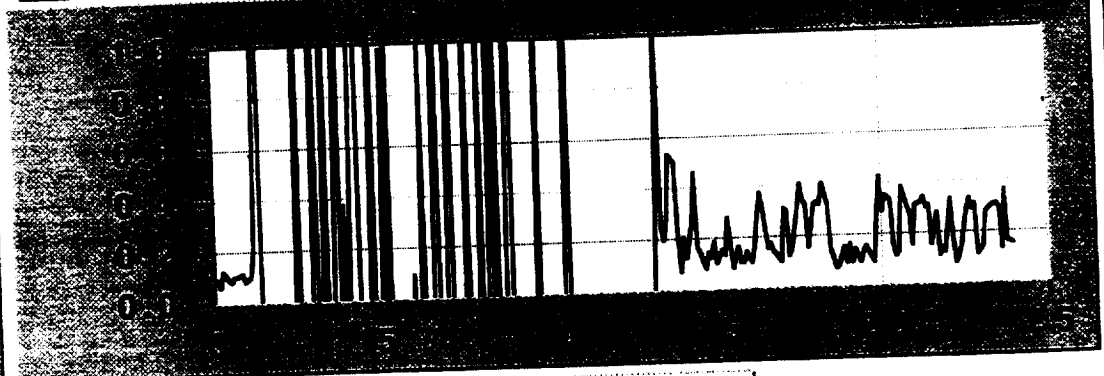
Drag Load
#1, lb



Time, sec

Plot C

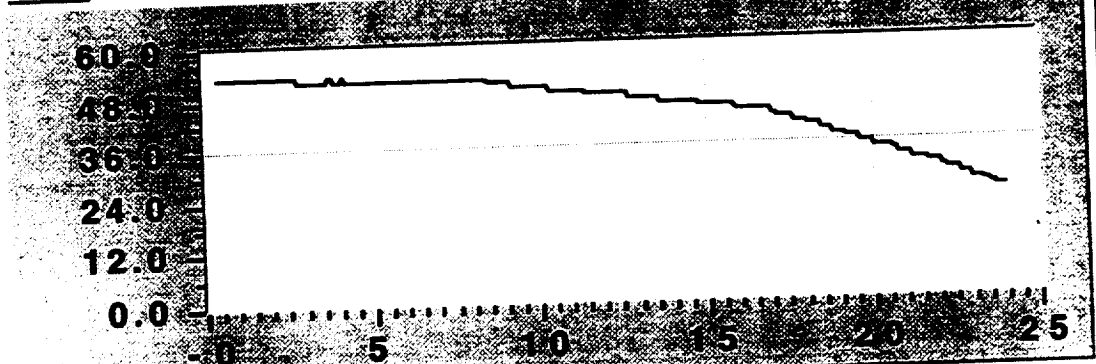
Drag
Friction
Coefficient



Time, sec

Plot D

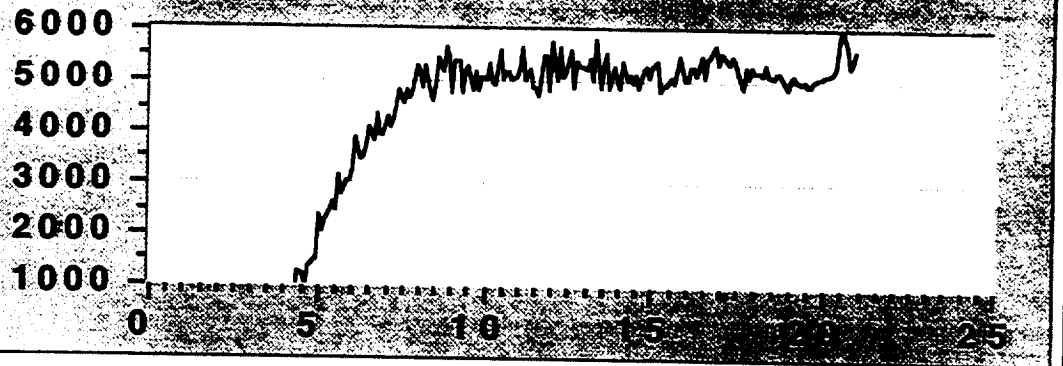
5th Wheel
Velocity,
mph



Time, sec

Run61

Plot A

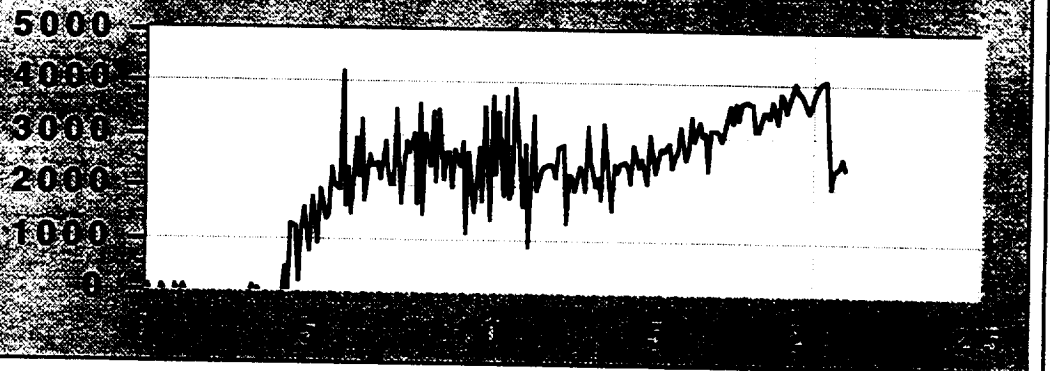


Return

Vertical
Load, lb

Plot B

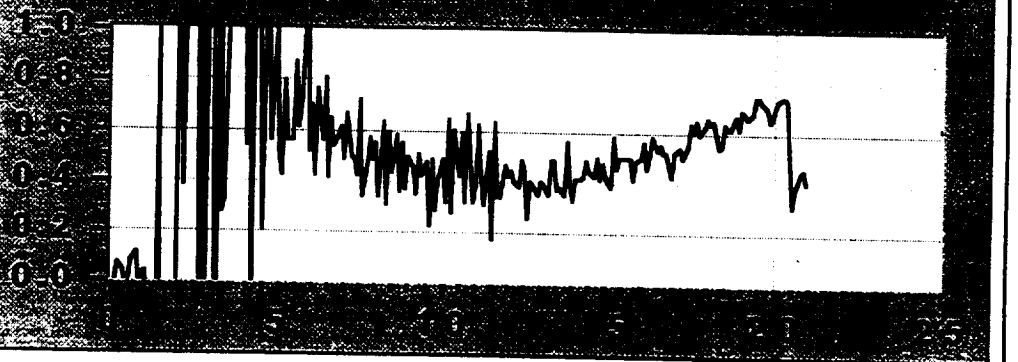
Time, sec



Drag Load
#1, lb

Plot C

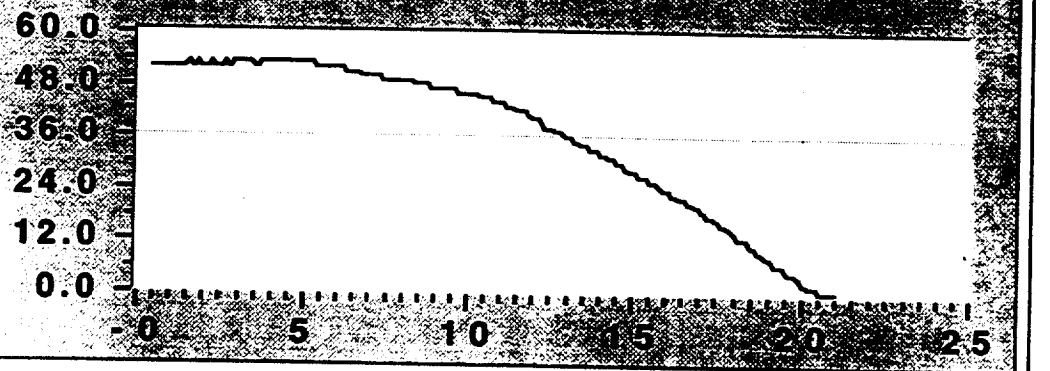
Time, sec



Drag
Friction
Coefficient

Plot D

Time, sec



5th Wheel
Velocity,
mph

Time, sec

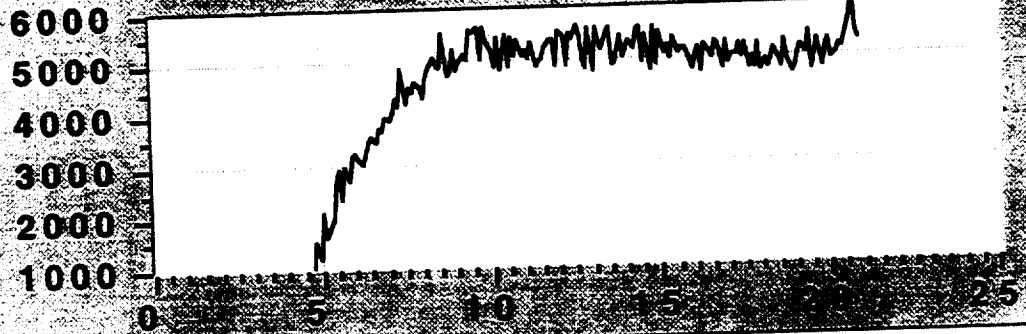
Run62

Plot A



Return

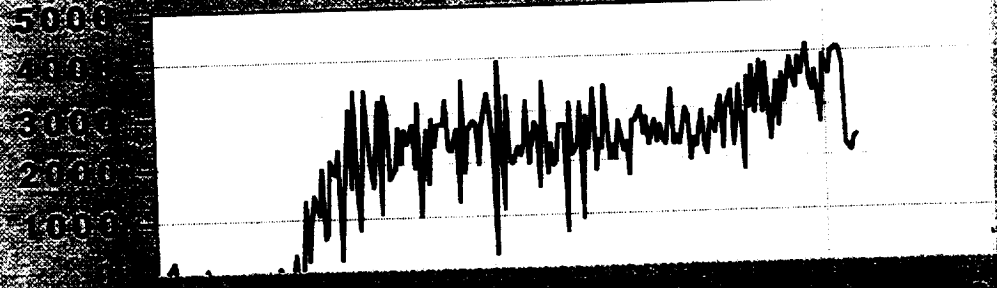
Vertical
Load, lb



Time, sec

Plot B

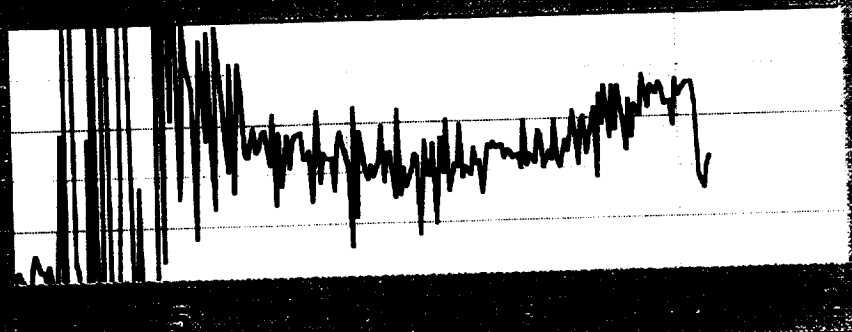
Drag Load
#1, lb



Time, sec

Plot C

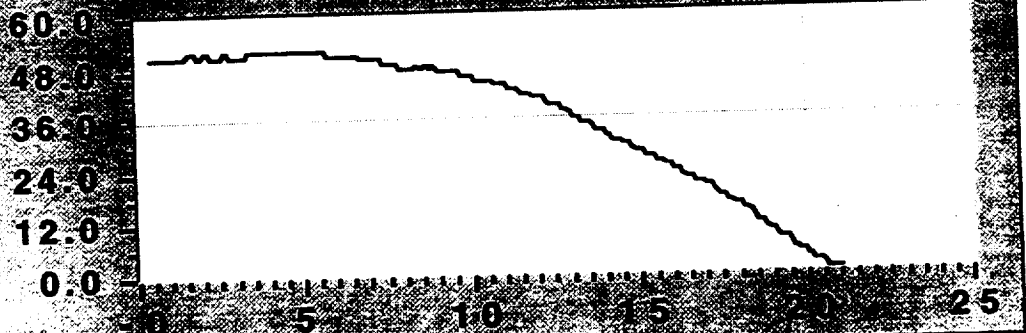
Drag
Friction
Coefficient



Time, sec

Plot D

5th Wheel
Velocity,
mph



Time, sec

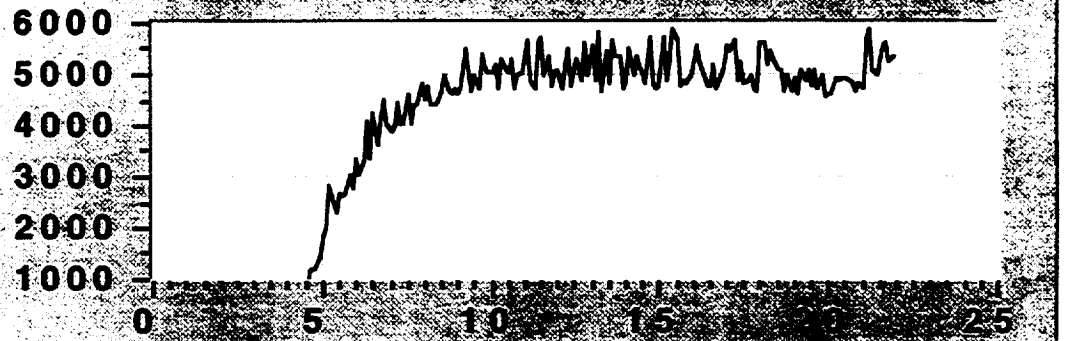
Run63

Plot A



Return

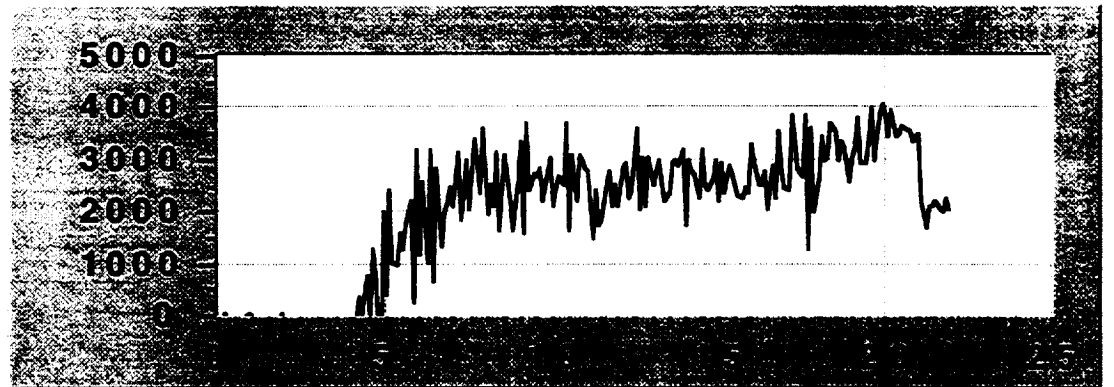
Vertical
Load, lb



Plot B

Time, sec

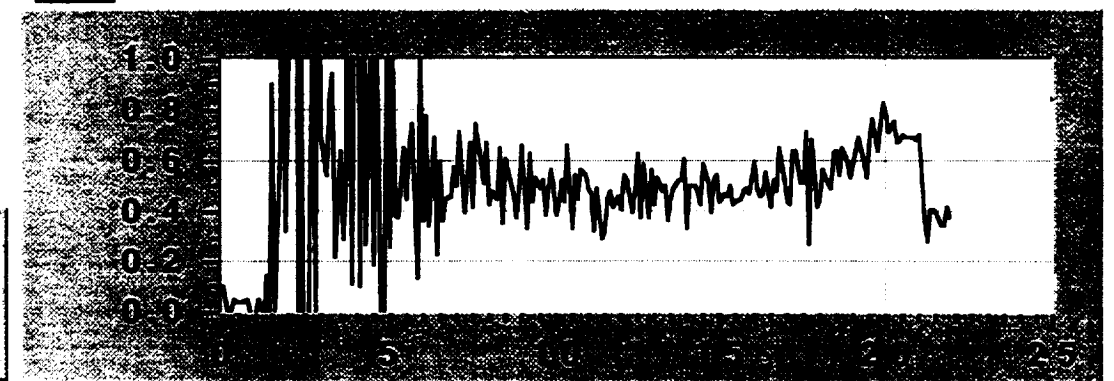
Drag Load
#1, lb



Plot C

Time, sec

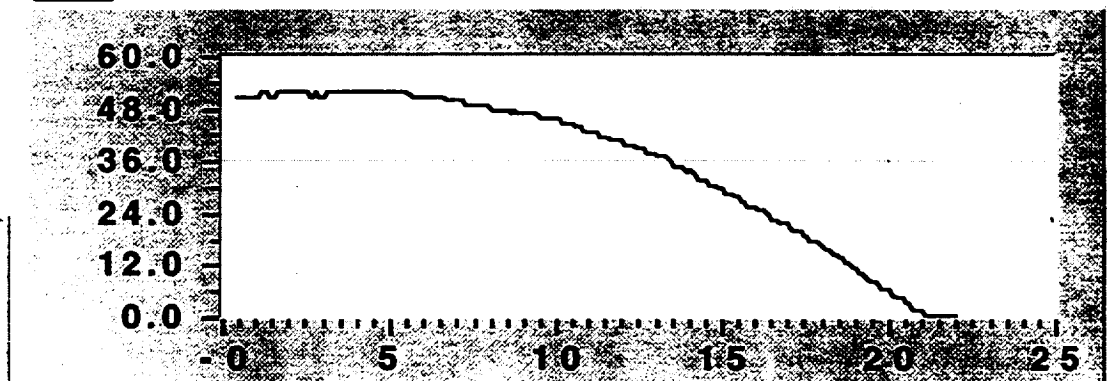
Drag
Friction
Coefficient



Plot D

Time, sec

5th Wheel
Velocity,
mph



Time, sec

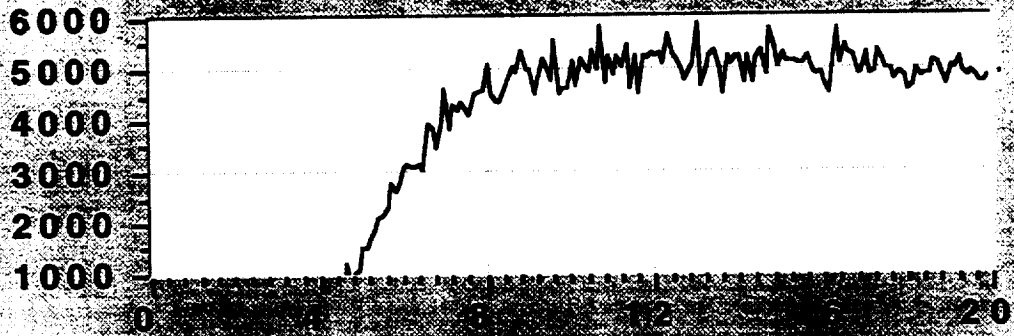
Run64

Plot A



Return

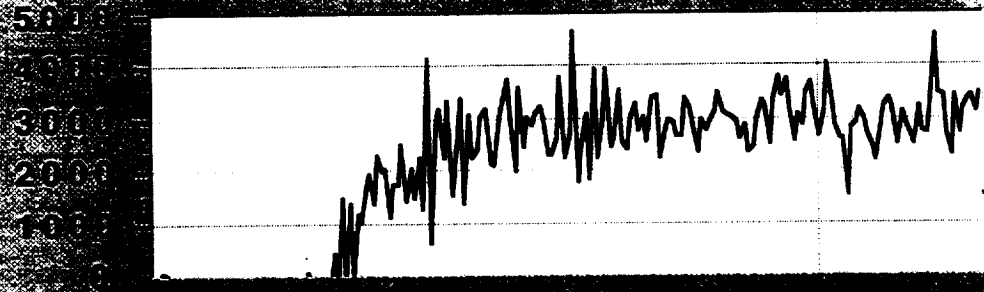
Vertical
Load, lb



Plot B

Time, sec

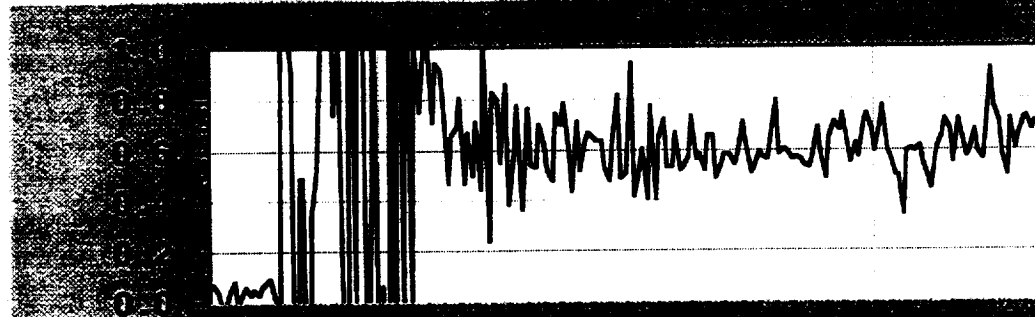
Drag Load
#1, lb



Plot C

Time, sec

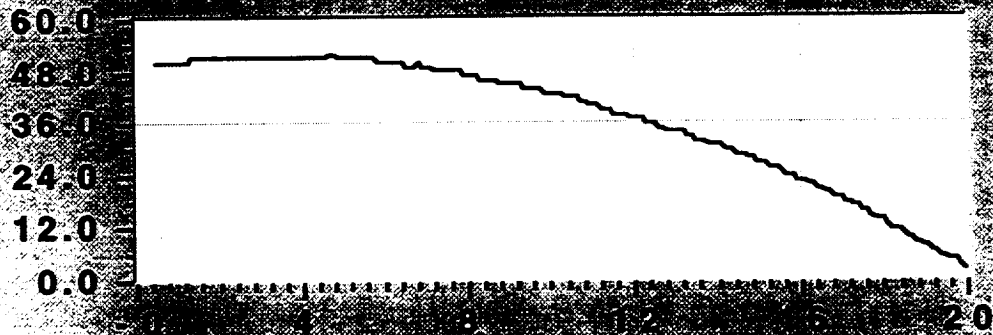
Drag
Friction
Coefficient



Plot D

Time, sec

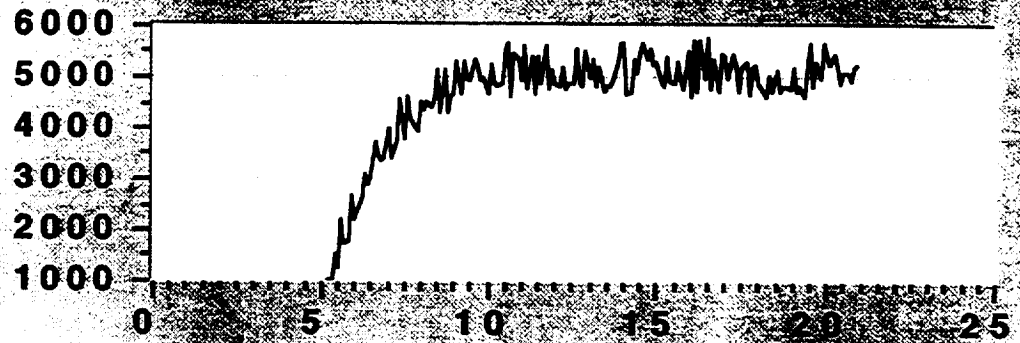
5th Wheel
Velocity,
mph



Time, sec

Run65

Plot A

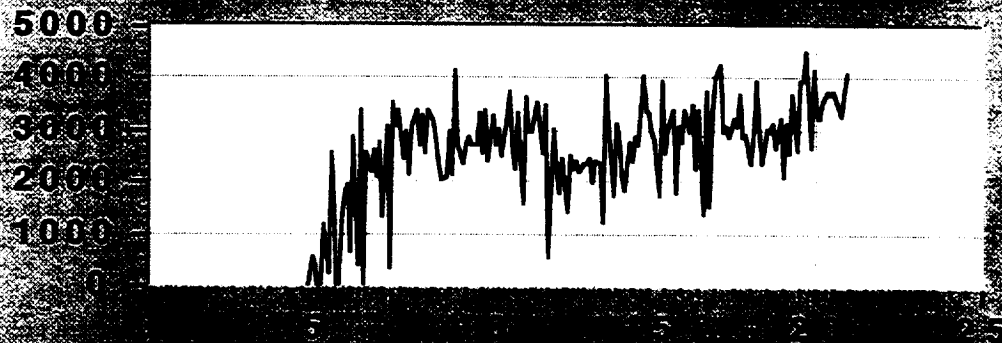


Vertical
Load, lb

Return

Plot B

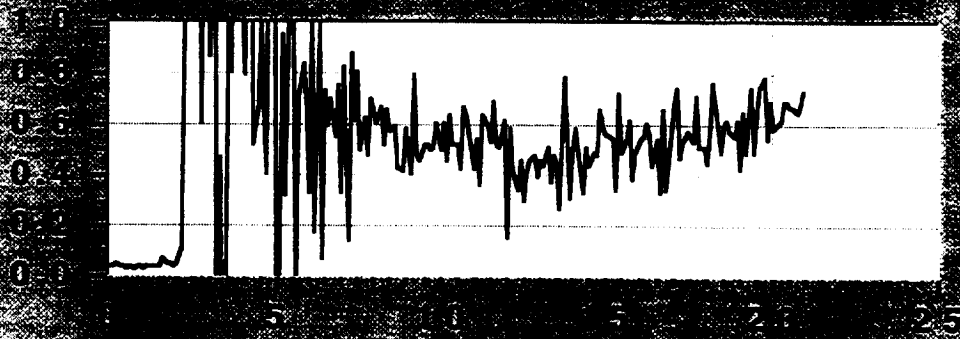
Time, sec



Drag Load
#1, lb

Plot C

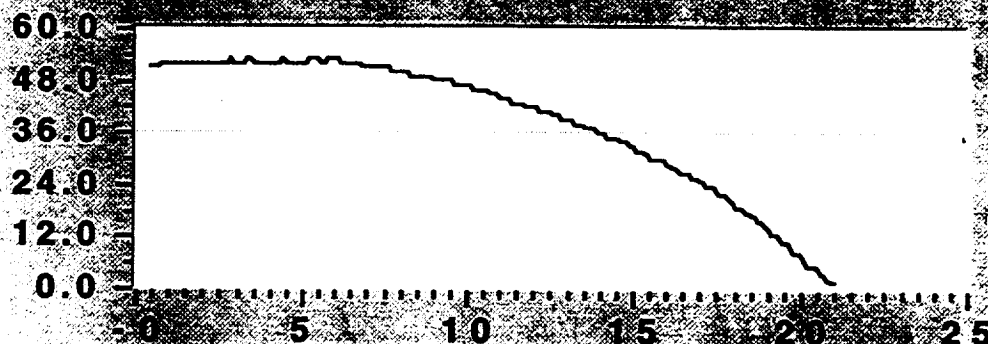
Time, sec



Drag
Friction
Coefficient

Plot D

Time, sec



5th Wheel
Velocity,
mph

Time, sec

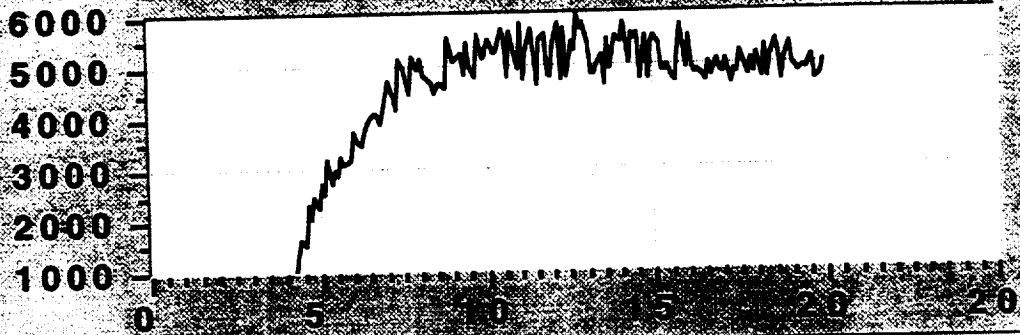
Run66



Return

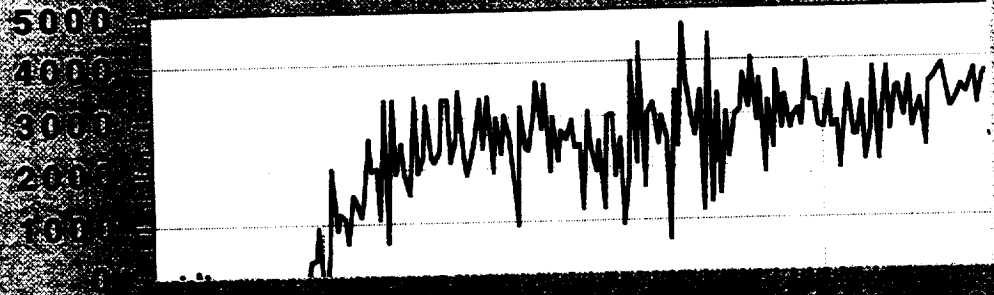
Vertical
Load, lb

Plot A



Time, sec

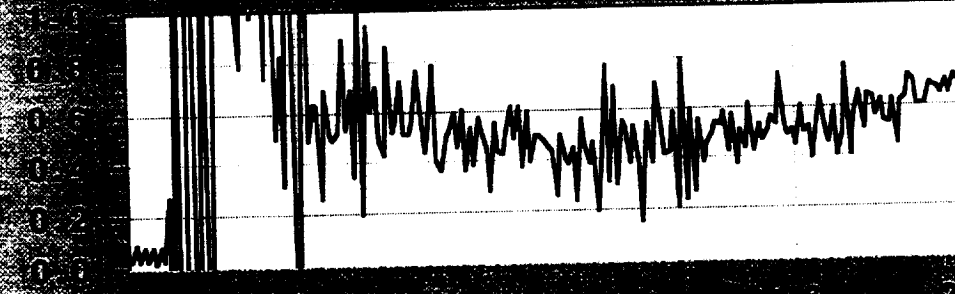
Plot B



Drag Load
#1, lb

Time, sec

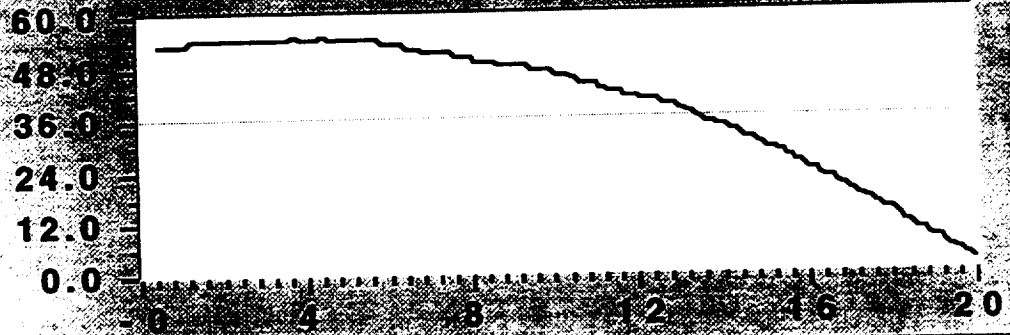
Plot C



Drag
Friction
Coefficient

Time, sec

Plot D



5th Wheel
Velocity,
mph

Time, sec

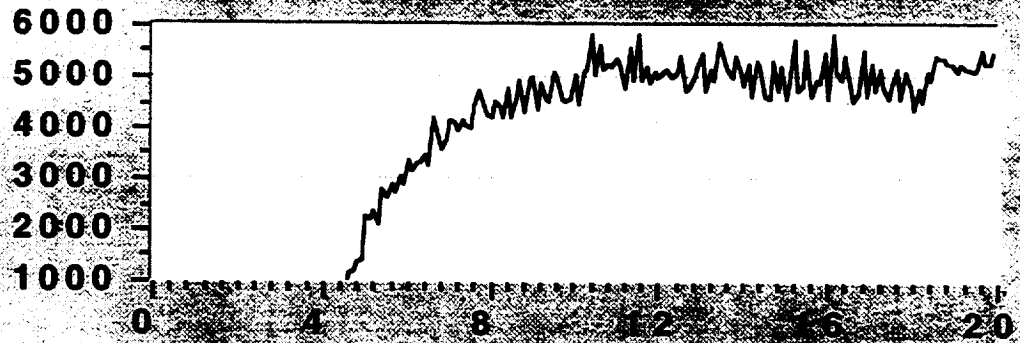
Run67

Plot A



Return

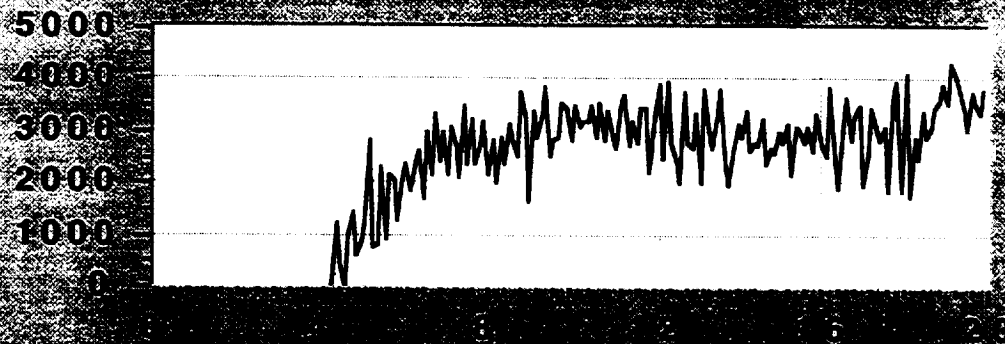
Vertical
Load, lb



Plot B

Time, sec

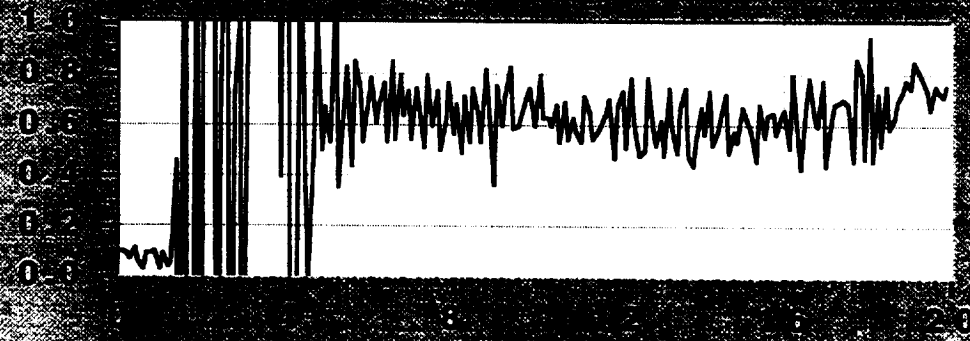
Drag Load
#1, lb



Plot C

Time, sec

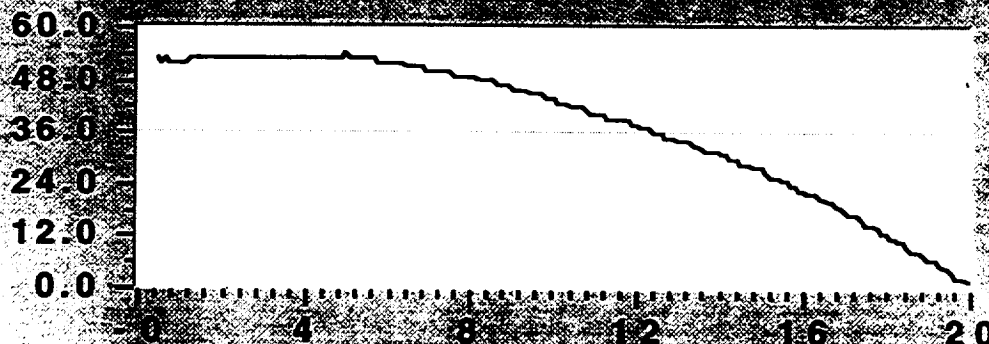
Drag
Friction
Coefficient



Plot D

Time, sec

5th Wheel
Velocity,
mph



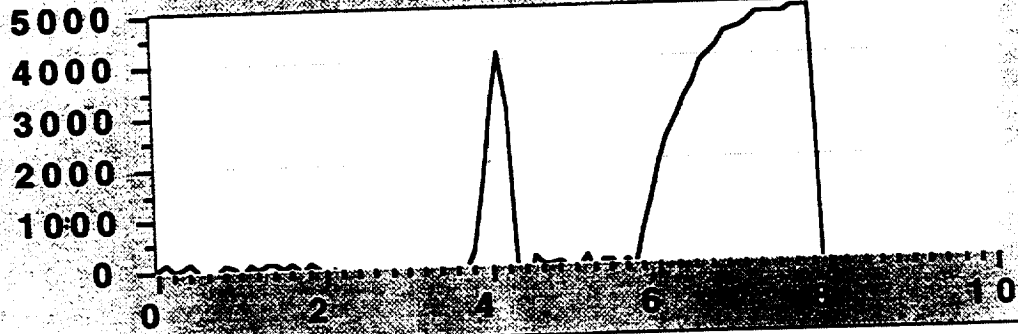
Time, sec

Run69

Plot A

Return

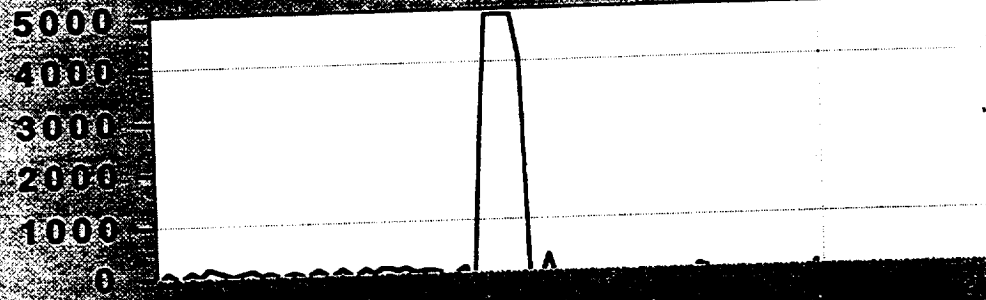
Vertical
Load, lb



Time, sec

Plot B

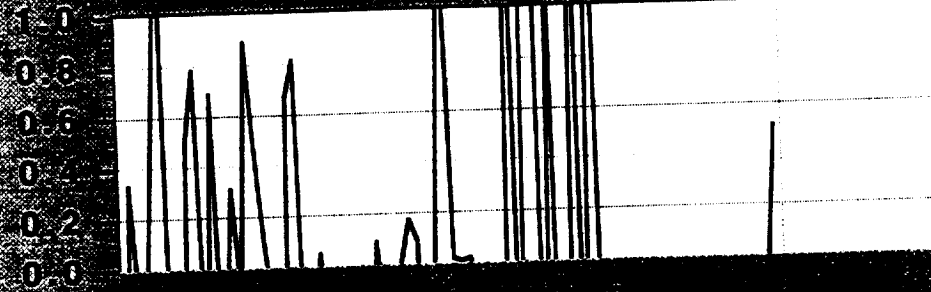
Side Load
#1, lb



Time, sec

Plot C

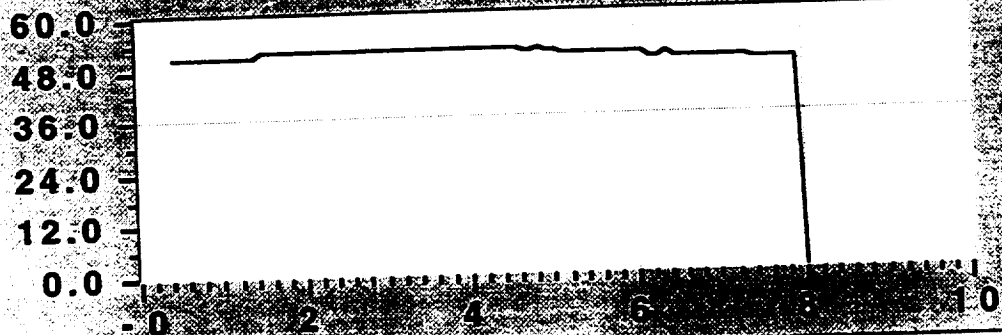
Side
Friction
Coefficient



Time, sec

Plot D

5th Wheel
Velocity,
mph



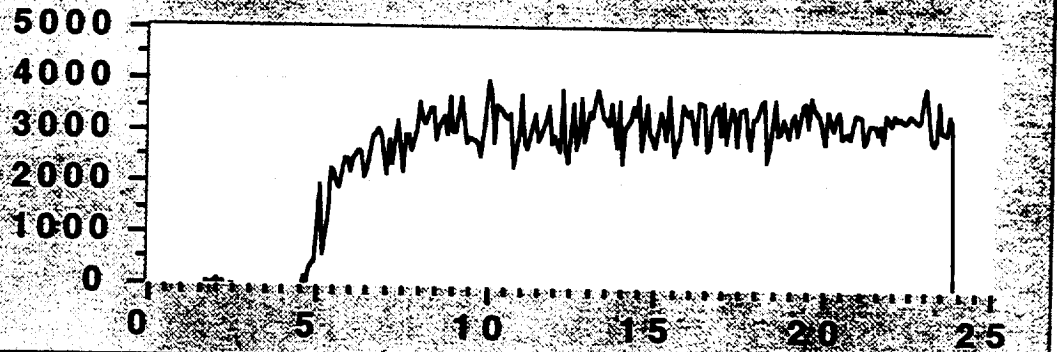
Time, sec

Run82

Plot A

Return

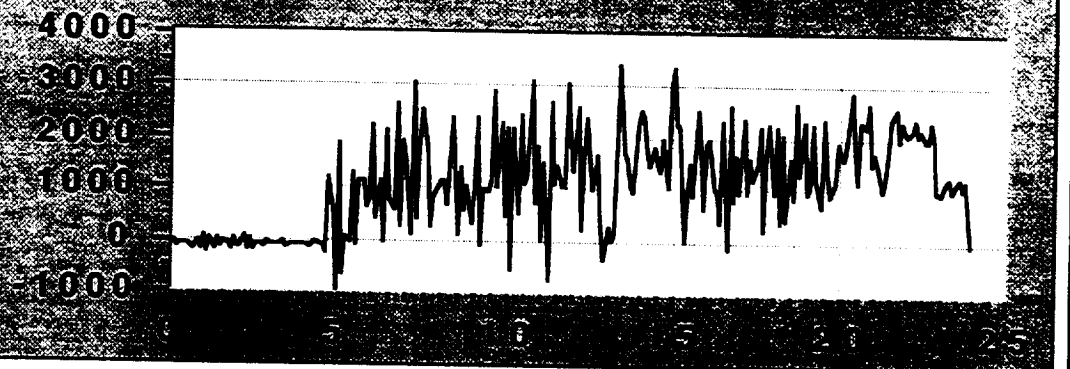
Vertical
Load, lb



Plot B

Time, sec

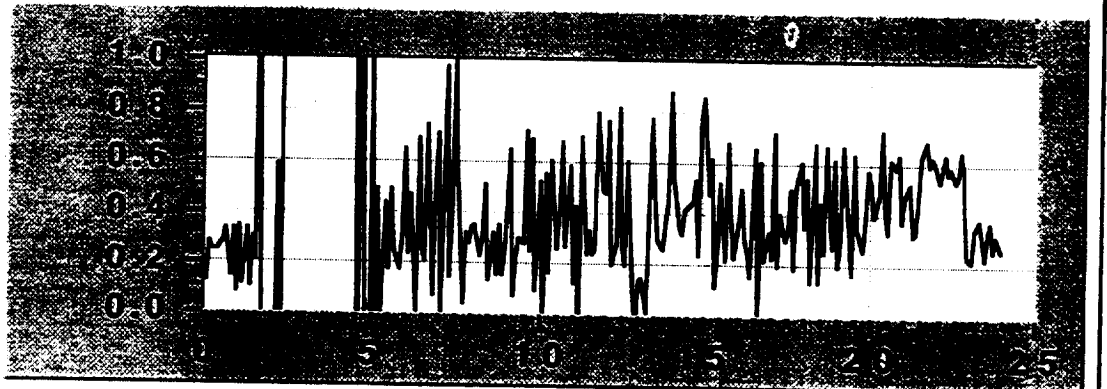
Drag Load
#1, lb



Plot C

Time, sec

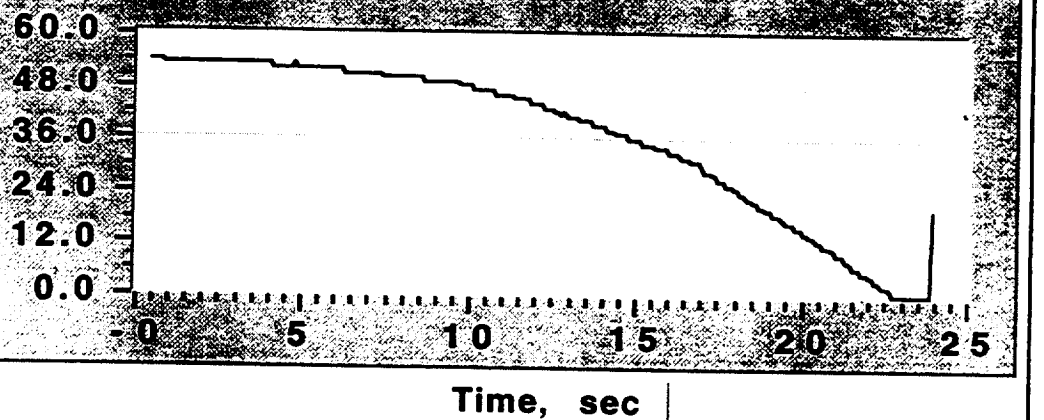
Drag
Friction
Coefficient



Plot D

Time, sec

5th Wheel
Velocity,
mph



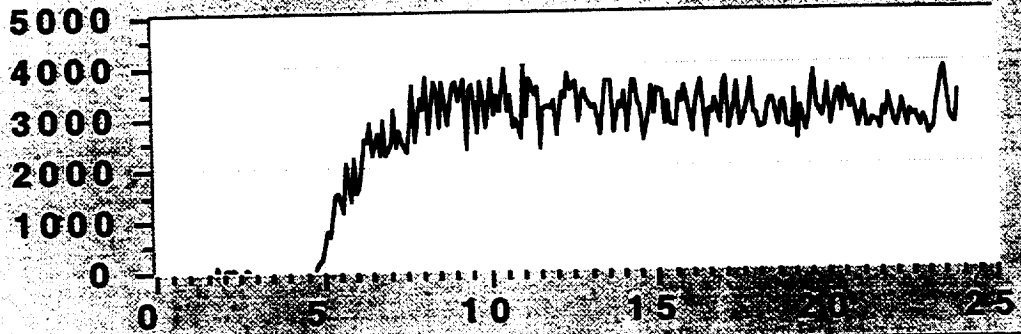
Run83

Plot A



Return

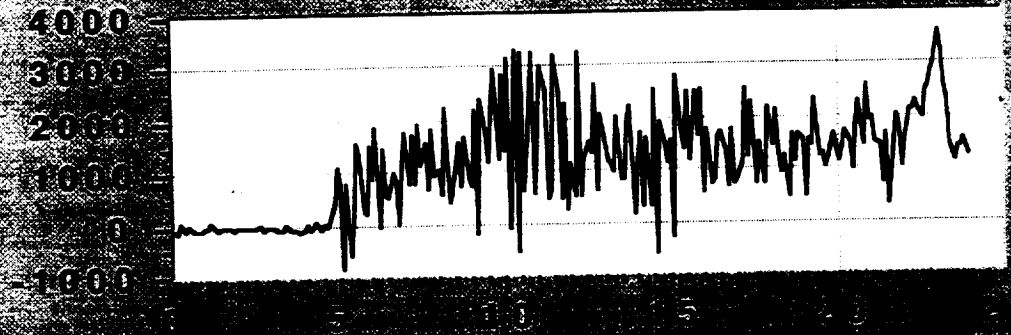
Vertical
Load, lb



Time, sec

Plot B

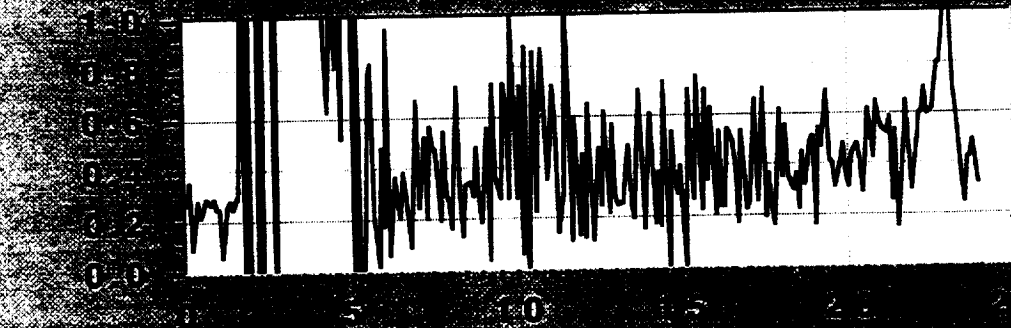
Drag Load
#1, lb



Time, sec

Plot C

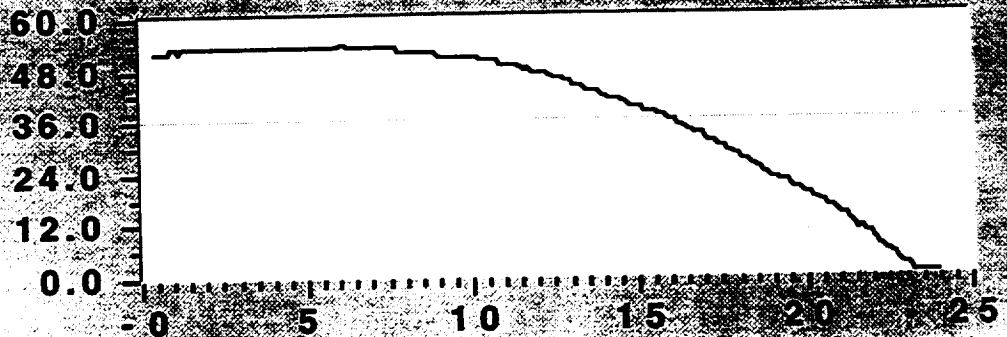
Drag
Friction
Coefficient



Time, sec

Plot D

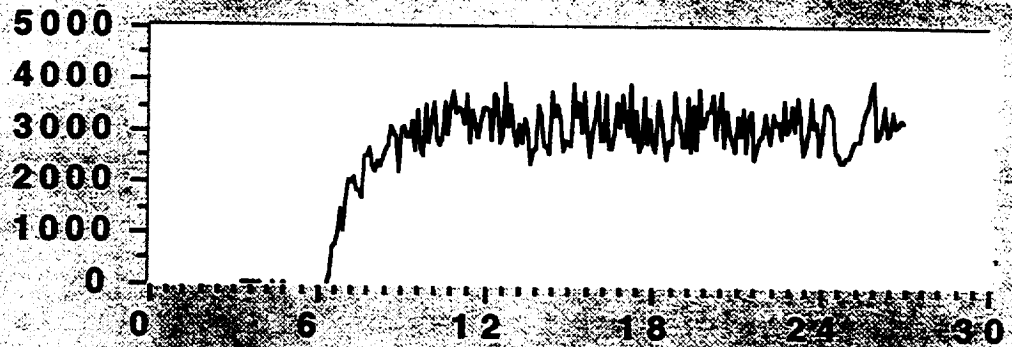
5th Wheel
Velocity,
mph



Time, sec

Run84

Plot A

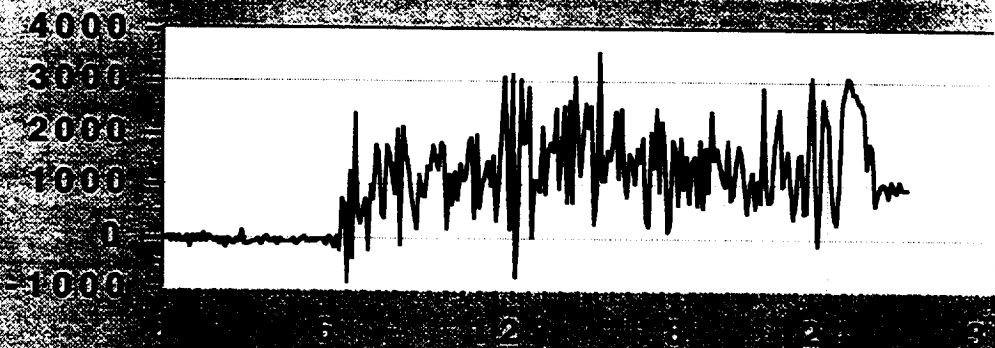


Return

Vertical
Load, lb

Plot B

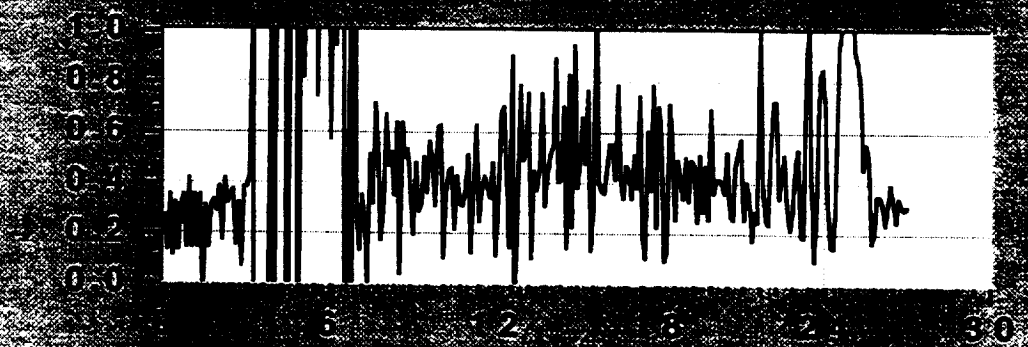
Time, sec



Drag Load
#1, lb

Plot C

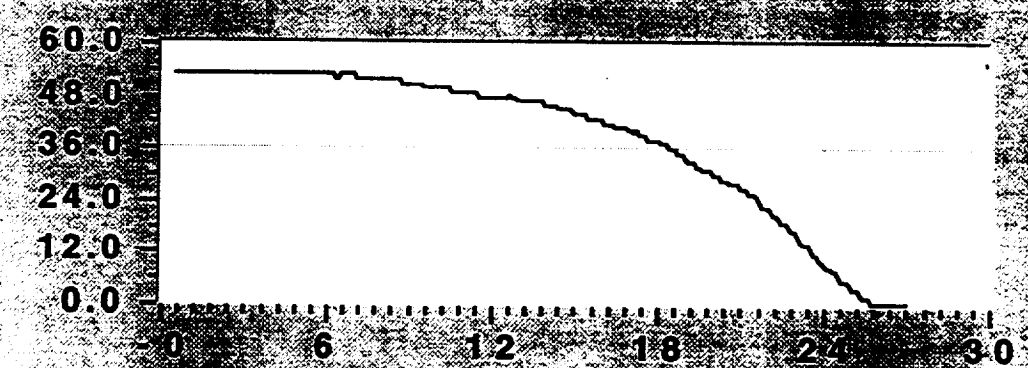
Time, sec



Drag
Friction
Coefficient

Plot D

Time, sec



5th Wheel
Velocity,
mph

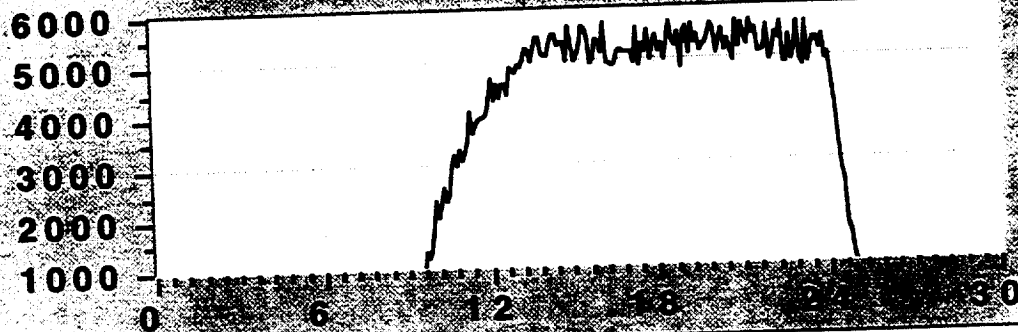
Time, sec

Run86

Plot A

Return

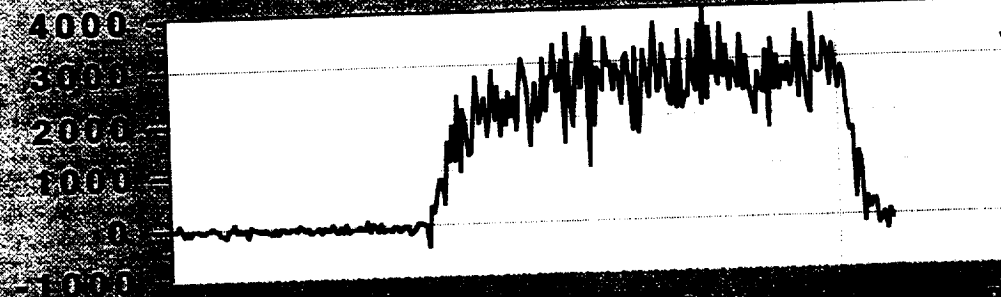
Vertical
Load, lb



Time, sec

Plot B

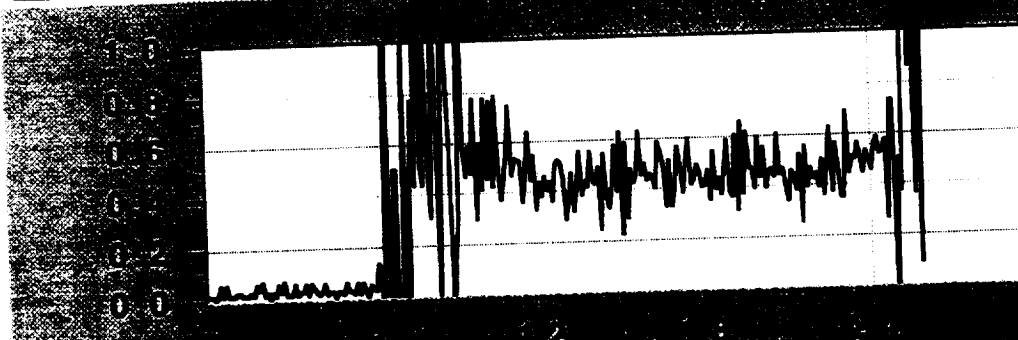
Drag Load
#1, lb



Time, sec

Plot C

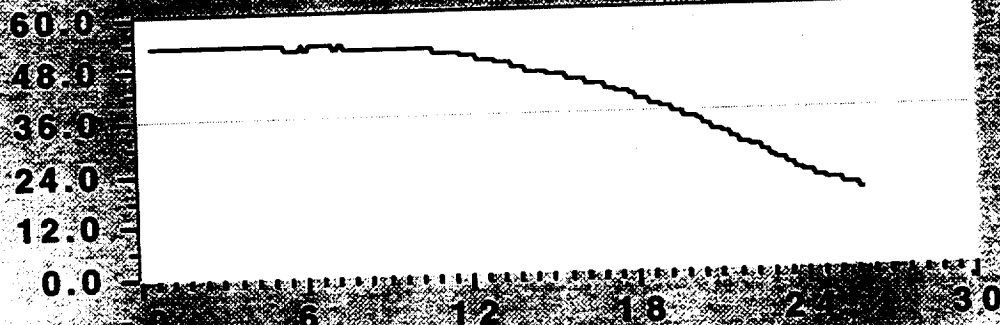
Drag
Friction
Coefficient



Time, sec

Plot D

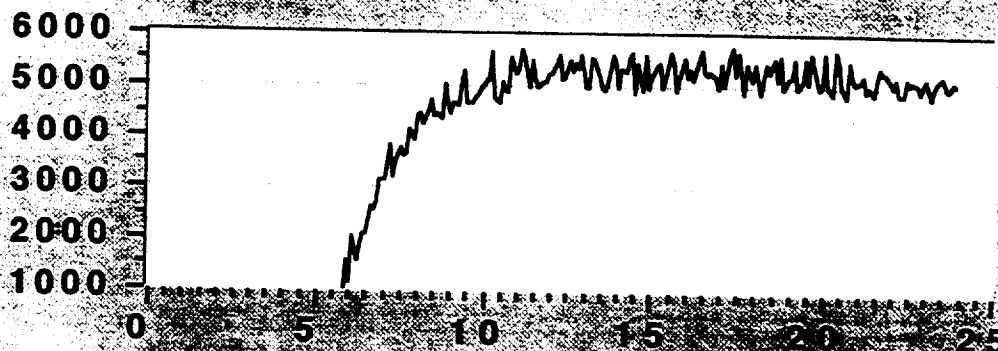
5th Wheel
Velocity,
mph



Time, sec

Run87

Plot A

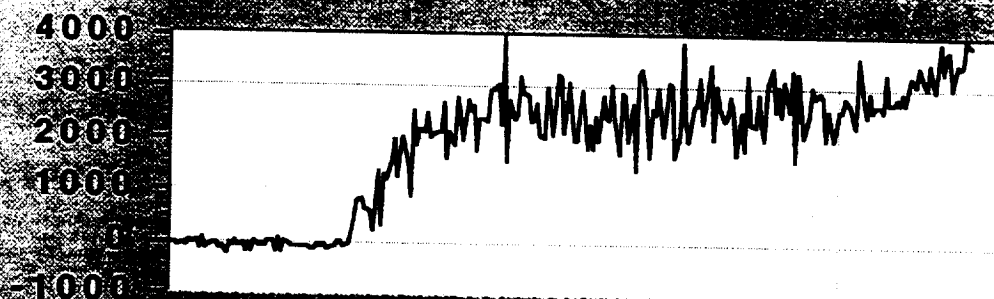


Return

Vertical
Load, lb

Plot B

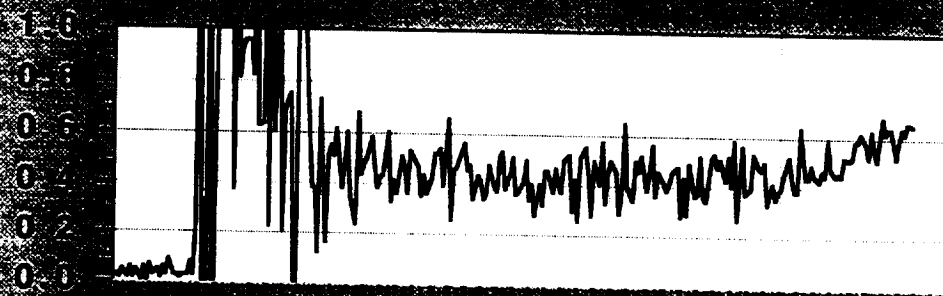
Time, sec



Drag Load
#1, lb

Plot C

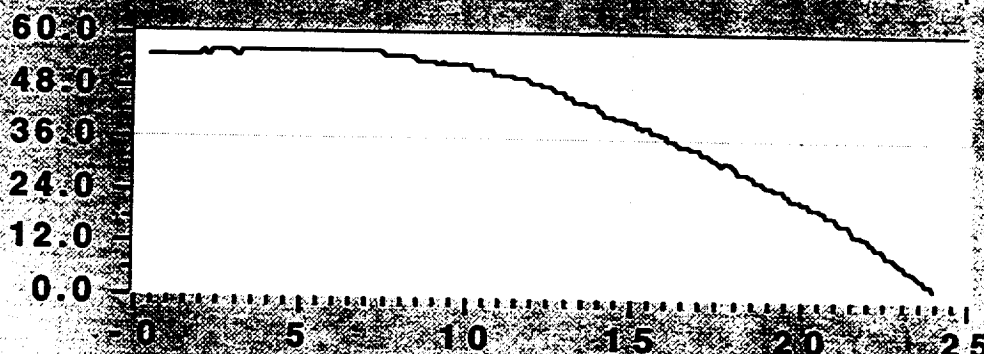
Time, sec



Drag
Friction
Coefficient

Plot D

Time, sec



5th Wheel
Velocity,
mph

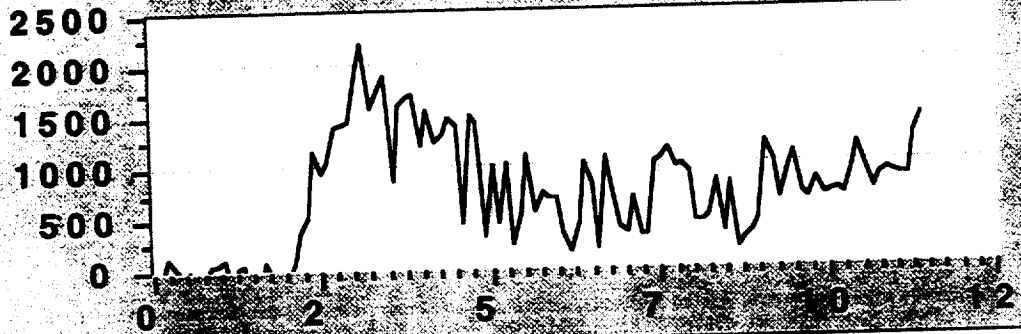
Time, sec

Run88

Plot A

Return

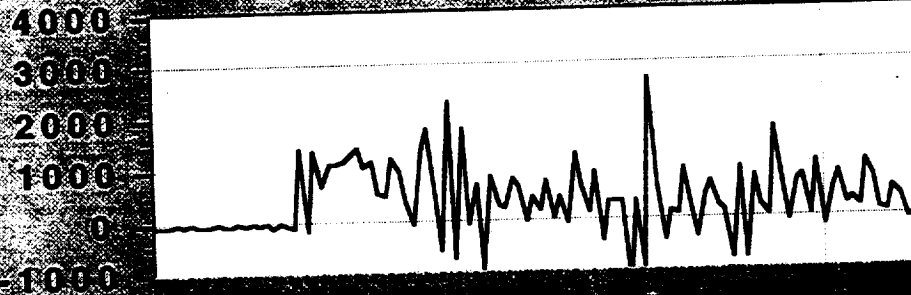
Vertical
Load, lb



Time, sec

Plot B

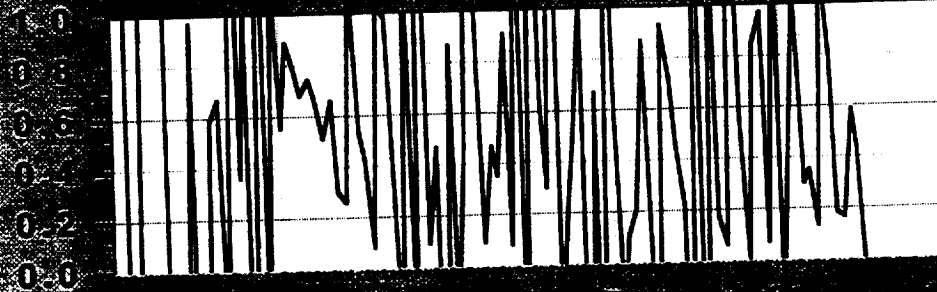
Drag Load
#1, lb



Time, sec

Plot C

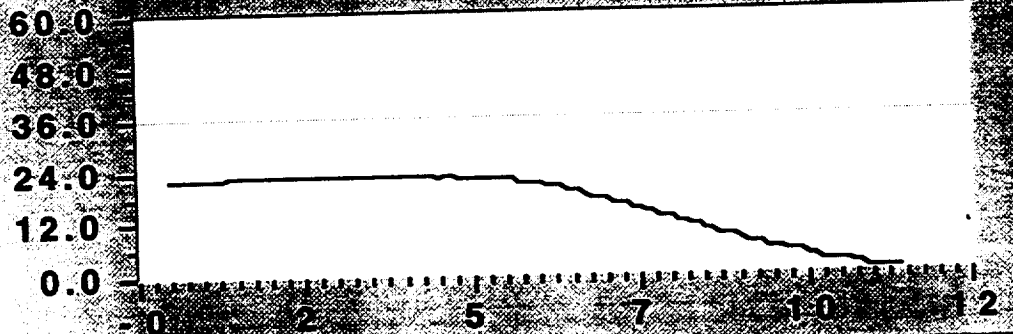
Drag
Friction
Coefficient



Time, sec

Plot D

5th Wheel
Velocity,
mph



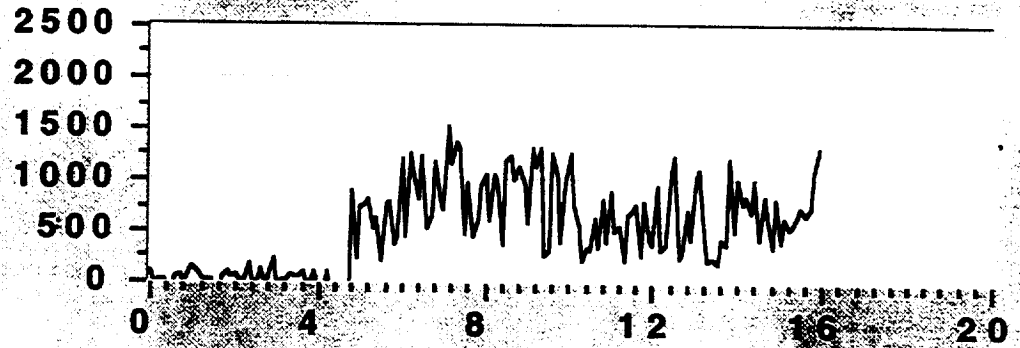
Time, sec

Run89

Plot A

Return

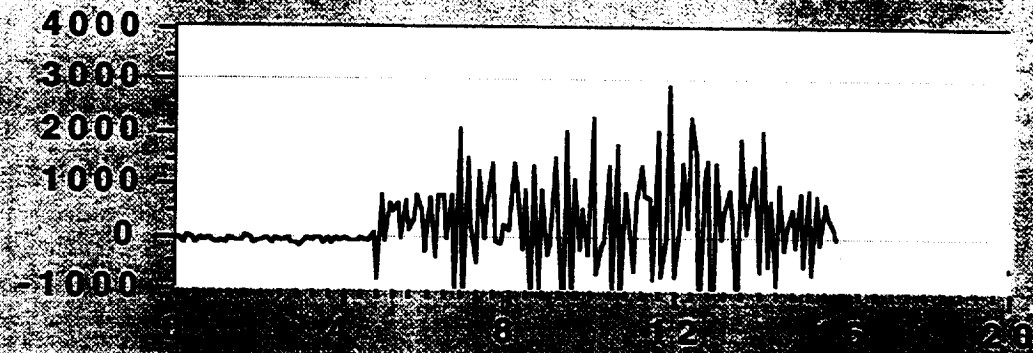
Vertical
Load, lb



Plot B

Time, sec

Drag Load
#1, lb



Plot C

Time, sec

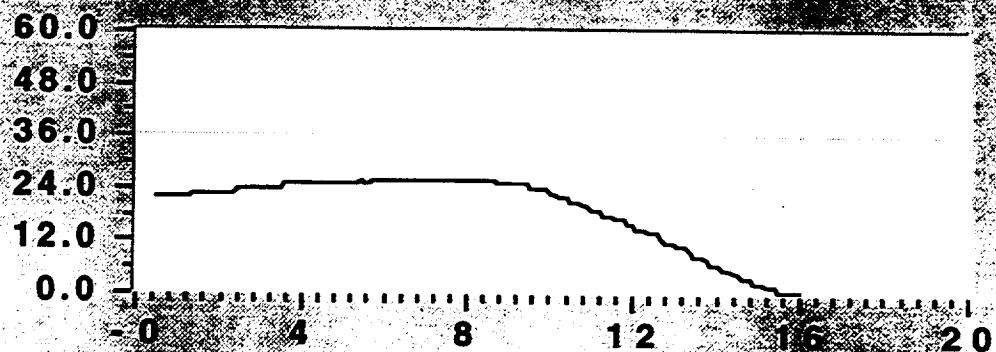
Drag
Friction
Coefficient



Plot D

Time, sec

5th Wheel
Velocity,
mph



Time, sec

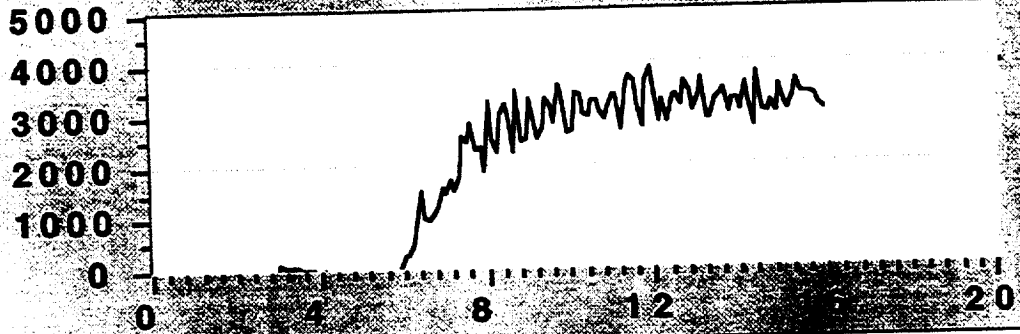
Run90

Plot A



Return

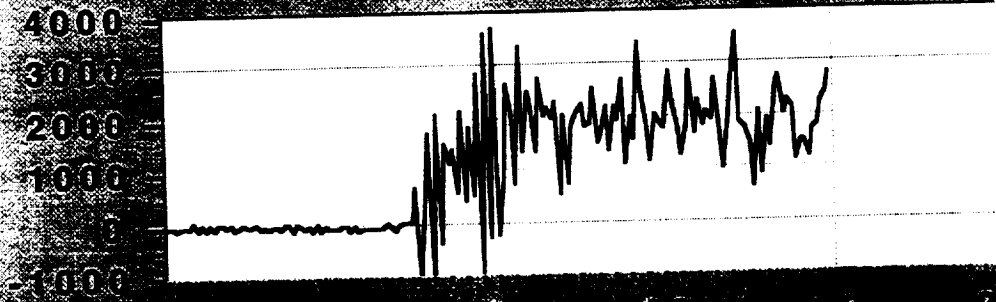
Vertical
Load, lb



Time, sec

Plot B

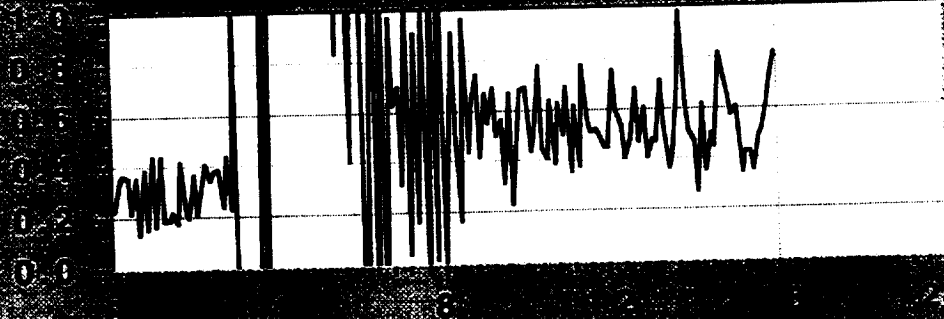
Drag Load
#1, lb



Time, sec

Plot C

Drag
Friction
Coefficient



Time, sec

Plot D

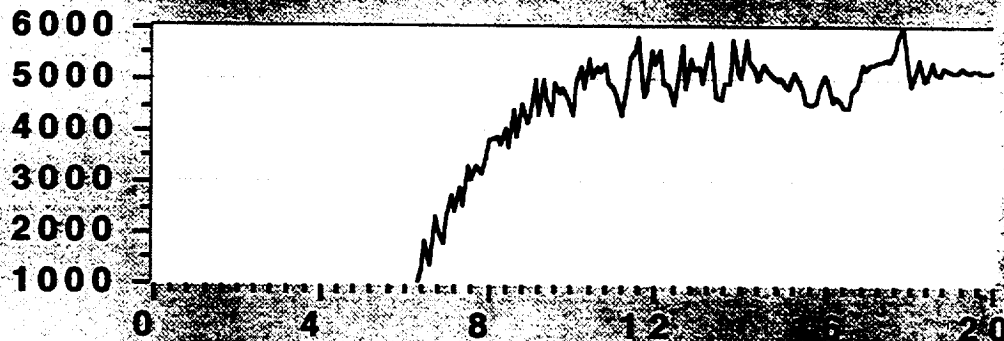
5th Wheel
Velocity,
mph



Time, sec

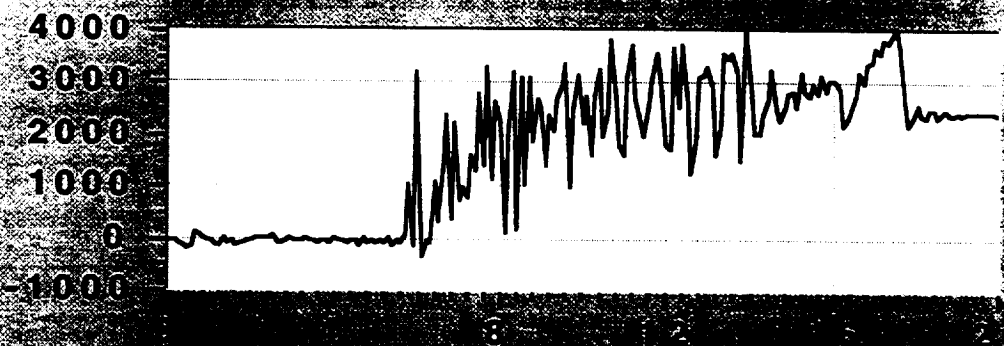
Run91

Plot A



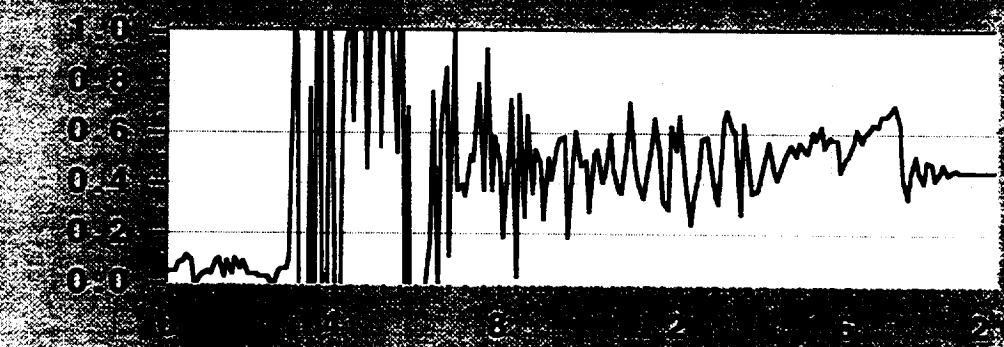
Plot B

Time, sec



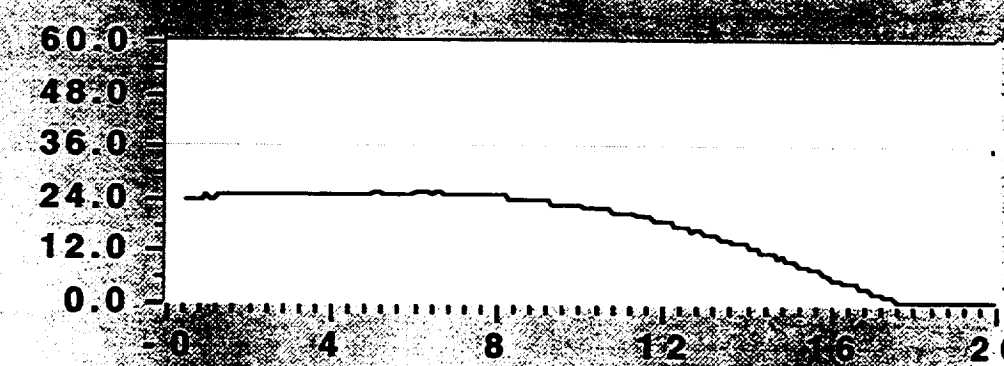
Plot C

Time, sec



Plot D

Time, sec



Return

Vertical
Load, lb

Drag Load
#1, lb

Drag
Friction
Coefficient

5th Wheel
Velocity,
mph

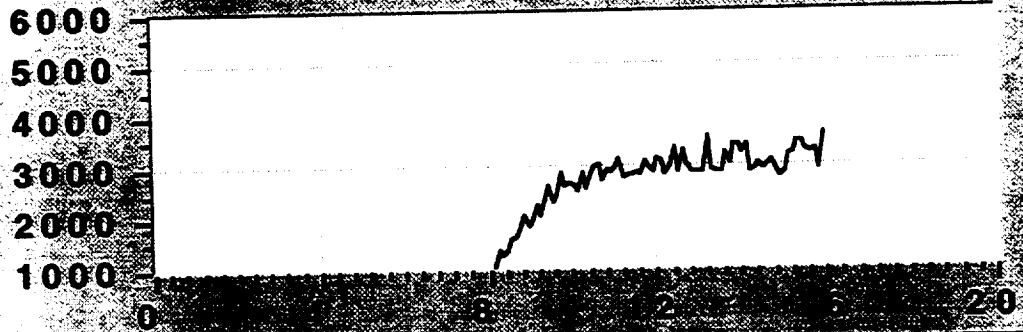
Run92

Plot A



Return

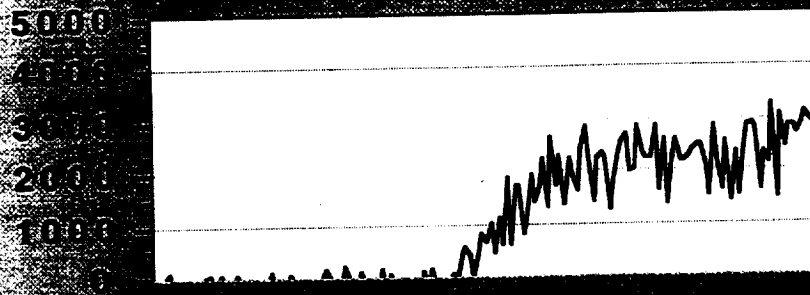
Vertical
Load, lb



Time, sec

Plot B

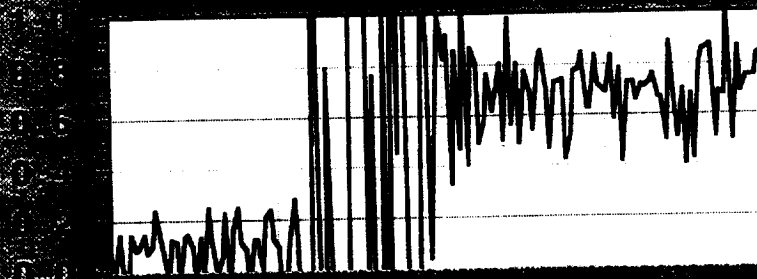
Drag Load
#1, lb



Time, sec

Plot C

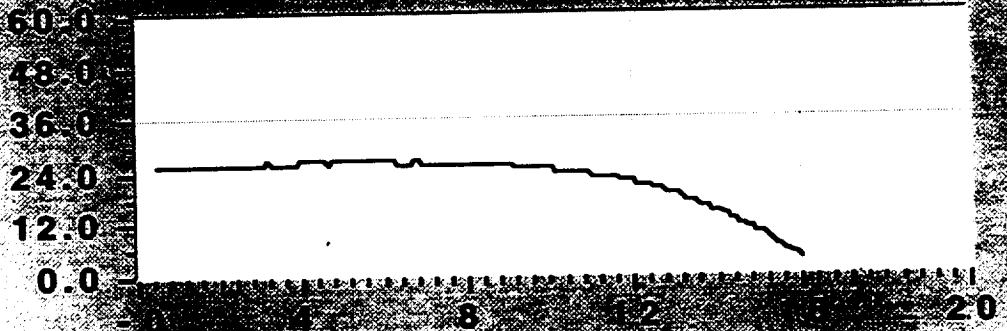
Drag
Friction
Coefficient



Time, sec

Plot D

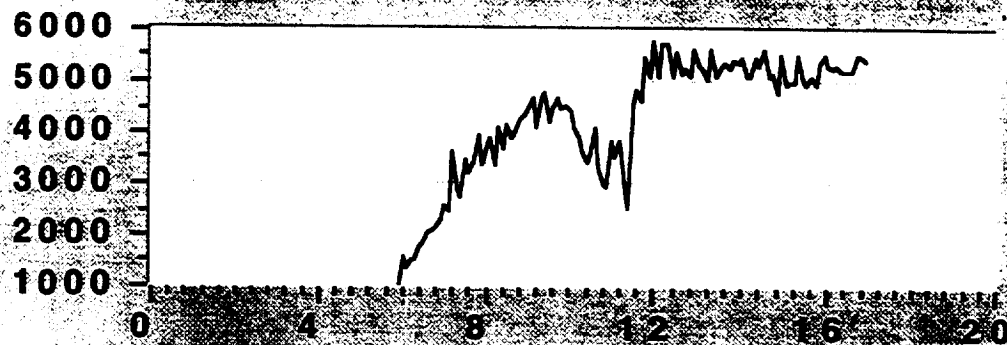
5th Wheel
Velocity,
mph



Time, sec

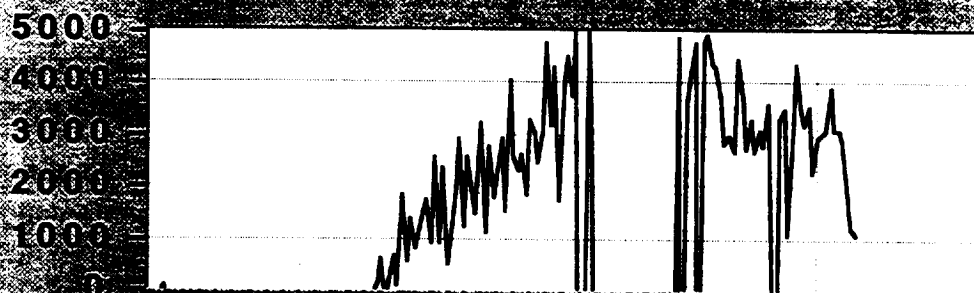
Run93

Plot A



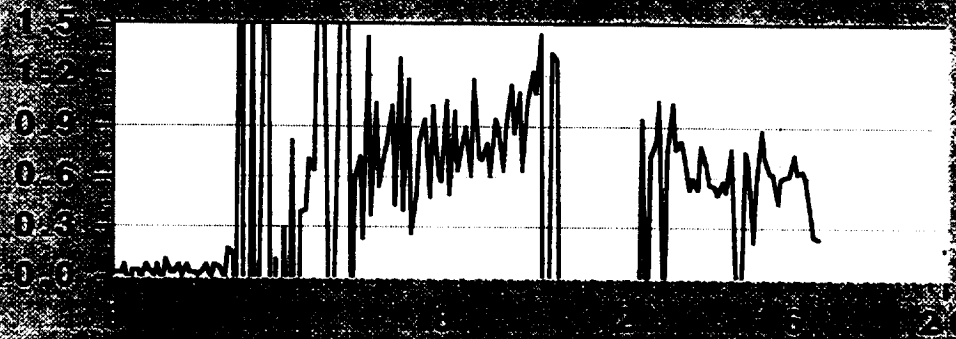
Plot B

Time, sec



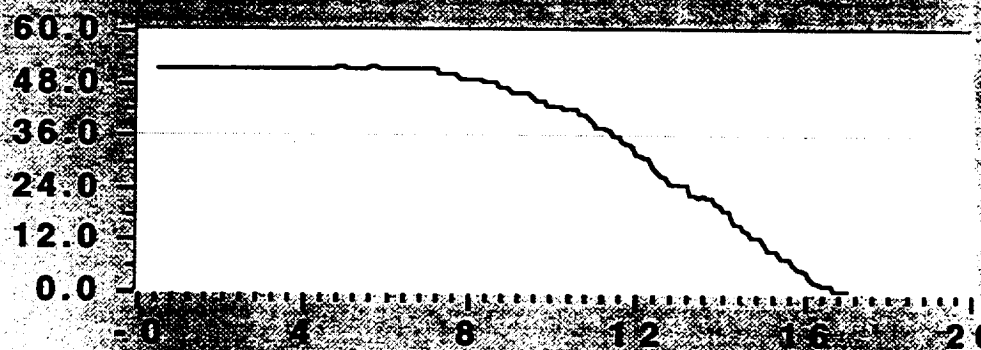
Plot C

Time, sec



Plot D

Time, sec



Return

Vertical
Load, lb

Drag Load
#1, lb

Drag
Friction
Coefficient

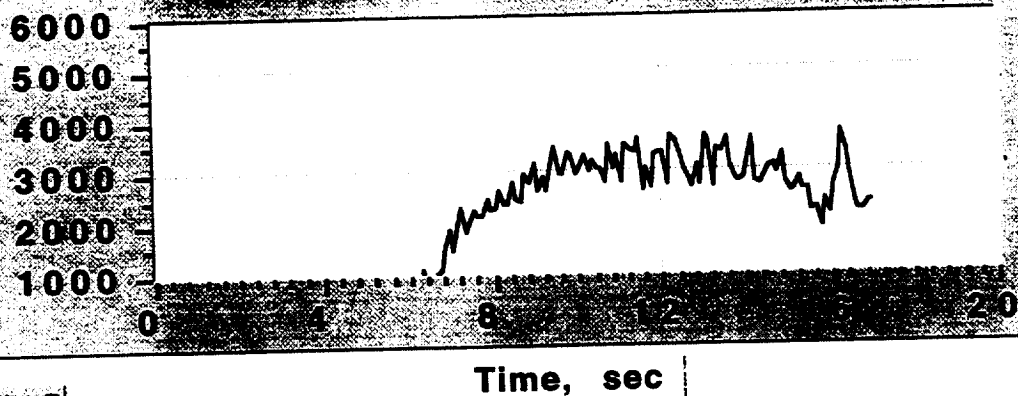
5th Wheel
Velocity,
mph

Run95

Return

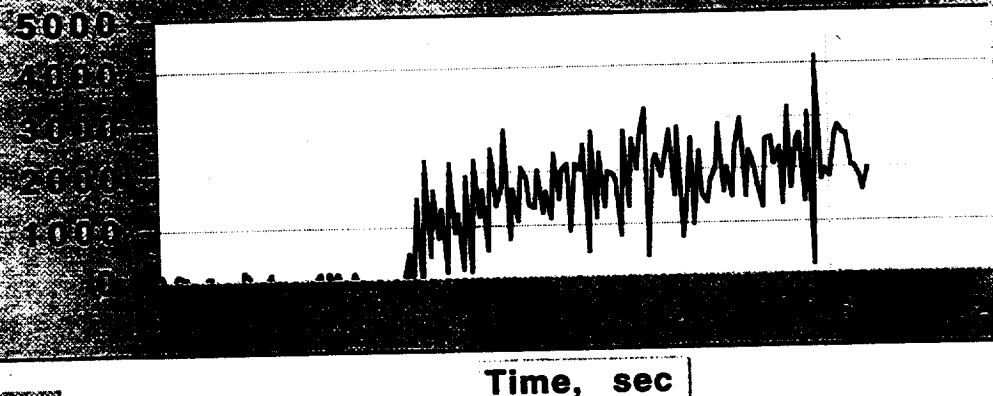
Vertical
Load, lb

Plot A



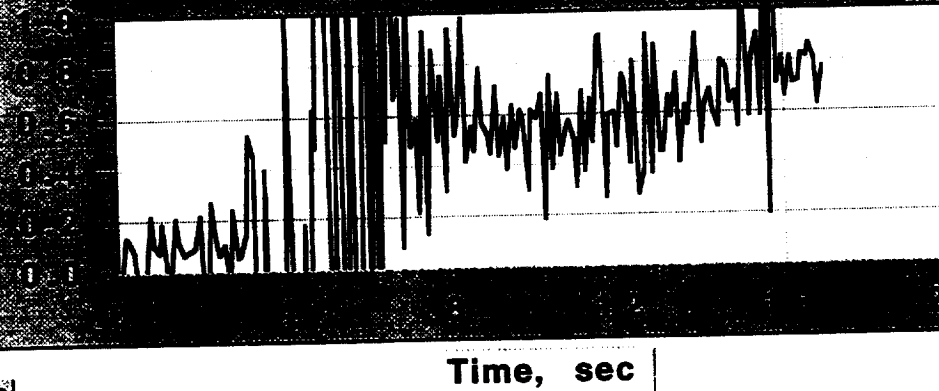
Drag Load
#1, lb

Plot B



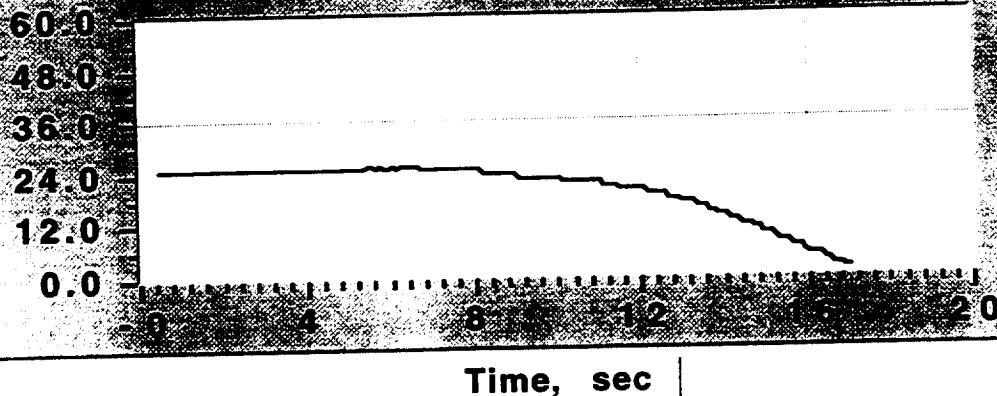
Drag
Friction
Coefficient

Plot C



5th Wheel
Velocity,
mph

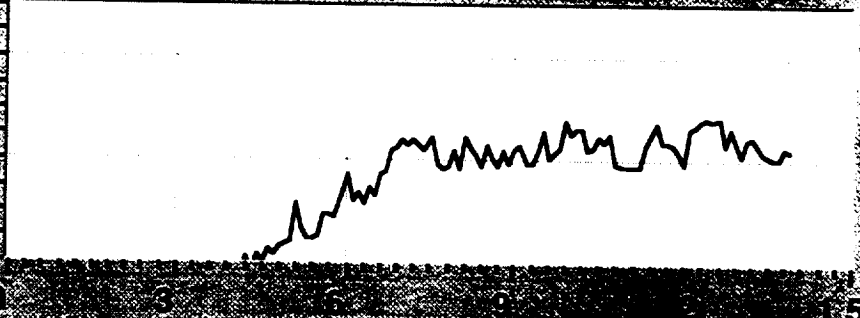
Plot D



Run102

Plot A

6000
5000
4000
3000
2000
1000



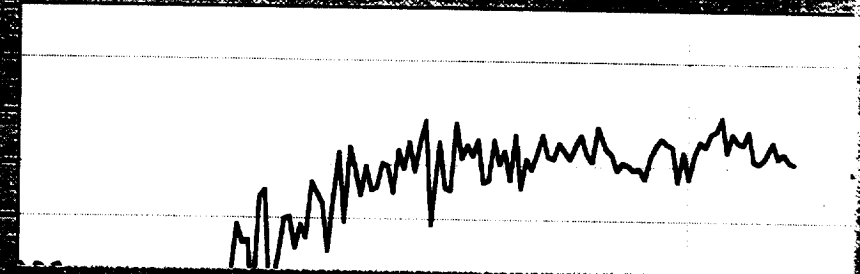
Return

Vertical
Load, lb

Plot B

Time, sec

5000
4000
3000
2000
1000

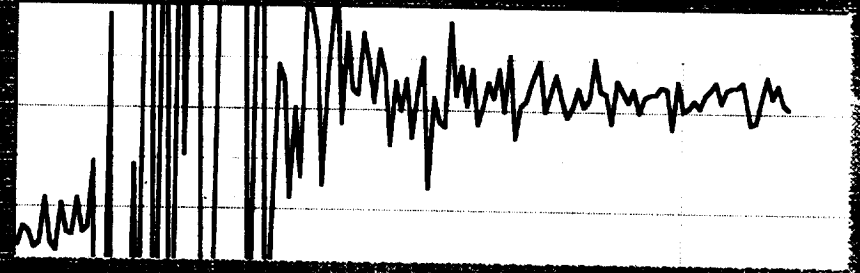


Drag Load
#1, lb

Plot C

Time, sec

1.0
0.8
0.6
0.4
0.2
0.0

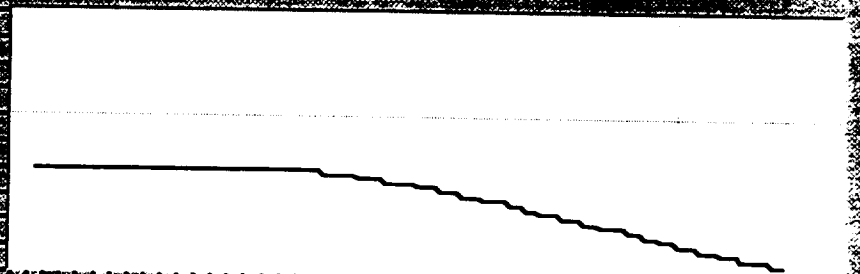


Drag
Friction
Coefficient

Plot D

Time, sec

60.0
48.0
36.0
24.0
12.0
0.0



5th Wheel
Velocity,
mph

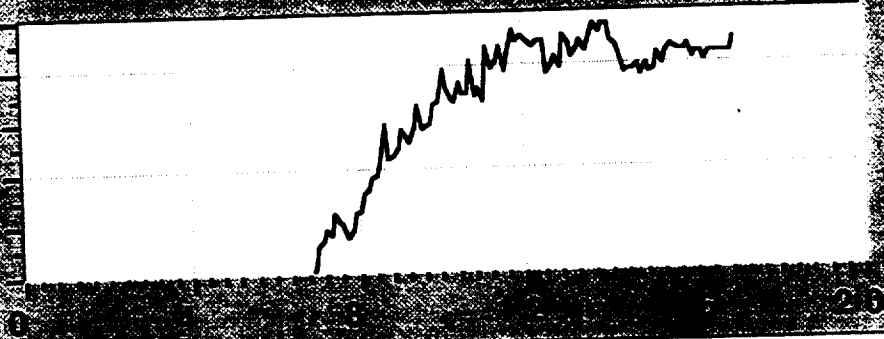
Run104

Plot A

Return

Vertical
Load, lb

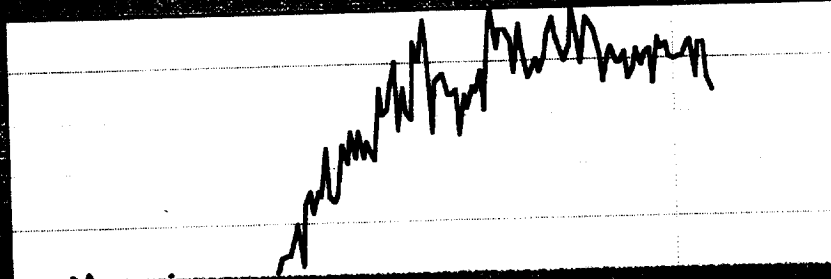
6000
5000
4000
3000
2000
1000
0



Plot B

Drag Load
#1, lb

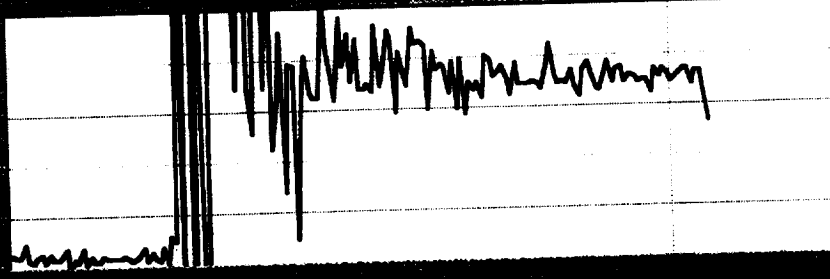
5000
4000
3000
2000
1000
0



Plot C

Drag
Friction
Coefficient

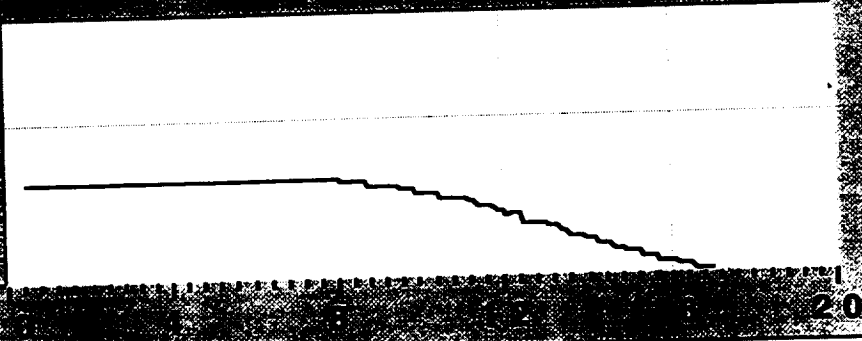
0.8
0.6
0.4
0.2
0.0



Plot D

5th Wheel
Velocity,
mph

60.0
48.0
36.0
24.0
12.0
0.0



Time, sec

Run106

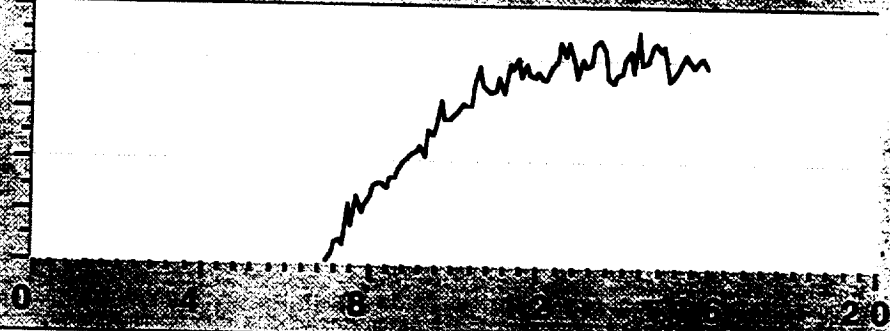
Plot A



Return

Vertical
Load, lb

6000
5000
4000
3000
2000
1000

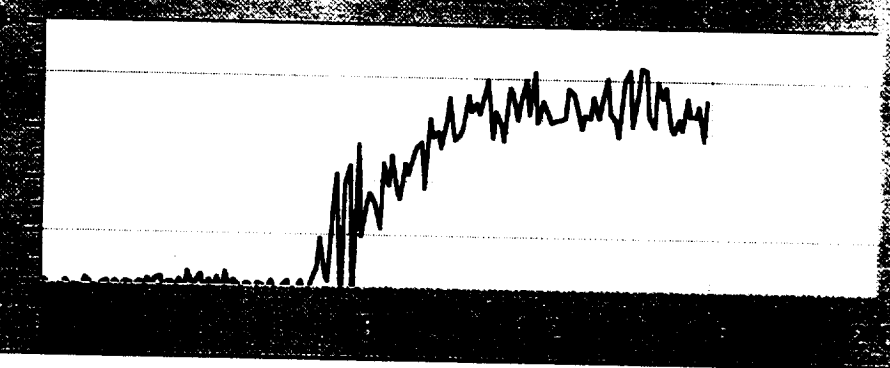


Plot B

Time, sec

Drag Load
#1, lb

5000
4000
3000
2000
1000

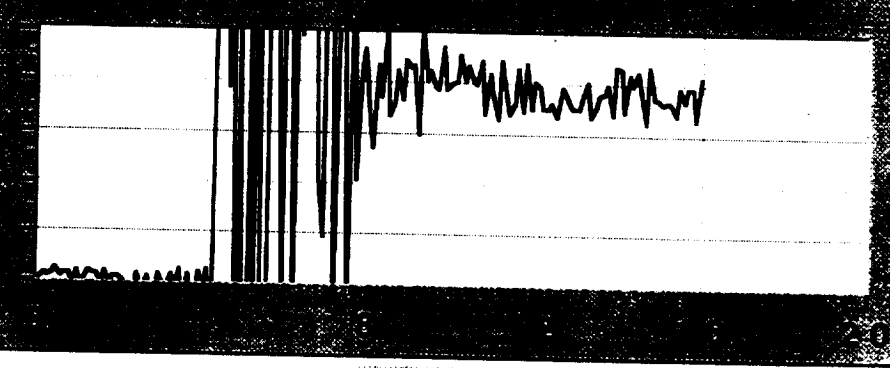


Plot C

Time, sec

Drag
Friction
Coefficient

1.0
0.8
0.6
0.4
0.2
0.0

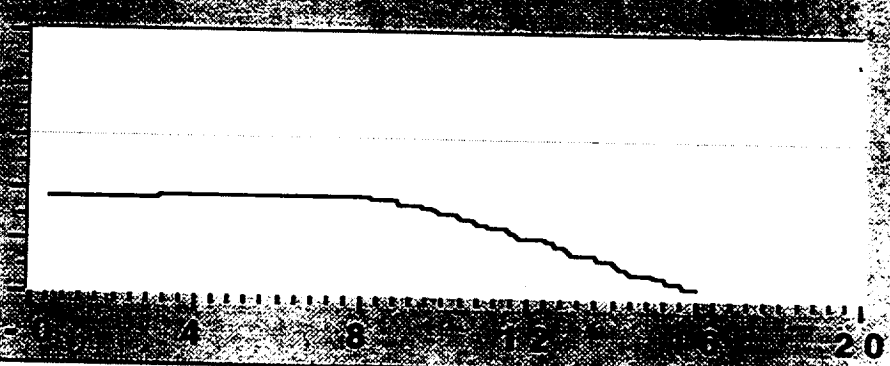


Plot D

Time, sec

5th Wheel
Velocity,
mph

60.0
48.0
36.0
24.0
12.0
0.0

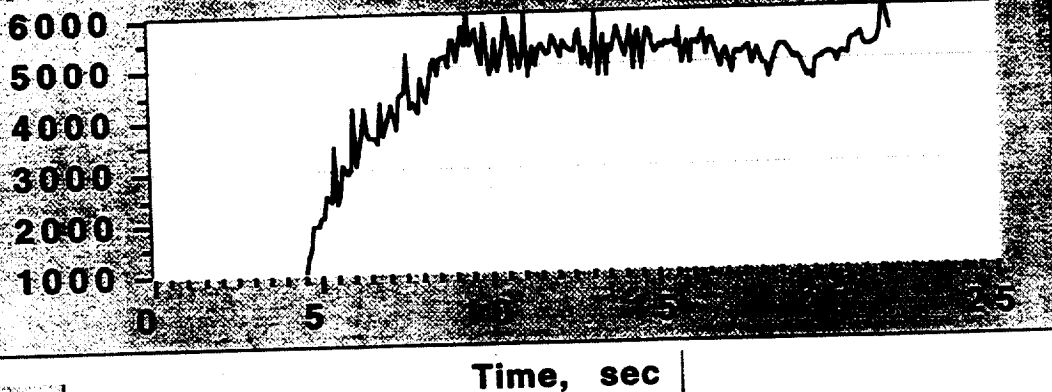


Run107

Plot A

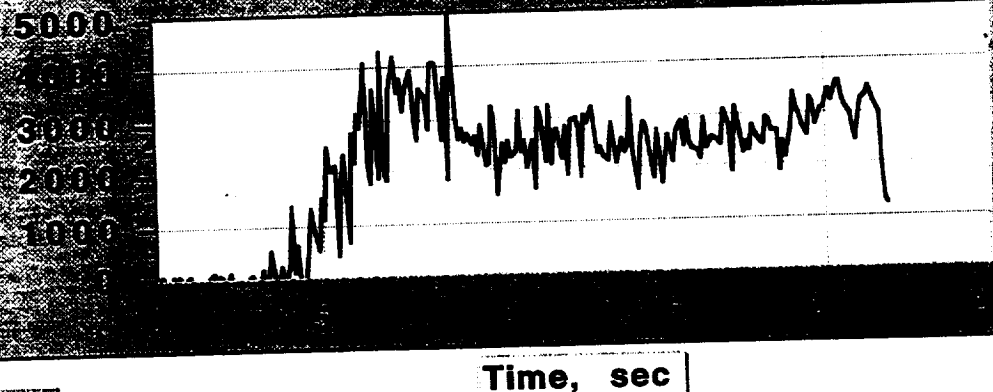
Return

Vertical
Load, lb



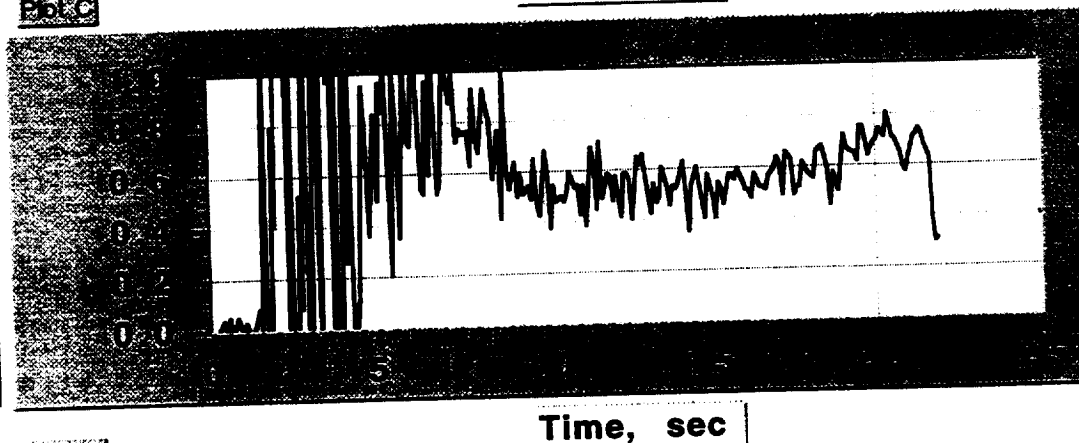
Plot B

Drag Load
#1, lb



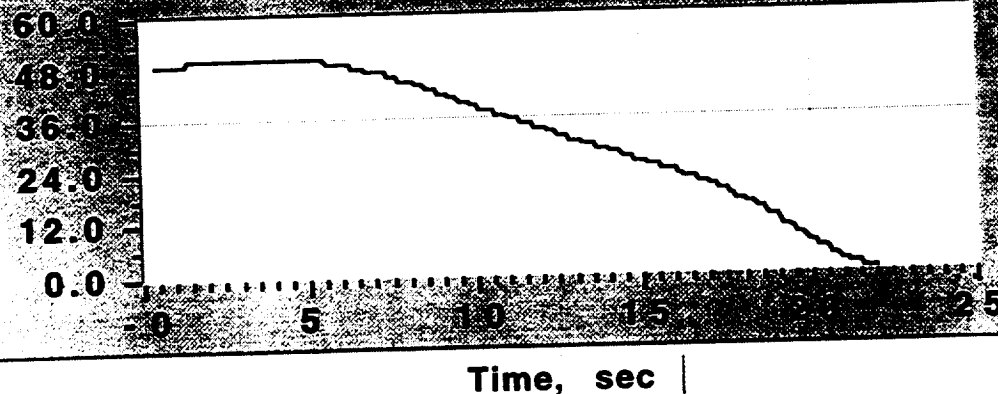
Plot C

Drag
Friction
Coefficient



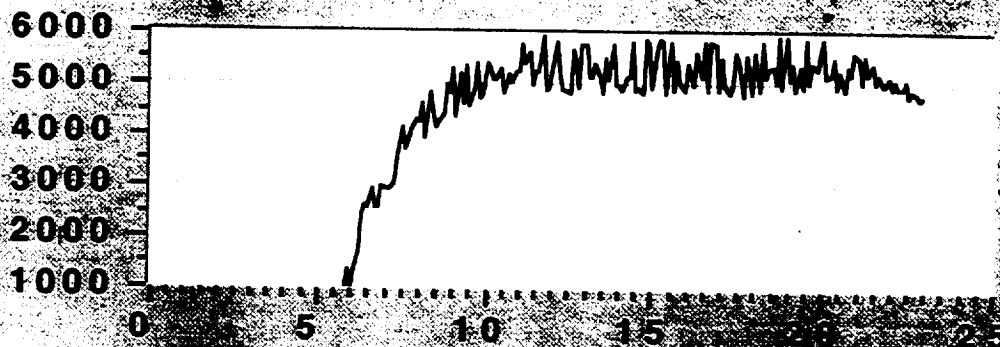
Plot D

5th Wheel
Velocity,
mph



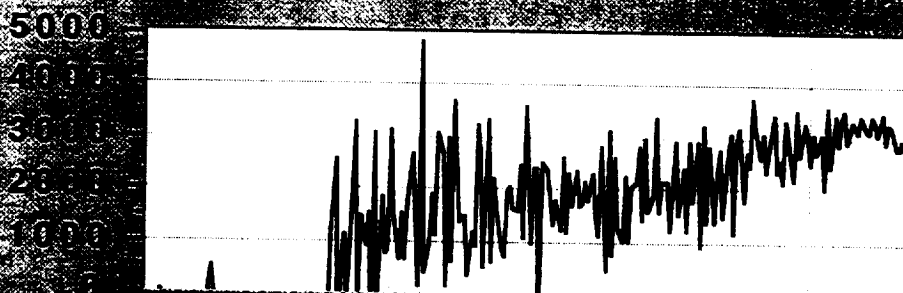
Run108

Plot A



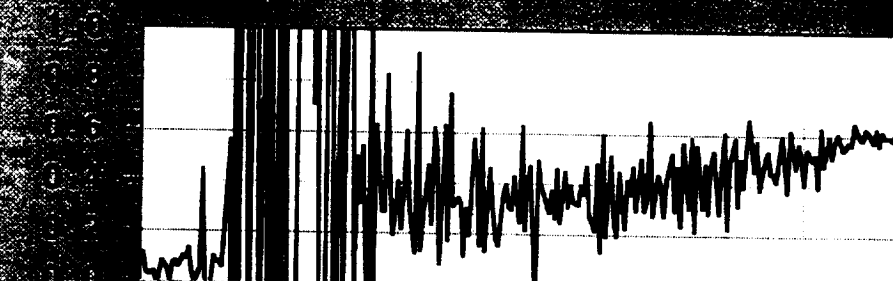
Plot B

Time, sec



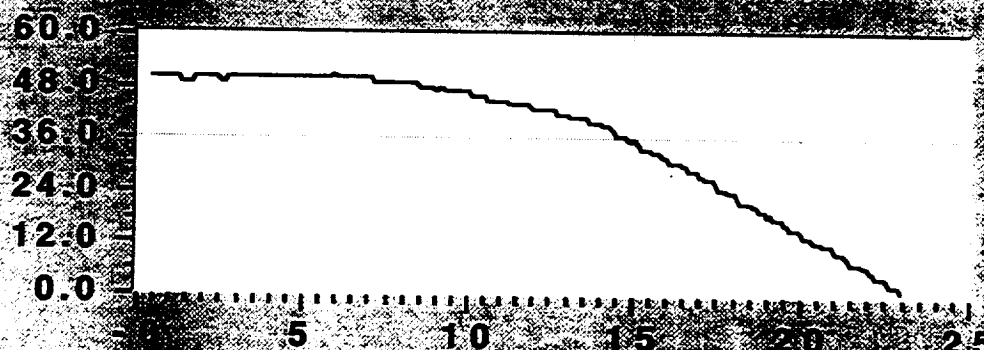
Plot C

Time, sec



Plot D

Time, sec



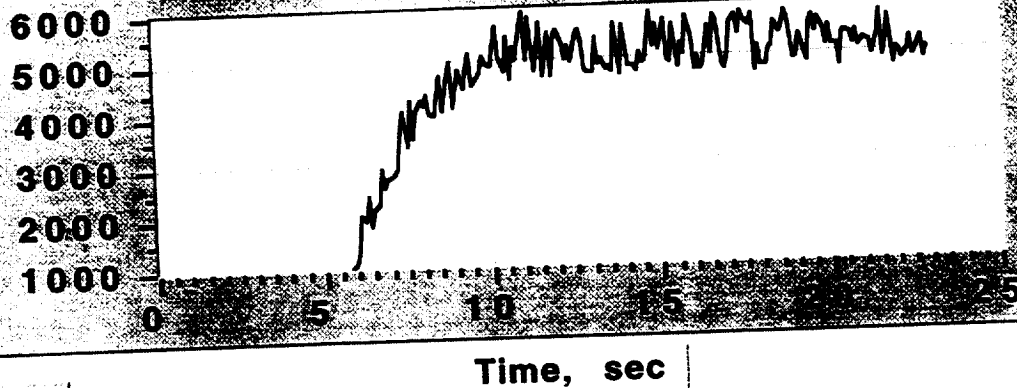
Run109



Return

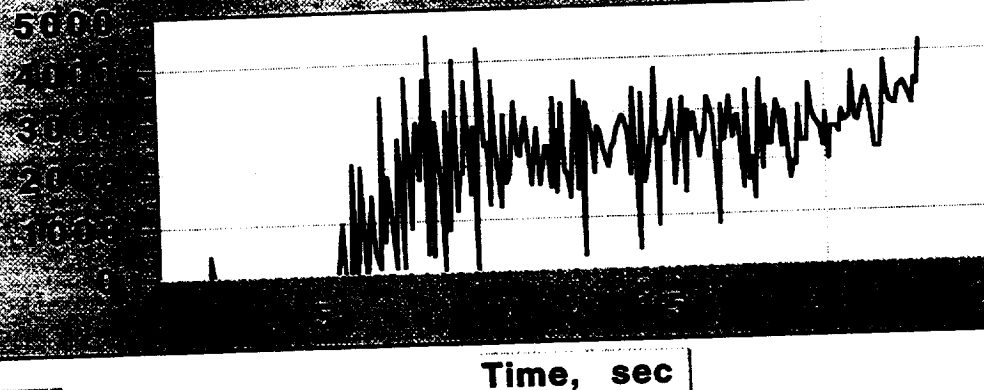
Vertical
Load, lb

Plot A



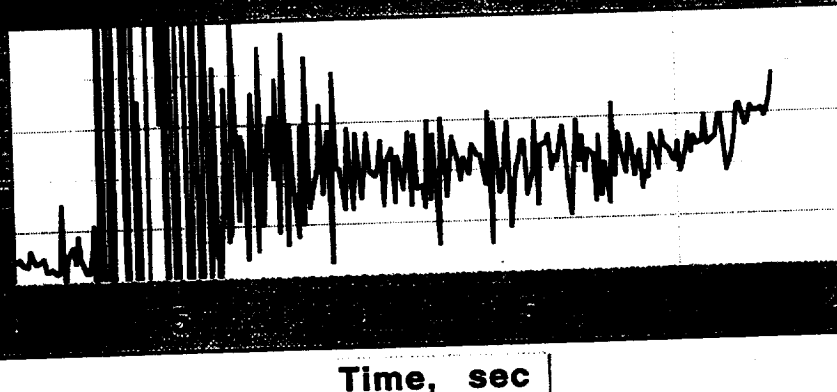
Drag Load
#1, lb

Plot B



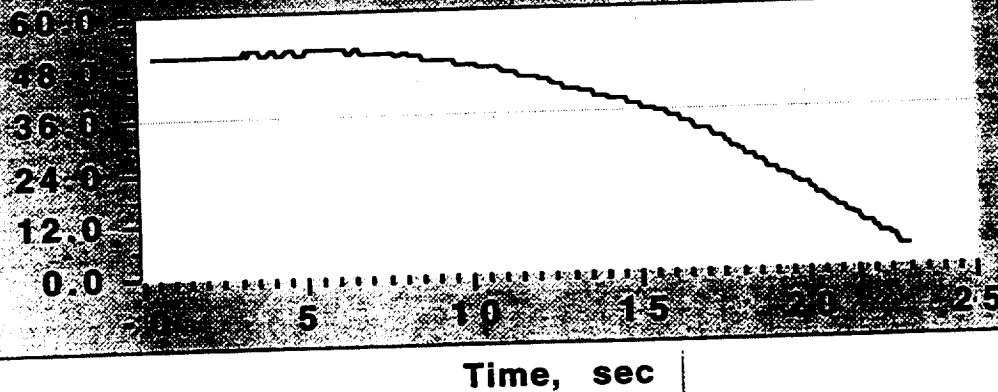
Drag
Friction
Coefficient

Plot C



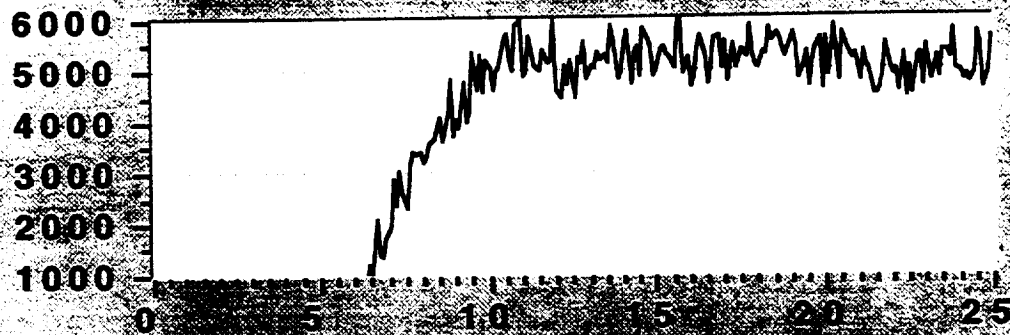
5th Wheel
Velocity,
mph

Plot D



Run110

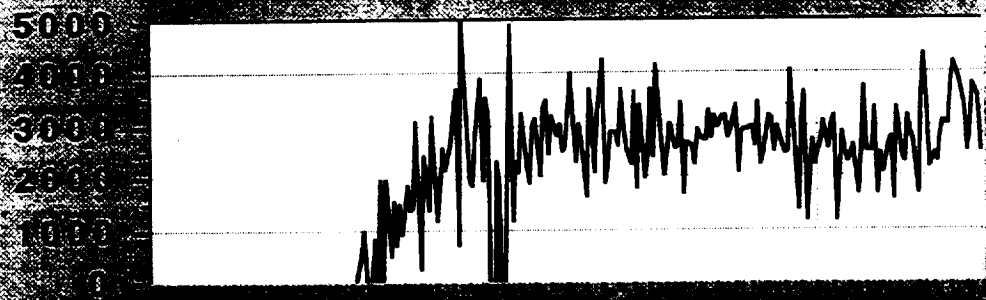
Plot A



Return

Vertical
Load, lb

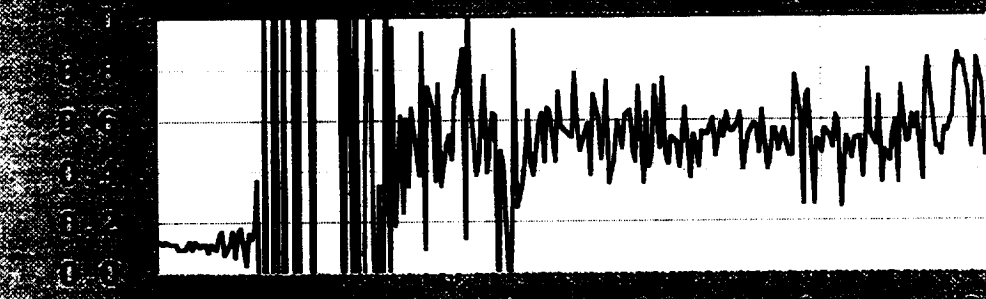
Plot B



Drag Load
#1, lb

Time, sec

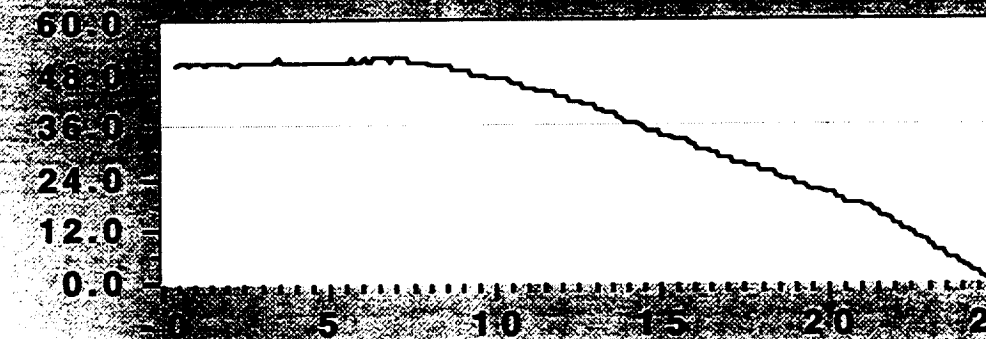
Plot C



Drag
Friction
Coefficient

Time, sec

Plot D



5th Wheel
Velocity,
mph

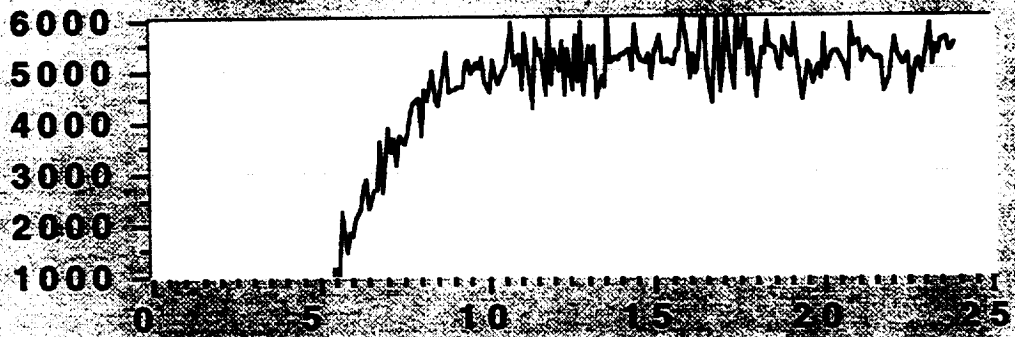
Time, sec

Run111

Return

Vertical
Load, lb

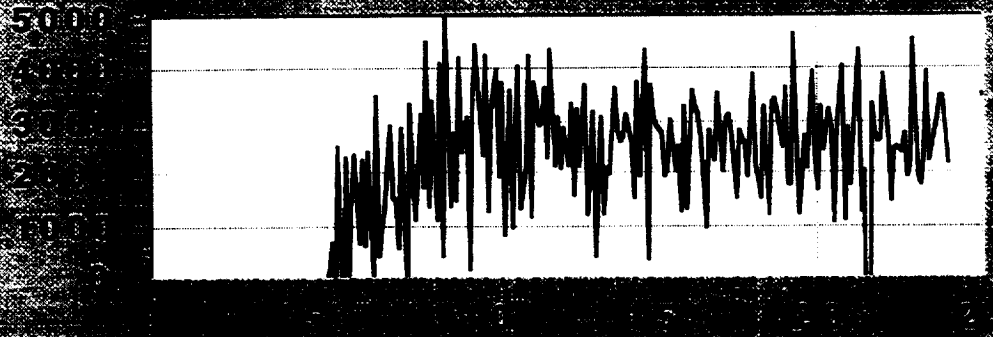
Plot A



Time, sec

Plot B

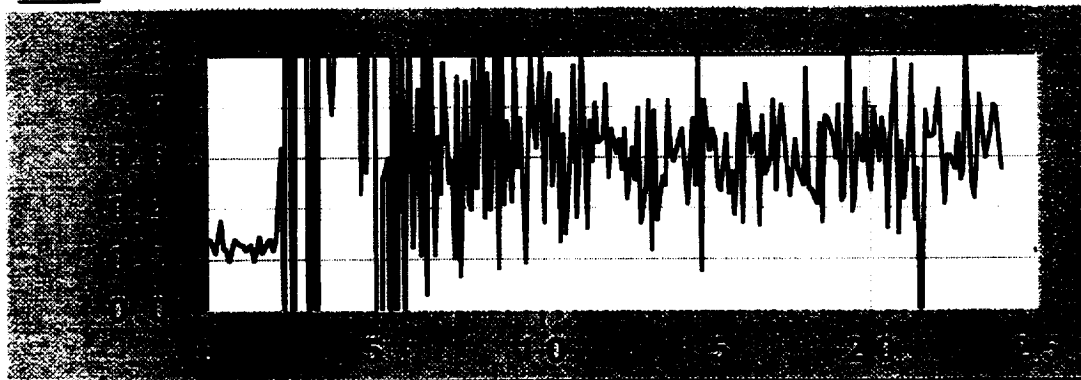
Drag Load
#1, lb



Time, sec

Plot C

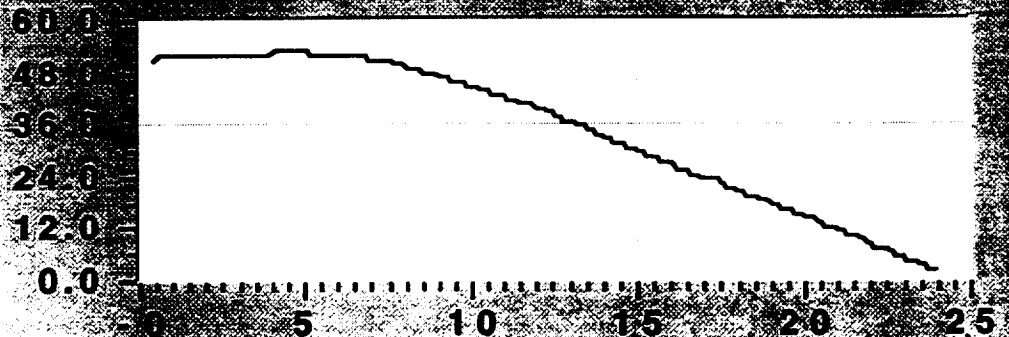
Drag
Friction
Coefficient



Time, sec

Plot D

5th Wheel
Velocity,
mph



Time, sec

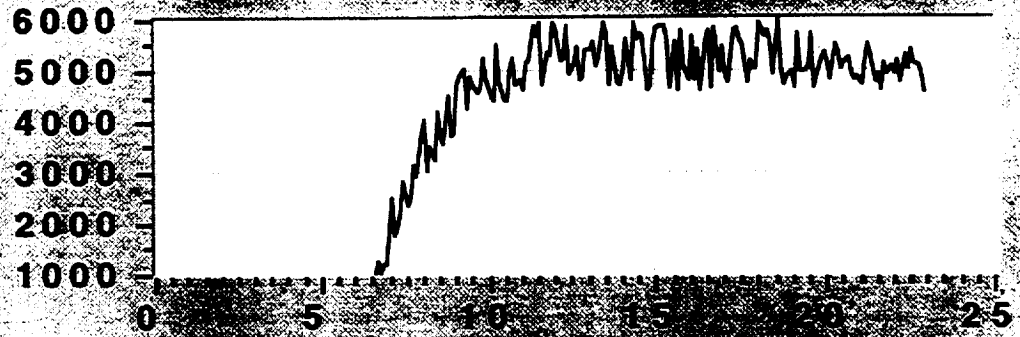
Run112

Plot A



Return

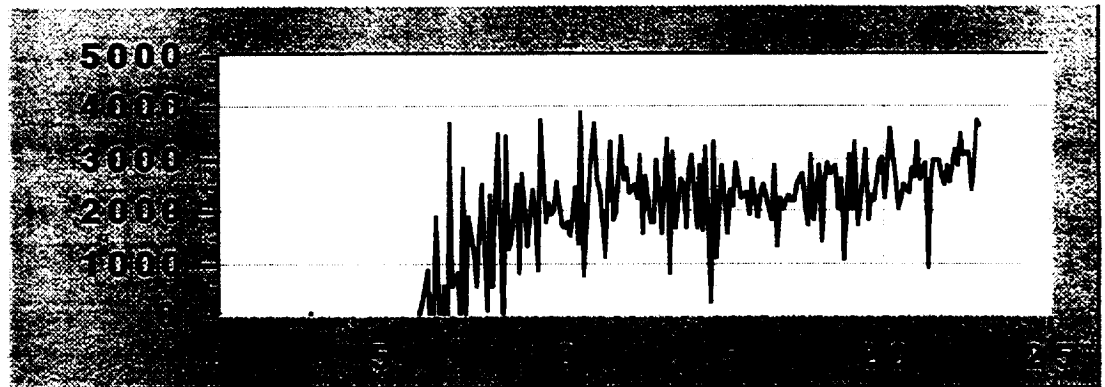
Vertical
Load, lb



Plot B

Time, sec

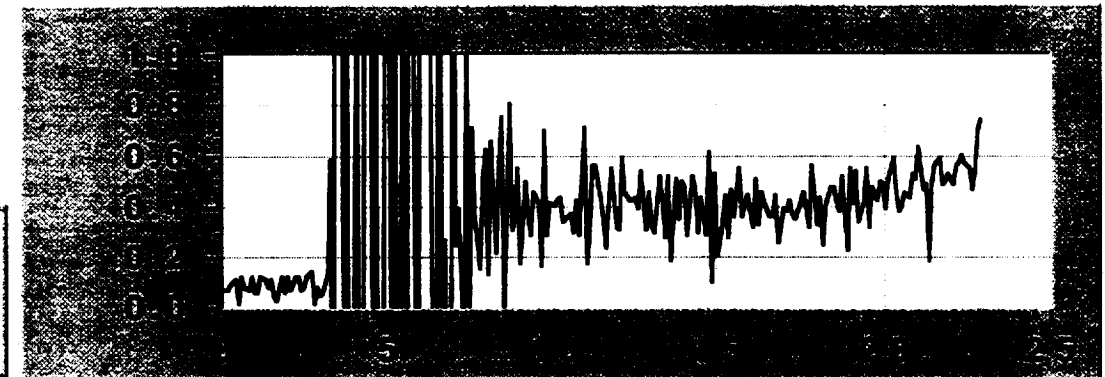
Drag Load
#1, lb



Plot C

Time, sec

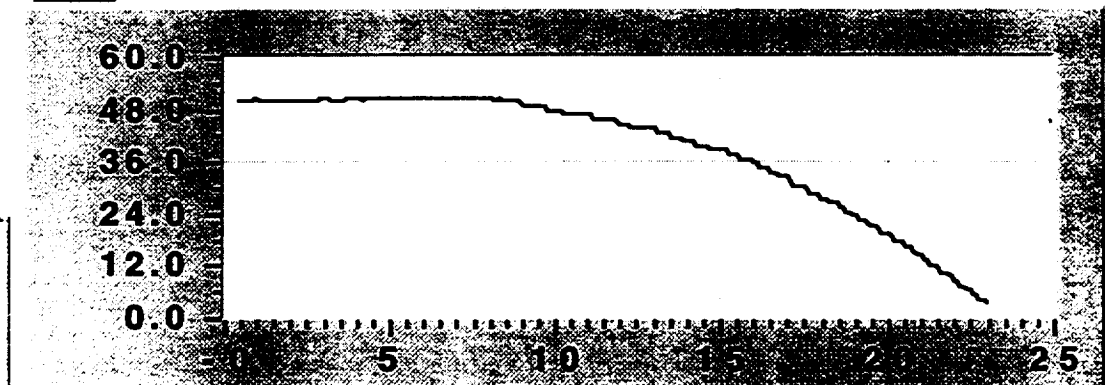
Drag
Friction
Coefficient



Plot D

Time, sec

5th Wheel
Velocity,
mph



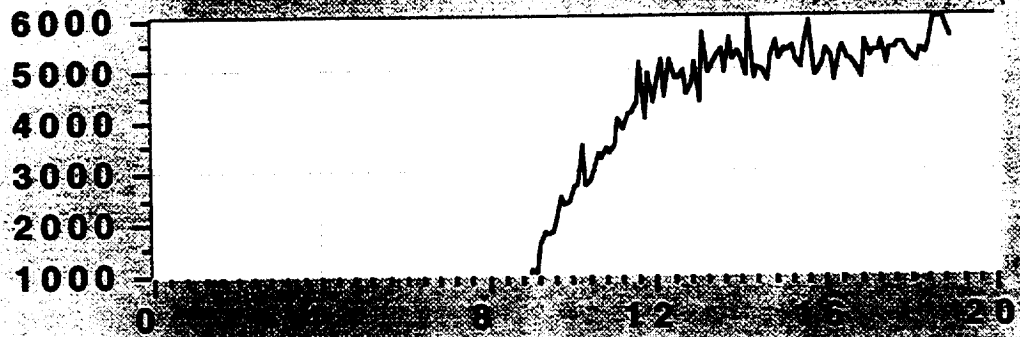
Time, sec

Run113

Plot A

Return

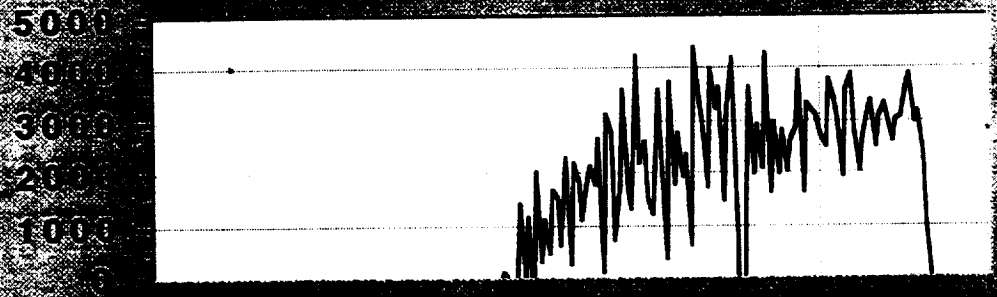
Vertical
Load, lb



Plot B

Time, sec

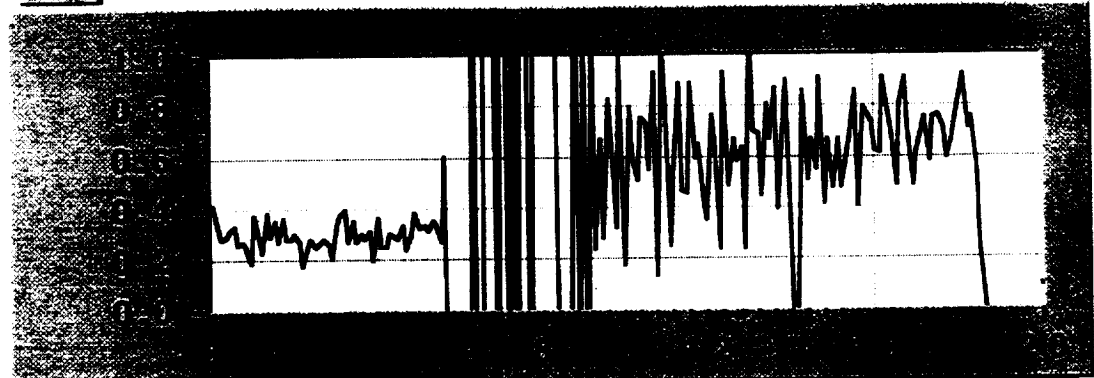
Drag Load
#1, lb



Plot C

Time, sec

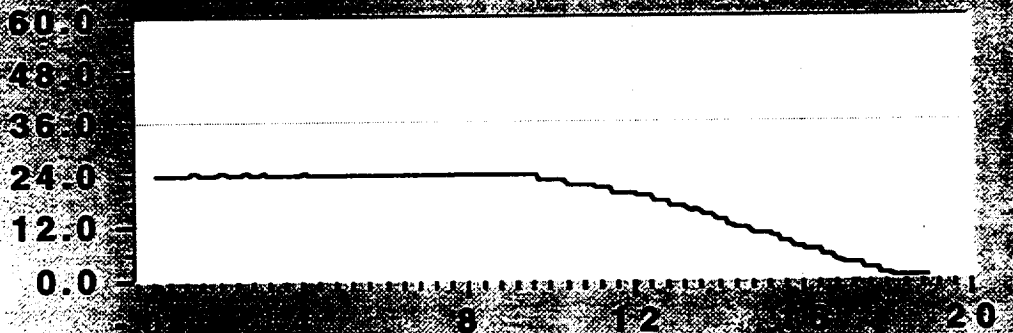
Drag
Friction
Coefficient



Plot D

Time, sec

5th Wheel
Velocity,
mph



Time, sec

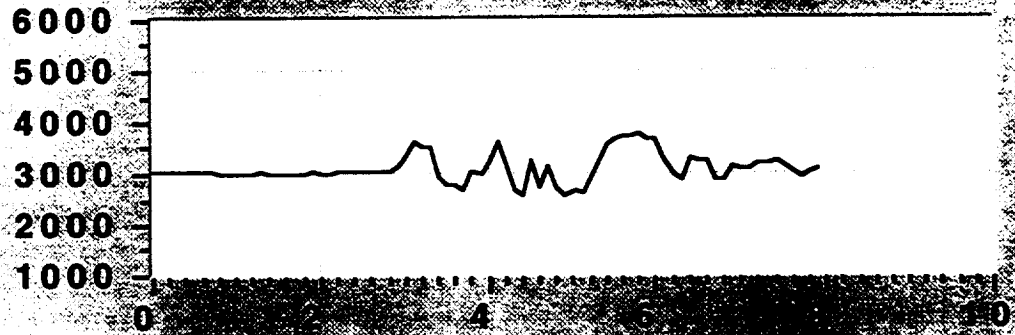
Run115

Plot A



Return

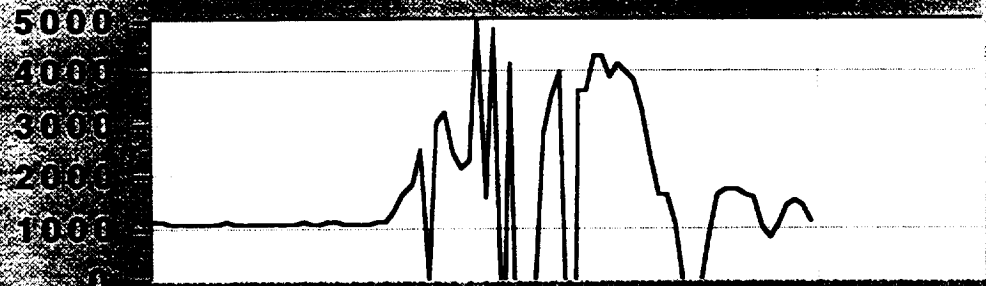
Vertical
Load, lb



Plot B

Time, sec

Drag Load
#1, lb



Plot C

Time, sec

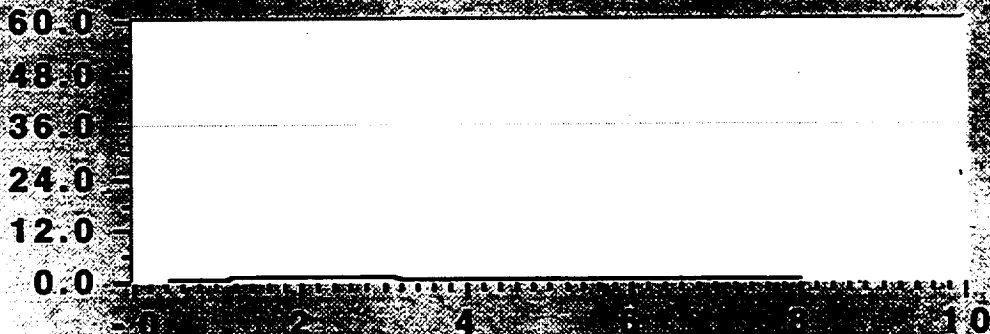
Drag
Friction
Coefficient



Plot D

Time, sec

5th Wheel
Velocity,
mph



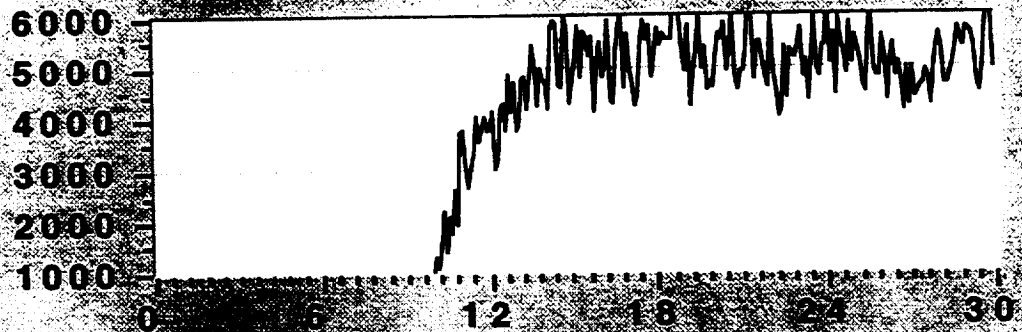
Time, sec

Run 117

Plot A

Return

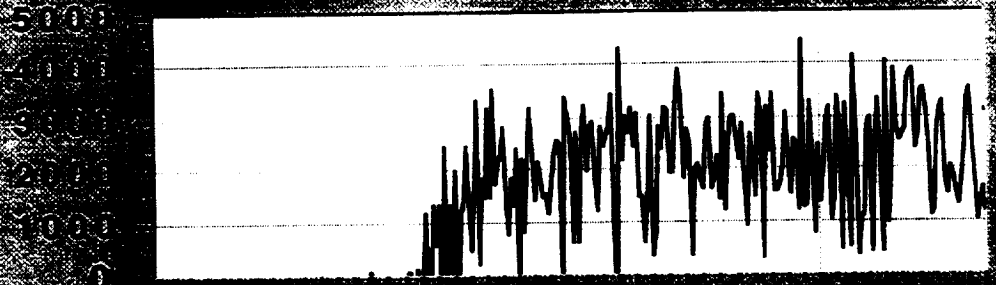
Vertical
Load, lb



Time, sec

Plot B

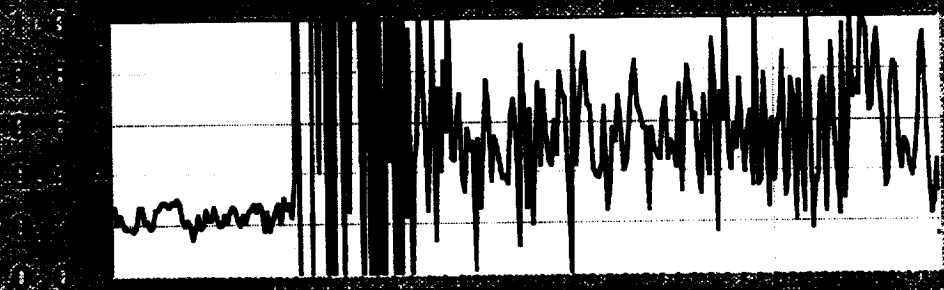
Drag Load
#1, lb



Time, sec

Plot C

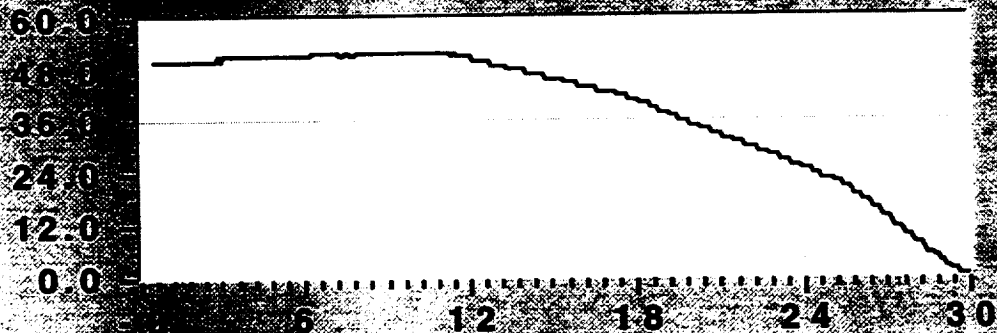
Drag
Friction
Coefficient



Time, sec

Plot D

5th Wheel
Velocity,
mph



Time, sec

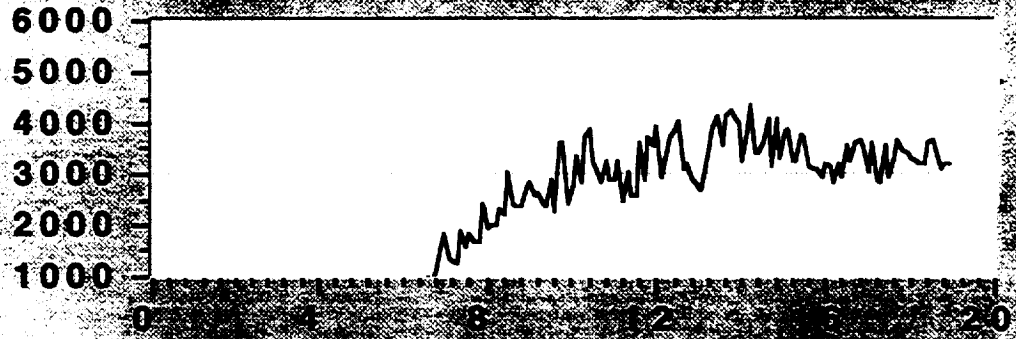
Run118



Return

Vertical
Load, lb

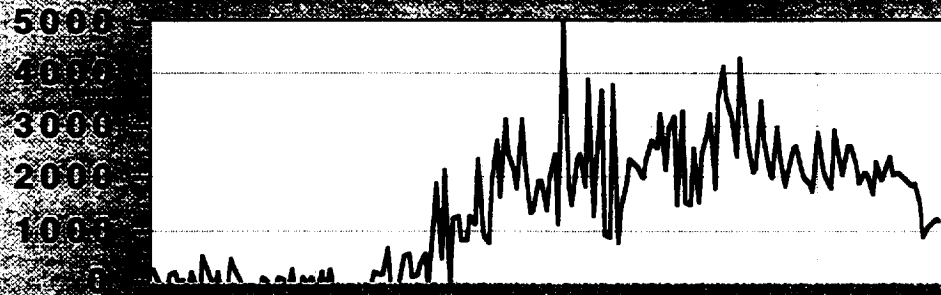
Plot A



Plot B

Time, sec

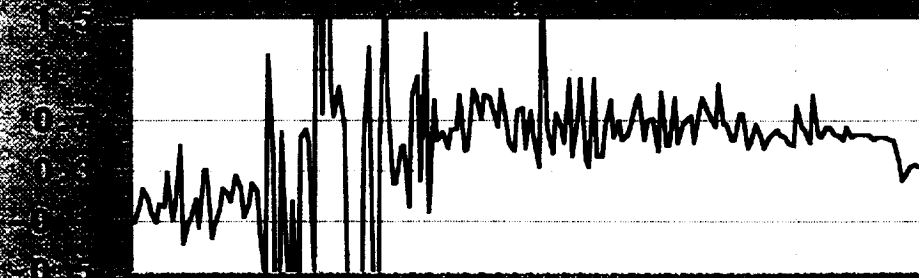
Drag Load
#1, lb



Plot C

Time, sec

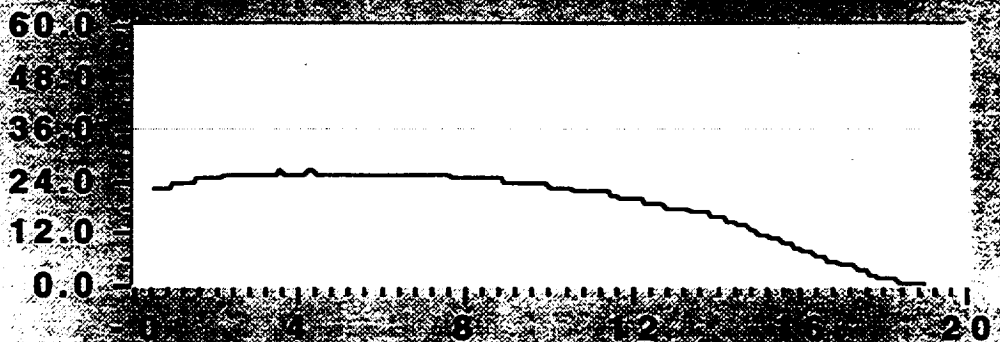
Drag
Friction
Coefficient



Plot D

Time, sec

5th Wheel
Velocity,
mph



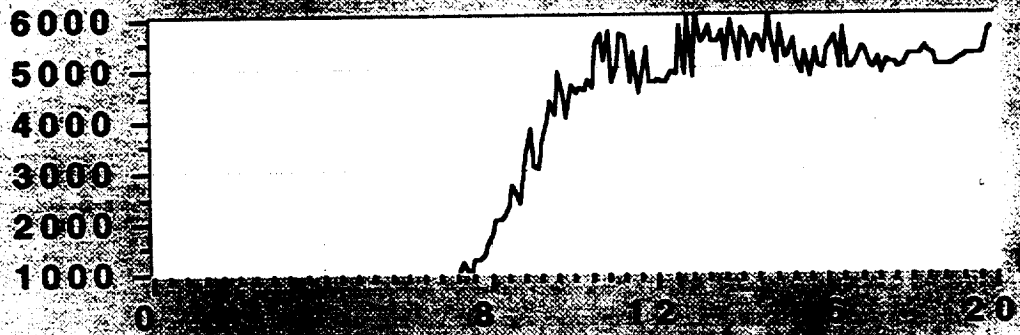
Time, sec

Run119

Plot A

Return

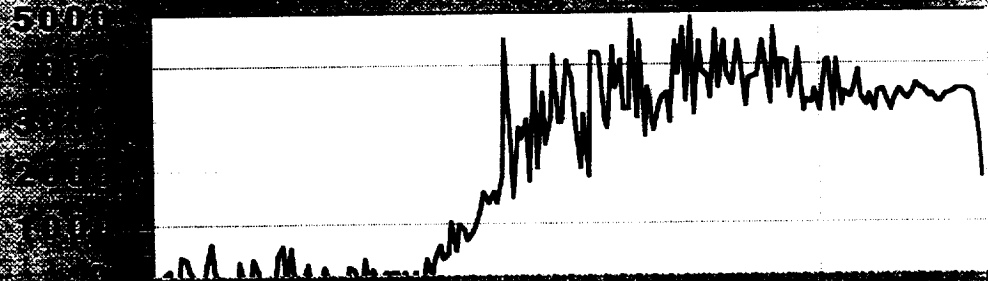
Vertical
Load, lb



Plot B

Time, sec

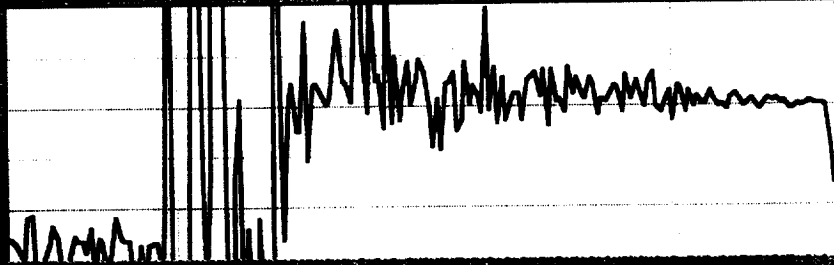
Drag Load
#1, lb



Plot C

Time, sec

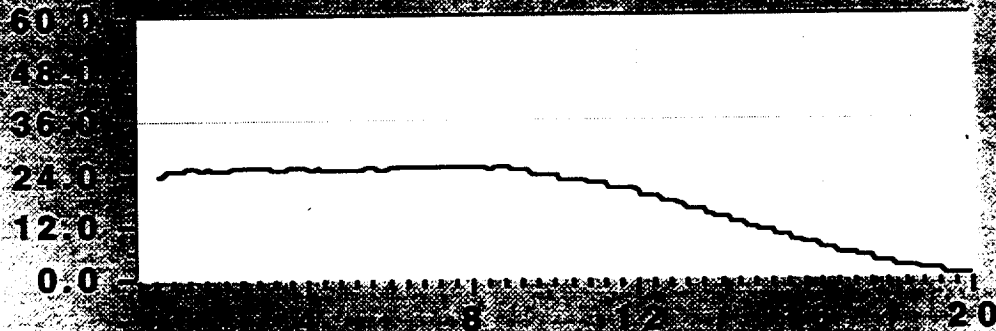
Drag
Friction
Coefficient



Plot D

Time, sec

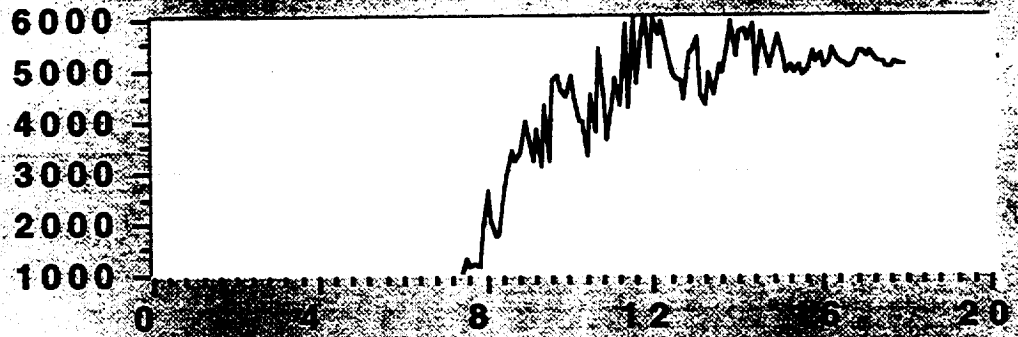
5th Wheel
Velocity,
mph



Time, sec

Run120

Plot A

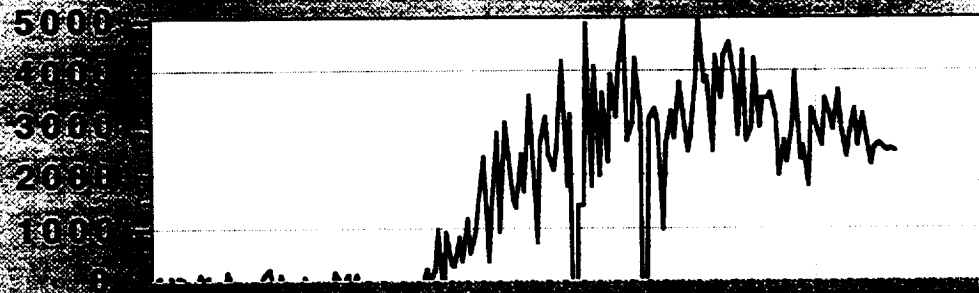


Return

Vertical
Load, lb

Plot B

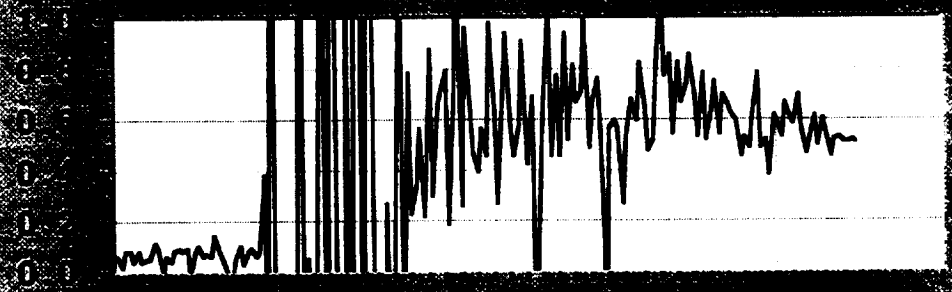
Time, sec



Drag Load
#1, lb

Plot C

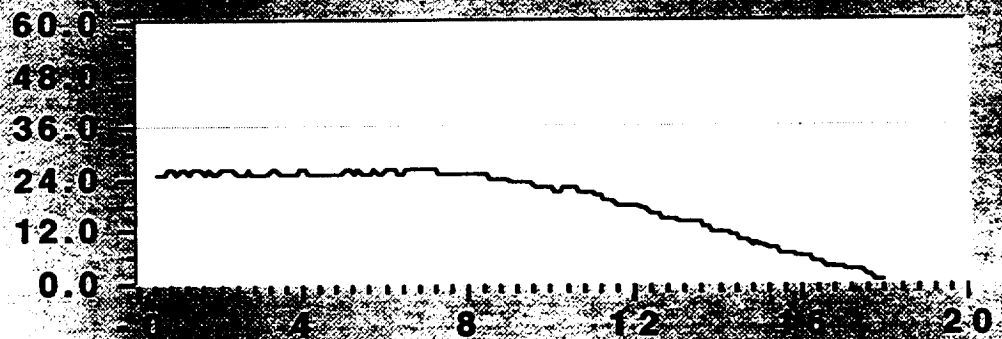
Time, sec



Drag
Friction
Coefficient

Plot D

Time, sec



5th Wheel
Velocity,
mph

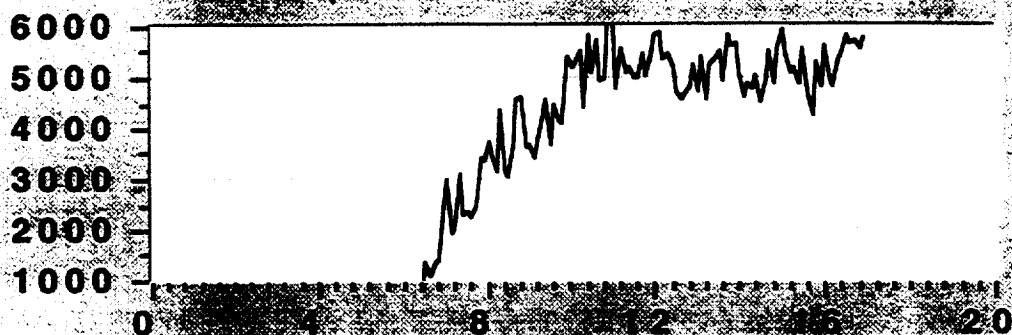
Time, sec

Run121

Plot A

Return

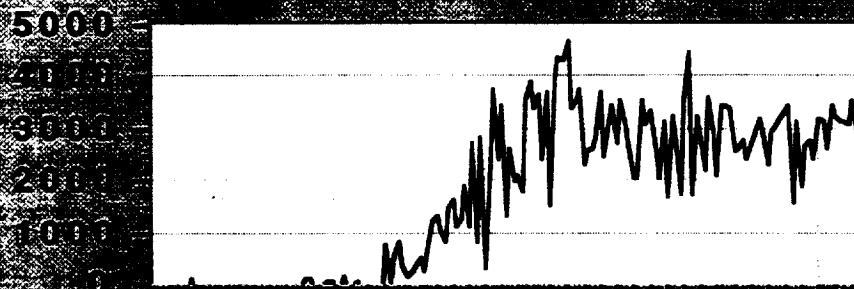
Vertical
Load, lb



Plot B

Time, sec

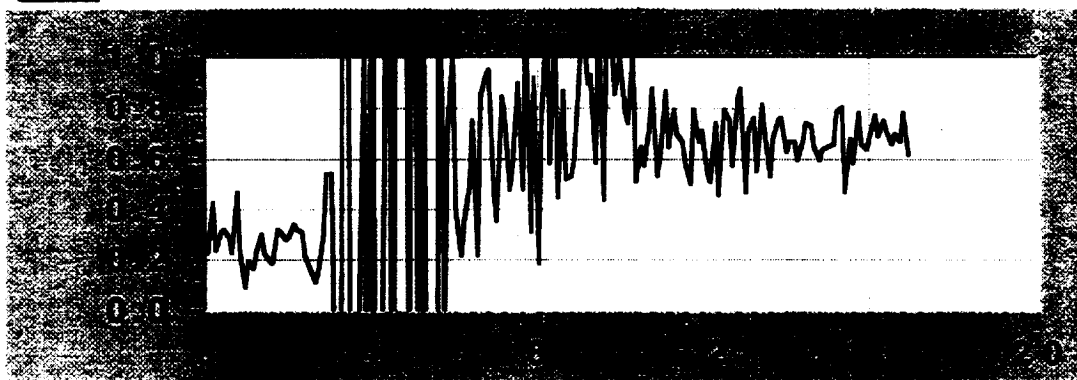
Drag Load
#1, lb



Plot C

Time, sec

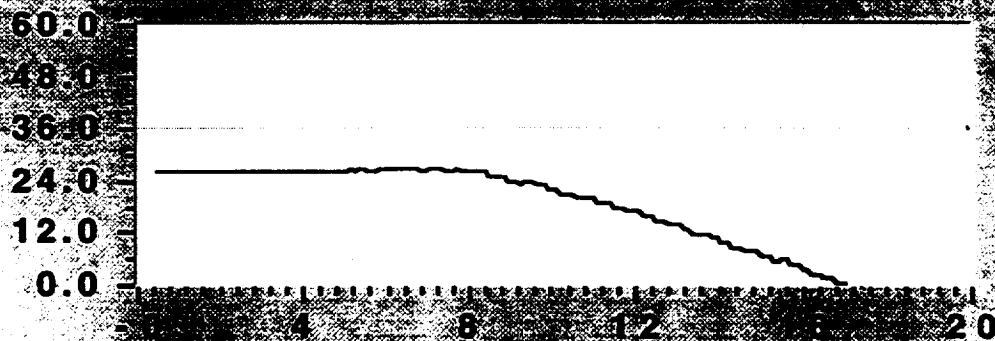
Drag
Friction
Coefficient



Plot D

Time, sec

5th Wheel
Velocity,
mph



Time, sec

REPORT DOCUMENTATION PAGE			Form Approved OMB No. 0704-0188	
Public reporting burden for this collection of information is estimated to average 1 hour per response, including the time for reviewing instructions, searching existing data sources, gathering and maintaining the data needed, and completing and reviewing the collection of information. Send comments regarding this burden estimate or any other aspect of this collection of information, including suggestions for reducing this burden, to Washington Headquarters Services, Directorate for Information Operations and Reports, 1215 Jefferson Davis Highway, Suite 1204, Arlington, VA 22202-4302, and to the Office of Management and Budget, Paperwork Reduction Project (0704-0188), Washington, DC 20503.				
1. AGENCY USE ONLY (Leave blank)		2. REPORT DATE June 2000		3. REPORT TYPE AND DATES COVERED Technical Memorandum
4. TITLE AND SUBTITLE X-38 Landing Gear Skid Test Report			5. FUNDING NUMBERS WU 522-62-11-02	
6. AUTHOR(S) George K. Gafka Robert H. Daugherty				
7. PERFORMING ORGANIZATION NAME(S) AND ADDRESS(ES) NASA Langley Research Center Hampton, VA 23681-2199			8. PERFORMING ORGANIZATION REPORT NUMBER L-17968	
9. SPONSORING/MONITORING AGENCY NAME(S) AND ADDRESS(ES) National Aeronautics and Space Administration Washington, DC 20546-0001			10. SPONSORING/MONITORING AGENCY REPORT NUMBER NASA/TM-2000-210293	
11. SUPPLEMENTARY NOTES Gafka: NASA Johnson Space Center, Houston, TX; Daugherty: NASA Langley Research Center, Hampton, VA				
12a. DISTRIBUTION/AVAILABILITY STATEMENT Unclassified-Unlimited Subject Category 05 Distribution: Nonstandard Availability: NASA CASI (301) 621-0390			12b. DISTRIBUTION CODE	
13. ABSTRACT (Maximum 200 words) NASA incorporates skid-equipped landing gear on its series of X-38 flight test vehicles. The X-38 test program is the proving ground for the Crew Return Vehicle (CRV), a gliding parafoil-equipped vehicle designed to land at relatively low speeds. The skid-equipped landing gear is designed to attenuate the vertical landing energy of the vehicle at touchdown using crushable materials within the struts themselves. The vehicle then slides out as the vehicle horizontal energy is dissipated through the skids. A series of tests was conducted at Edwards Airforce Base (EAFB) in an attempt to quantify the drag force produced while "dragging" various X-38 landing gear skids across lakebed regions of varying surface properties. These data were then used to calculate coefficients of friction for each condition. Coefficient of friction information is critical for landing analyses as well as for landing gear load and interface load analysis. The skid specimens included full- and sub-scale V201 (space test vehicle) nose and main gear designs, a V131/V132 (atmospheric flight test vehicles) main gear skid (actual flight hardware), and a newly modified, full-scale V201 nose gear skid with substantially increased edge curvature as compared to its original design. Results of the testing are discussed along with comments on the relative importance of various parameters that influence skid stability and other dynamic behavior.				
14. SUBJECT TERMS X-38, Crew Return Vehicle, Landing Gear, Skid, Lakebed, Friction, Friction Coefficient, Drag, Drag Coefficient, Stability, Edwards Air Force Base			15. NUMBER OF PAGES 115	
			16. PRICE CODE A06	
17. SECURITY CLASSIFICATION OF REPORT Unclassified	18. SECURITY CLASSIFICATION OF THIS PAGE Unclassified	19. SECURITY CLASSIFICATION OF ABSTRACT Unclassified	20. LIMITATION OF ABSTRACT UL	

NSN 7540-01-280-5500

Standard Form 298 (Rev. 2-89)
Prescribed by ANSI Std. Z-39-18
298-102